UNIVERSITEIT VAN PRETORIA
UNIVERSITY OF PRETORIA
YUNIBESITHI YA PRETORIA

Monitoring of tool wear in turning operations using vibration measurements

by

Cornelius Scheffer

Submitted in partial fulfilment of the requirements for the degree MEng in the Faculty of Engineering, University of Pretoria

December 1999

UNIVERSITEIT VAN PRETORIA
UNIVERSITY OF PRETORIA
YUNIBESITHI YA PRETORIA

Monitoring of tool wear in turning operations using vibration measurements

by

Cornelius Scheffer

Supervisor: Prof. PS. Heyns

Department of Mechanical and Aeronautical Engineering

Degree: MEng

SUMMARY

This study investigates the use of vibration and strain measurements on machine tools in order to identify the propagating wear of the selected tools. Two case studies are considered, one of which was conducted in the plant of a South African piston manufacturer. The purpose of the first case study was to investigate the feasibility of vibration monitoring to identify tool wear, before attempting to implement a monitoring system in the manufacturing plant. During this case study, data from a turning process was recorded using two accelerometers coupled to a PL202 real time FFT analyser. Features indicative of tool wear were extracted from the sensor signals, and then used as inputs to a Self-Organising Map (SOM). The SOM is a type of neural network based on unsupervised learning, and can be used to classify the input data into regions corresponding to new and worn tools. It was also shown that the SOM can also be used very efficiently with discrete variables.

One of the main contributions of the second case study was the fact that a unique type of tool was investigated, namely a synthetic diamond tool specifically used for the manufacturing of aluminium pistons. Data from the manufacturing of pistons was recorded with two piezoelectric strain sensors and a single accelerometer, all coupled to a DSPT Siglab analyser. A large number of features indicative of tool wear were automatically extracted from different parts of the original signals. These included features from time and frequency domain data, time series model coefficients as features and features extracted from wavelet packet analysis. A correlation coefficient approach

was used to automatically select the best features indicative of the progressive wear of the diamond tools. The SOM was once again used to identify the tool state. Some of the advantages of using different map sizes on the SOM were also demonstrated. A near 100% correct classification of the tool wear data was obtained by training the SOM with two independent data sets, and testing it with a third independent data set.

It was also shown that the monitoring strategy proposed in the second case study can be fully automated and can be implemented on-line if the manufacturer wishes to. Some of the contributions of this study are the use of the SOM for tool wear classification, and conclusions regarding the wear modes of the synthetic diamond tools.

Keywords: Neural Networks, Self-Organising Map (SOM), Vibration, Process Monitoring, Diamond Tools, Machining, Turning, Tool Condition Monitoring (TCM), Tool Wear, Wavelets.

Monitering van beitelslytasie in draai-operasies deur middel van vibrasiemetings

deur
Cornelius Scheffer
Studieleier: Prof. PS. Heyns

Departement van Meganiese en Lugvaartkundige Ingenieurswese
Graad: MIng

OPSOMMING

Hierdie studie ondersoek die gebruik van vibrasie- en vervormingsmetings op snybeitels gedurende draai-operasies met die doel om die slytasie van sekere soorte beitels te identifiseer. Twee gevallestudies word bespreek, waarvan een in die aanleg van 'n Suid-Afrikaanse suiervervaardiger onderneem is. Die doel van die eerste gevallestudie was om die moontlike toepaslikheid van vibrasiemetings om beitelslytasie te identifiseer te ondersoek, voordat daar met werk in die vervaardigingsaanleg voortgegaan word. Gedurende die eerste gevallestudie is data opgeneem deur die gebruik van twee versnellingmeters gekoppel aan 'n PL202 intydse FFT analiseerder. Seinkarakteristieke wat die beitelslytasie kan aandui is uit die data onttrek, en was as die insette vir 'n *Self-Organising Map* (SOM) gebruik. Die SOM is 'n tipe neurale netwerk wat sonder enige interaksie van die gebruiker leer, en die insetdata kan verdeel in areas wat met nuwe en gebruikte beitels ooreenstem. Daar is ook aangetoon dat die SOM diskrete veranderlikes effektief kan hanteer.

Een van die bydraes van die tweede gevallestudie is die feit dat 'n unieke tipe beitel vir die eksperimente gebruik is, naamlik 'n kunsmatige diamantbeitel, wat spesifiek vir suiervervaardiging gebruik word. Data vanaf die vervaardigingsproses is opgeneem deur twee piezo-elektriese vervormingsensors en 'n enkele versnellingsmeter, gekoppel aan 'n DSPT Siglab analiseerder. 'n Groot hoeveelheid seinkarakteristieke wat beitelslytasie kan aandui is automaties vanuit verskillende dele van die oorspronklike seine onttrek. Dit sluit in karakteristieke vanuit tyd en frekwensie domein data, tydreeks modelkoëffisiënte

asook karakteristieke onttrek van *wavelet packet* analises. 'n Korrelasiekoëffisiënt-metode is gebruik om die karakteristieke te identifiseer wat die slytasie van die diamantbeitels die beste beskryf. Die SOM is weer eens ingespan om die graad van slytasie op die beitel te klassifiseer. Die voordele van die gebruik van verskillende hoeveelhede neurone op die SOM is ook aangetoon. 'n Byna 100% korrekte klassifikasie van die graad van slytasie is verkry deur die SOM te leer met twee onafhanklike datastelle en dit te toets met 'n derde onafhanklike datastel.

Daar is ook aangetoon dat die algehele strategie vir slytasiemonitering in die tweede gevallestudie ten volle geoutomatiseer kan word, en ook intyds geïmplementeer kan word indien die vervaardiger dit sou verlang. Bydraes van hierdie studie met relevansie tot die vakliteratuur, sluit in die gebruik van die SOM vir slytasie data klassifisering, asook die gevolgtrekkings wat gemaak is rakende die slytasiemodusse van die kunsmatige diamant-beitels.

Sleutelterme: Neurale Netwerke, *Self-Organising Map (SOM)*, Vibrasie, Proses Monitering, Diamant Beitels, Masjinering, Draai-operasies, Toestandsmonitering, Beitel Slytasie, *Wavelets*.

ACKNOWLEDGEMENTS

The author wishes to thank the following people and organisations for their valuable contributions to this study:

- Prof. P.S. Heyns for his professional supervision and support. His special interest in this work was an inspiration for the successful completion of this project.
- Federal Mogul (Pty) Ltd (formerly AE Goetze) for permission to perform measurements at their Roodepoort plant. A special word of thanks to Mr. Ed Shimbles and Mr. Neels Wentzel for their help in planning and conducting the experiments.
- The author gratefully acknowledges the NRF, LGI and University of Pretoria for the financial support provided for this project.

Table of contents

NOMENCLATURE

Uppercase

A_n	wavelet approximations of packet n
A, B	constants for learning rate function for SOM
AMV_b	base line Absolute Mean Value
AMV_i	current Absolute Mean Value at instant i
C	Taylor equation constant, wavelet coefficients
CF	crest factor
cA_n	wavelet coefficients approximations of packet n
cD_n	wavelet coefficients details of packet n
D_n	wavelet details of packet n
E	energy of wavelet packet (Shannon entropy)
K	kurtosis
L	surface length
N_{i1}	1-neighbourhourhood of neurone i
$RAMV_i$	Ratio of Absolute Mean Value at instant i
R_a	roughness average
R_p	maximum height of a surface profile from the centre line
R_{pm}	mean of the maximum height values for a number of chosen off-cuts
R_q	rms roughness average
R_{ti}	peak to valley roughness
R_{tm}	mean peak to valley value
R_v	maximum depth of a surface profile from the centre line
R_y	largest peak to valley value
S	skewness, original signal for wavelet analysis
$S_x(f)$	one sided PSD function
T	total accumulated time, tool life in Taylor equation
V	cutting speed
W	waviness
X_{max}	maximum value of $x(t)$
X_{rms}	rms value of $x(t)$

Lowercase

$a_1, a_2 \ldots a_p$	AR coefficients
$b_1, b_2 \ldots b_q$	MA coefficients
c	subscript denoting Best-Matching Unit for SOM
fl	lower frequency cut-off for frequency band energy
fh	upper frequency cut-off for frequency band energy
h	height of surface profile above or below the centre line
$h_{c(x),i}$	neighbourhood function for SOM
k	summation index of ARMA model
$\boldsymbol{m}_c(t)$	Best Matching Model for SOM
$\boldsymbol{m}_I$	model vectors for SOM
n	material exponent in Taylor equation, index of AR, MA, and ARMA models, number of off-cuts for roughness assessment
p	order of AR model
q	order of MA model
$\boldsymbol{r}_c$	location of BMU on SOM grid
$\boldsymbol{r}_i$	location of unit i on SOM grid
s_i	signal sample i
t	time index, training step for SOM
u	sequence for MA model
$\boldsymbol{x}$	sample vector for SOM
$\bar{x}$	mean value of $x(t)$
$\boldsymbol{x}_I$	observation sample for SOM
$x(n)$	AR, MA or ARMA model of $x(t)$
$x(t)$	sensor observation
y	ideal trend value
$\bar{y}$	mean of ideal trend vector

Greek symbols

$\alpha(t)$	learning rate function of SOM
ρ	correlation coefficient
σ^2	variance
ψ	wavelet function
ψ_{xb}^2	frequency band energy

Abbreviations

AC	Adaptive Control
ACC	Adaptive Control Constraint
ACO	Adaptive Control Optimisation
AE	Acoustic Emission
AFM	Atomic Force Microscopy
AI	Artificial Intelligence
ANOVA	Analysis of Variance
AR	Auto Regressive
ARMA	Auto Regressive Moving Average
BMU	Best-Matching Unit
CAD	Computer Aided Design
CNC	Computerised Numerical Control
CWT	Continuous Wavelet Transform
DWT	Discrete Wavelet Transform
FFT	Fast Fourier Transform
FM	Federal Mogul
FN	Fuzzy Net
FRF	Frequency Response Function
IDWT	Inverse Discrete Wavelet Transform
KBES	Knowledge Based Expert Systems
MA	Moving Average
MRR	Metal Removal Rate
NC	Numerical Control
OR	Operations Research
PC	Personal Computer
PDC	Polycrystalline Diamond Compact
PSD	Power Spectral Density

rms	root mean square
SOM	Self-Organising Map
STFT	Short-Time Fourier Transform
SURE	Stein's Unbiased Risk Estimate

CHAPTER 1

INTRODUCTION AND LITERATURE

1.1 Introduction

The use of flexible manufacturing equipment has gained more ground in recent years due to the high demands of a fast growing industry. In order to justify the investment associated with the purchase of such equipment, it is necessary to achieve the maximum possible utilisation of each machine. Furthermore, manufactured goods have to be supplied with sufficient quality and low cost. Monitoring of the manufacturing process plays a very important role to avoid down time of the machine, or to prevent unwanted conditions such as chatter vibration, excessive tool wear or tool breakage. This is also very important in the unmanned machining environment, where the process must be absolutely reliable, and be able to operate non-stop without an operator checking for errors.

Increasing interest has been shown in the design of process control systems for manufacturing. This interest is driven by the rapid development of advanced sensor technology, signal processing and the successful implementation of intelligent control systems. Modern monitoring systems are generally required to operate on-line, and must be able to interpret the working conditions at any given time. The growing need in industry present various opportunities and challenges for research, and the development of new products. One of these challenges lies in devising methods for the complete optimisation of the machining process. Optimisation of machining processes can be divided into many sub problems, for example:

- Optimisation of the machining parameters.
- Maximisation of the process output.
- Minimisation of operating costs.
- Minimisation of the tool wear.

These sub problems are often related, and one problem may constrain another, such as the optimisation of machining parameters with tool wear as a constraint. Many of these problems have been researched for various processes. A wide variety of techniques have been developed and implemented, for industrial and academic purposes. Due to the wide variety of manufacturing processes, it is not possible to apply a single technique to all operations. It is not uncommon for a monitoring system to be reliable for one process, but unsatisfactory for the next. However, a number of techniques exist that can be used for different processes, if the necessary adjustments are made to them.

It is widely accepted that intelligent, sensor based manufacturing is vital to achieve reliable operation of a manufacturing process [1]. Sophisticated signal processing supply information about the manufacturing conditions that enables optimisation, control and decision making criteria. Due to the many factors that influence manufacturing process, they are very difficult to model mathematically. Therefore, sensors are generally needed to solve the optimisation problems described above. Sensors supply the information that researchers are unable to determine from pure mathematical modelling. Using this information, it is however possible to determine empirical equations describing the process.

This study deals with tool wear monitoring. However, studies of surface roughness and process optimisation are very often found in conjunction with tool wear studies. In order to get a better understanding on the subject of wear monitoring, a wide range of literature in the fields of process monitoring, process optimisation, tool wear and surface roughness monitoring were studied. In this chapter, the literature from the various fields dealing with Tool Condition Monitoring (TCM) are discussed.

1.2 Process monitoring

1.2.1 Sensors for process monitoring

A wide variety of sensors for process monitoring are available today. The most common sensors found in the industry are force, power and acoustic emission sensors. Others include [1,2]:

- Flame detector
- Sound level sensor
- Lubrication oil detector
- Touch sensor
- Edge position sensor
- Limit sensor
- Clamping force sensor
- Speed sensor
- Torque sensor
- Smoke sensor
- Image sensor
- Temperature sensor
- Tool wear sensor
- Accelerometer (vibration)
- Seismic sensor
- Tool damage sensor
- Current sensor
- Acoustic Emission (AE) sensor

- pH sensor
- Level meter
- Thermal deformation sensor
- Temperature distribution sensor
- Humidity sensor
- CO_2 gas sensor
- Machined surface roughness sensor
- Coolant temperature sensor
- Chip monitoring sensor
- Dust sensor
- Pressure sensor

These sensors and many more have found their rightful place in the manufacturing industry. Most of them are only used for a specific monitoring objective. The focus of monitoring may fall on one or more of the following areas [1]:

1. The machine (diagnostics and performance).
2. The tools for machining (wear, lubrication and alignment).
3. Workpiece (surface roughness, tolerance, geometry).
4. Process (chip formation, energy consumption, temperature).

The development of smart sensor technology also present new and exciting developments for the manufacturing industry [1,3,4,5]. With smart sensors, the time needed for signal processing are reduced significantly, thus enabling faster response for an on-line control scheme. These sensors can also possess abilities such as self-calibration, self-diagnostics, signal conditioning and decision making. This development, together with sophisticated signal processing software, makes inexpensive, fast and accurate measurements possible. With control systems that can respond at almost the same instant as sensor measurement, changes to the machine parameters can be made to optimise the machining conditions. Numerous optimisation techniques for control systems exist that could be used to improve machining speed and quality.

As will be shown further in this chapter, the emphasis in current international research is to integrate sensor systems. This enables more accurate and robust characterisation of a process. Integrated sensor systems can handle noisy input data, which is caused by random disturbances in the machining process. The sensor integration systems include learning schemes such as neural networks, and have the capability to handle complex processes which defy mathematical modelling.

1.2.2 Applications of monitoring systems

Applications for tool wear and surface roughness monitoring systems are found in a wide range of modern manufacturing industries. The on-line monitoring of tool wear allows timely tool replacement with minimum down time. A few examples are:

- The automotive industry.
- Manufacturing of machine components.
- Mass production of household items.
- Computerised Numerical Control (CNC) machining optimisation.
- Electrical / Mechanical product manufacture.

It has been shown that monitoring systems are most often used in turning and drilling processes, with milling and grinding in second place, according to Dornfeld *et al.* [1]. They also suggest that no monitoring system should be expected to operate with 100% reliability, although failures almost always occur due to human error. In most cases the demand for a monitoring scheme is to monitor tool breakage, tool wear and collision. Most manufacturers state that reliable operation of the manufacturing process is more important than quality monitoring. Some industries may have monitoring requirements that have never been explored. However uncertain these demands may be at the moment, the already existent need in the manufacturing industry for reliable monitoring systems is evident.

1.3 Tool wear monitoring

1.3.1 Introduction

The monitoring of cutting tool wear is a more complex task than expected, because tool wear induces very small changes in a process with a very wide dynamic range. Furthermore it is difficult to identify whether a change in a signal is caused by tool wear or a change in the cutting conditions. The task of tool wear monitoring can be subdivided into a number of stages [6]:

- Sensor selection and deployment.
- Generation of a set of features indicative of tool condition.
- Classification of the collected and processed information as to determine the amount of tool wear.
- A further step, which is not always included, is what we do about it, like the control or optimal tool replacement strategy.

Through the years, a number of different types of wear geometry have been identified, depending on the following [6,7,8]:

- Cutting tool material.
- Workpiece material.
- Tool geometry.
- Cutting conditions.

Tool wear is also generally divided into five distinct stages, namely [9]:

1. Initial stage of wear.
2. Regular stage of wear.
3. Micro-breakage stage of wear.
4. Fast wear stage.
5. Tool breakage.

Most authors identify the initial, regular and fast wear stage with their monitoring strategy. It is also assumed by some authors that tool wear only consists of the initial, regular and fast wear stages. It has been established by various researchers that the initial and fast (before tool breakage) stages wear occur more rapidly than the regular stage. The reason for this behaviour is not clear from any of the surveyed literature.

1.3.2 Tool failure modes

It is important to identify the different tool failure modes in order to select appropriate operating conditions for machining. The most widely researched tool failure modes are flank wear, breakage (fracture), crater wear and plastic deformation [10]. Other modes include notching (groove wear), cracking and chipping. Notching and chipping changes the tool nose curvature. Figure 1.1 displays the tool failure modes, as depicted by Rao [11]. Flank and crater wear are generally accepted as the normal tool failure modes, because the other failure modes can be avoided by selecting the proper machining parameters. The growth of flank and crater wear are directly related to the cutting time (or length of cut), unlike some of the other failure modes which can occur unexpectedly, even with a new tool.

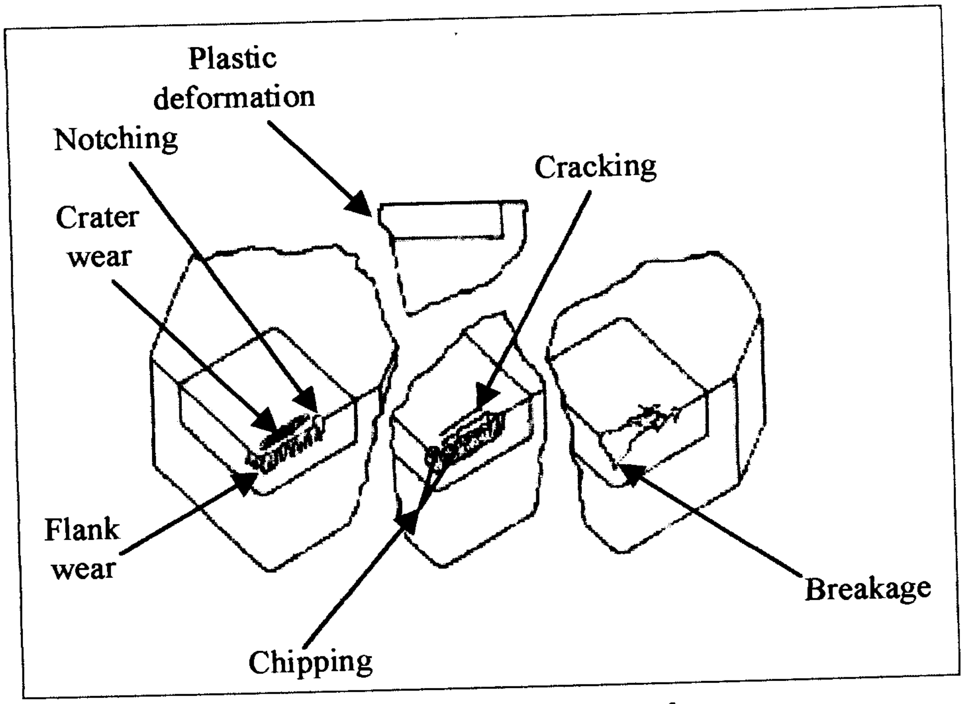

Figure 1.1: Tool failure modes

It is already well established that flank wear has the greatest influence on the workpiece dimensions and surface quality [11]. For this reason flank wear has been widely researched, and ways and means of predicting it has been the pursuit of researchers for many years. However, this study demonstrates that certain tools can exhibit different dominant modes of failure, such as the synthetic diamond tools investigated in Chapter 4. A brief discussion of the different tool failure modes are made here:

A. Flank wear

Flank wear is the volumetric loss at the top of the tool tip edge, and is mainly caused by abrasion. It is of course normal that a tool will wear out at some or other stage, depending on the type of work it has been subjected to. Some authors affirm that the flank wear in coated tools first occurs due to abrasion, and, as the cutting process continues, the temperature also increases and diffusion also occurs [9]. Flank wear normally occurs at lower operating speeds.

B. Fracture

Fracture is a mode of failure characterised by breakaway of material on the tool edge. Fracture occurs when the feed-rate is too high, or when a tool is used with too low fracture strength.

C. Crater wear

Crater wear is a mode of failure predominantly caused by diffusion of tool material into the chip when operating at high speeds. The tool-chip interface temperature governs this mode of failure. This is in its turn a function of the speed and feed-rate.

D. Plastic deformation

Plastic deformation starts when the temperature of the tool tip reaches a certain value. This implies that the tool yield strength is lowered below the existent normal stress. Further plastic deformation results in a temperature increase that causes complete failure. Keeping the temperature increase at the tool tip edge lower than a critical value can prevent this failure mode.

1.3.3 Tool wear monitoring techniques

A. Direct and Indirect systems

A number of approaches to monitor tool wear exist. These techniques can be divided in two categories, namely direct and indirect. Direct methods always deal with a measurement of volumetric loss at the tool tip, while indirect methods seek a pattern in sensor data from the process to detect a failure mode [1]. Direct methods are of less importance to this study. In general, direct methods are sensitive to dirt and chips, and therefore they are not commonly accepted in industry.

Indirect methods will be discussed in greater detail. Indirect methods are said to be less accurate than direct methods, but have found more acceptance in industry, due to the fact that most indirect methods are easily interpreted, cost-effective, and in some instances more reliable than direct methods. Also, for some applications, it might not be possible to use a direct monitoring method, due to the nature of the process.

B. Continuous and Intermittent systems

The second important distinction to be made with tool wear monitoring systems is between continuous and intermittent systems [1]. In the case of continuous systems, the measurement variable is available throughout the machining process. This enables the on-line classification of the process, and ensures that sudden changes can be reacted upon in time. This study will focus on continuous systems.

In the case of intermittent systems, the variable is only recorded during intervals in the machining process. This method has many obvious disadvantages, which includes time losses and high costs. One practical application of an intermittent system can be the detecting of a tool or wear measurement on a magazine of tools, while the machine is using a different tool.

C. Sensors for tool wear monitoring

Monitoring usually takes place in very hostile environments. Subsequently, sensors used for tool wear monitoring should be robust and simple to operate. The use of multiple sensors can enhance the performance of tool wear monitoring systems, because each sensor is independently related to the tool wear. Sensors used for TCM must meet certain requirements, such as [1]:

- Measurement as close to the machining point as possible.
- No reduction in the static and dynamic stiffness of the machine tool.
- No restriction of working space and cutting parameters.
- Wear and maintenance free, easy to replace and of low cost.
- Resistant to dirt, chips and mechanical, electromagnetic and thermal influences.
- Function independent of tool and workpiece.
- Adequate metrological characteristics.
- Reliable signal transmission, e.g. from rotating to fixed machine components.

1.3.4 Tool Condition Monitoring (TCM) systems

A discussion on some TCM systems follows. Surface roughness analysis is also a indirect TCM method, but will be discussed in a separate section, because it is a wider field of study not only dependent on tool wear.

A. Mathematical modelling: Analytical and empirical

Analytical mathematical models can be very useful to study the effects of tool geometry on the various machining parameters, but these models are too complex to be of any value in a real-time TCM system. The non-linear, stochastic and time invariant nature of machining processes, make modelling very difficult [6]. A transformation between the signal characteristics and the physical law representing the process is necessary to establish such a model. Because of the complexity of the process, modelling of the physical law cannot be performed analytically in most instances.

The only remaining option is empirical modelling which can be performed parametrically or non-parametrically. Parametric modelling usually represents only an adaptation of the analytical model and is of limited capability. This method also requires the inputs of an expert familiar with the relational mechanisms and an ability to translate these into simple rules [10]. Non-parametric modelling methods are based on a statistical description of natural phenomena.

Empirical models have been used with great success for describing many manufacturing processes. Grabec *et al.* [13] used empirical modelling for estimating tool sharpness on a lathe, for the determination of surface roughness in a grinding process, and for classifying surface quality of paper. Ruiz *et al.* [14] used a multi-sensor empirical approach to estimate tool wear, and identified tool wear with three different empirical identification methods.

A common mathematical model for the case of tool wear can be generated by Taylor's tool life equation [11]. The equation is:

$$VT^n = C \tag{1.1}$$

The equation provides a relationship between cutting speed V, and tool life T, and two parameters, n and C, depending on tool and workpiece material. The Taylor parameters are generally determined empirically if they are unknown. This method is useful in establishing a tentative value for the expected tool life. It was found from experiments that the Taylor equation could yield estimates within ± 35 percent of the actual tool life. This equation is common in the literature and various versions have been adapted to enhance the equation's performance.

The use of an analytical model for force reconstruction for wear identification was proposed by Braun *et al.* [15]. This model can be used for the prediction of chatter onset. Ravindra *et al.* [16] proposed a mathematical model based on multiple regression analysis. The model describes the wear-time and wear-force relationships for turning operations. Good correlation was found between the cutting force and progressive tool wear.

B. Force-based monitoring

It is well established that worn tools cause an increase in the cutting force components [1,17,18]. Many types of sensors have been developed to monitor the cutting force in different directions for a number of processes. These include [1]:

- Direct measurement dynamometers
  These sensors are based on the piezoelectric effect and can measure dynamic cutting forces very accurately. However, these sensors are expensive and in most cases not protected from overload, and therefore not widely used in industry yet. There is also some difficulty in protecting the sensors against cutting lubricant. Force-measuring tool turrets have been developed that can measure three force components, but are still of a very high cost.

- Plates and rings
  Force-measuring plates can be fitted relatively easy on turning machines between the turret housing and the cross slide, or between the turret disc and slide. These thin plates are fitted with piezoelectric force measuring sensors. These sensors have some advantages, but in some cases they are subject to many disturbing factors, such as thermal expansion.

- Pins, extension sensors
  These sensors are suitable for tool breakage monitoring in rough machining. The sensors are fitted on force-carrying machine components to detect the cutting force indirectly. The identification of a suitable fitting position can only be determined experimentally, which is a disadvantage.

- Measurement of displacement
  Non-contact sensors to detect the displacement or bending of tools can be mounted directly on the tool [19]. However, these sensors are subjected to the high risk of damage and disturbance due to chips, dirt and cooling lubricant.

- Force-measuring bearings
  Bearings and bushes can be specially fitted with strain gauges in certain positions to measure cutting forces. Force-measuring bearings require a low-pass filter due to disturbance from the ball contact frequency, and therefore high frequency signal

processing is not possible. The force-measuring bushes are only accepted in special cases because they reduce the rigidity of the machine.

- Force and torque at spindles
  These systems can be very complex because they have to monitor the torque of the spindle with high resolution, and within the entire range of the motor. Furthermore, the signal must be transmitted on a non-contact basis. The installation of such systems is not possible on most machines because of a constraint on the available space for sensor mounting.

C. Measurement of motor current

The measurement of motor current is an easy alternative to the above systems and can be installed without much difficulty. A wide range of sensors are available for this purpose. However, due to fluctuations in the signal due to friction, the system is not always absolutely accurate. Also, tool breakage is not detected directly, but only after damage has occurred. Spindle power is also proportional to the cutting force in the primary motion, which is not always sensitive enough for tool wear monitoring. The cutting process consumes only a small portion of the measured power of the spindle, which also makes monitoring difficult. However, monitoring systems based on the principle of spindle current can be successful when used with the right process [18].

D. Vibration

Piezoelectric accelerometers can measure the machine vibration caused by oscillations of cutting forces. It has been shown by previous authors that the vibration levels change with tool wear (see references below). Accelerometers fulfil the environmental requirements for tool wear monitoring because they are generally resistant to the aggressive media present in machining operations. Accelerometers can be of low cost, and can measure vibration levels within a very wide frequency range. For these reasons, accelerometers are often used for TCM [9,18,20-26].

One of the main difficulties of monitoring the tool life through vibration is to identify the frequency range that is actually influenced by tool wear, since most machining processes consist of many factors that produce vibrations that are not related to tool wear. The frequency range for ordinary machining operations is usually between 0 – 10 kHz. Bonifacio and Diniz [9] suggest that the useful signal falls between 0 – 8 kHz. Some authors found that two ranges of frequencies are sensitive to tool wear: The first relatively close to 0 Hz and the second at a higher value, mostly below 8 kHz [9]. It would seem that the frequency range sensitive to tool wear is absolutely dependent on the specific machining operation, and have to be determined experimentally. A 'global' range that would satisfy all machining operations does not exist.

E. Acoustic Emission (AE)

Cutting processes produce elastic stress waves which propagate through the machine structure. Different sources in the cutting process generate these stress waves known as Acoustic Emission (AE). Sources of AE in metal cutting are:

- Friction on the tool face and flank.
- Plastic deformation in the shear zone.
- Crack formation and propagation.
- Impact of the chip at the workpiece.
- Chip breakage.

The fact that crack formation generate AE, makes AE very useful for tool breakage detection. Although a wide range of AE sensors exist, only a few can withstand the hostile environments of machining processes. AE sensors specially designed for TCM purposes exist, which can be attached to the machine tool surface. However, a new concept is to use a coolant stream to transmit the AE waves from the tool to the sensor. The advantage is that the distance between the cutting area and the sensor is reduced, and thereby damping effects are minimised. Some problems with this approach is that bubble free coolant is required, and monitoring may be disturbed when chips pass through the coolant stream. Another approach is to use non-contact transmission of the signal, allowing measurement near the process. Many AE based tool wear and breakage monitoring systems have been implemented successfully [18,27-31].

F. Other methods

Some of the other methods for indirect / direct tool wear monitoring (excluding surface roughness approaches) are:

- Ultrasonic systems [32].
- Use of a non-contact capacitive sensor [33].
- Vision systems [34,35].
- Laser scatter methods [36].
- Stereo imaging [37].

1.3.5 Decision making techniques

With the sensor information from the different TCM systems described in the previous section, a decision must be made regarding the tool condition. This decision is generally referred to as the *classification*. In complex problems it is always better to combine knowledge from sensor data in some way for best results. The functions of a modern TCM system is shown in figure 1.2 [6].

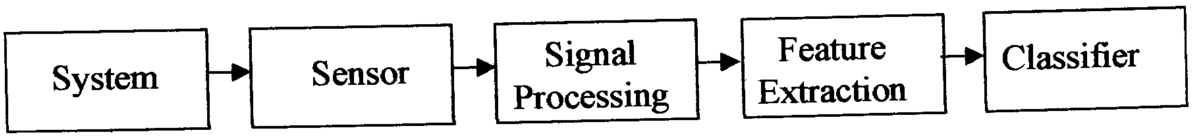

Figure 1.2: Functions of TCM system

A discussion on classification techniques for TCM follows here, with an introductory discussion on *features*, on which most classification techniques are based.

A. Features

Most decision making techniques for process monitoring are based on features. Information from the force, vibration or AE signal acquired during machining can be used for the monitoring of the cutting tool. Features can be extracted from these signals that show effective and consistent trends towards tool wear. Once these features are extracted through preliminary processing of the signal, the tool state can be predicted with a pattern recognition or other classification technique [38].

These features can be derived from time and / or frequency domain data, for example:

- Mean.
- Variance.
- Skewness.
- Kurtosis.
- Crest Factor.
- Power in a specific frequency band, by means of the Fast Fourier Transform (FFT).
- Auto Regressive (AR) and Auto Regressive Moving Average (ARMA) coefficients.

One useful approach in the literature is the use of AR and ARMA coefficients. AR coefficients computed for a signal represent the characteristic behaviour of the signal. When the signal change during the cutting operation as a result of tool wear, the model coefficients also change and can then be utilised to monitor the progressive tool wear. Hence, AR coefficients can also be used as features for pattern recognition [38].

El-Wardany *et al.* [20] found that the instantaneous Ratio of Absolute Mean Value ($RAMV_i$) was useful in eliminating false alarms that occurs when monitoring drill wear and breakage in conjunction with kurtosis and cepstrum analysis. They state that the kurtosis value is useful in identifying transients and spontaneous events within vibration signals. Cepstrum analysis is used to identify a series of harmonics or side bands in the power spectrum and to estimate their relative strength. Drill breakage consistently caused a peak at the quefrency corresponding to one spindle revolution. $RAMV_i$ was used to trigger the onset of kurtosis and cepstrum analysis. It is calculated as follows:

$$RAMV_i = \frac{AMV_i}{AMV_b} \tag{1.2}$$

Where AMV_b represents a base line instantaneous Absolute Mean Value calculated at the start of the drilling process, and AMV_i is the current Absolute Mean Value calculated at the i-th revolution of the spindle.

B. Trending, threshold

A very simple decision making technique can be based on the normal 'trending' of the features. When a certain feature, or a set of features, reach certain pre-established set limits, an estimation of the tool condition can be derived. Certain threshold values for the features can be established that can be related to a certain tool condition. These thresholds must be determined experimentally. The difficulty with this method is to determine the correct threshold value, especially under diverse cutting conditions.

C. Ratio

Some authors suggested that two frequency ranges must be identified from the original signal [9]. The one range must be sensitive to tool wear, the other must be insensitive. For instance, if the measurement was made from 0 – 8000 Hz, it must be split (using appropriate filters) into a 0 – 4000 Hz signal, and a 4000 – 8000 Hz signal. If the lower range is more sensitive to tool wear, a ratio between the two ranges can be calculated. If this ratio exceeds a certain pre-established value, it can be deducted that the end of the tool life has been reached.

This can also apply for a ratio between the signal recorded from a fresh tool to that compared with a worn tool. The problem with this method is that it is unable to account for tool breakage. When the tool breaks, a sudden fall of the signal occurs, and the rationing method will not detect the breakage.

D. Neural networks

The use of neural networks as a secondary, more sophisticated signal processing and decision making technique have been researched and implemented by many authors in various fields of manufacturing. This is also very true for TCM [6,39-53]. The use of a neural network makes the decision making much more accurate because it can use a lot of independent data simultaneously to make a correct decision or classification. The extraction of the underlying information and the robustness towards distorted sensor signals are two of the most attractive features of neural networks.

This also applies for sensor integration schemes for TCM, by which data from a selection of sensors are used for classification. Combining features from the vibration, AE, force and current signals can result in a network that can predict the tool state at any given time [6]. The most common neural network tested in machining operations is the Backpropagation algorithm.

Despite the current popularity of backpropagation as a supervised learning algorithm, its need for a correct tool classification in every training sample limits its successful application for on-line tool wear monitoring. This is because the machine operation must be interrupted in order to acquire correct information about tool condition. Since the system must handle numerous combinations of tool-type, material, and cutting conditions, a supervised learning procedure like backpropagation is undesirable. Thus, it would be helpful to have a neural network that can utilise unsupervised training samples

[6]. The use of a self-organising neural network that can utilise unsupervised training samples will be demonstrated in this study. The successful implementation of neural networks is dependent on the proper selection of the network structure, as well as the availability of reliable training data.

E. Fuzzy logic

Many authors [54-59] have researched the concept of fuzzy logic to classify tool wear. It has been shown that fuzzy logic systems demonstrate a great potential for use in intelligent manufacturing applications. While neural-network models cannot directly encode structured knowledge, fuzzy systems can directly encode structured knowledge in a numerical framework. Additionally, fuzzy control systems is capable of estimating functions of systems with only a partial description of the systems' behaviour. This is very difficult to construct by simply using neural-network models.

Neural networks and fuzzy systems are also combined into a so-called Fuzzy Net (FN). FN systems are able to facilitate a simple training procedure for a complex system such as a machining process. FNs require little memory and have the capability to adapt to the process when changes are made. An in-process FN system to monitor tool breakage were designed and implemented successfully by Chen and Black [54], concentrating on end milling operations.

F. The coherence function method

Li *et al.* [21] found that the coherence function of two crossed accelerations can be used as an easy and effective way to identify tool wear and chatter. They found that with progressive tool wear, the autospectra of the two accelerations and their coherence function increase gradually in magnitude around the first natural frequencies of the cross-bending vibration of the tool shank. As the tool approaches a severe wear stage, the peaks of the coherence function increase to values close to unity. This was also proved in theory by the authors. However, there are two conditions to be fulfilled when using this approach: The first is the careful selection of sensor locations on the tool shank. The second is the high-speed computation required for real-time monitoring on the tool performance, as well as the need for a fast FFT co-processor.

G. Other methods

There also exist a number of other decision making methods, which include:

- Knowledge Based Expert Systems (KBES) [10].
- Pattern recognition algorithms [38].

1.4 Surface roughness analysis

1.4.1 Introduction

Surface roughness is one of the most important factors in evaluating the quality of the machining operation. Because it is sometimes easier to measure the surface roughness of the machined component than to measure the amount of wear on the tool, surface roughness estimation can be utilised to monitor the tool wear [60].

Cutting conditions, such as cutting speed, feed rate, depth of cut, tool geometry and material properties of the tool and workpiece, significantly influence the surface finish of the workpiece material. If these factors are known and set correctly, an in-process surface roughness measurement system can also indicate a worn tool [12,61].

Surface inspections in industry have been conducted typically as a post-process operation, which is both time consuming and uneconomical since a number of non-conforming parts can be produced prior to inspection. This underlines the importance of devices to monitor surface finish continuously without interrupting the machining process.

Several methods have been researched to estimate surface roughness on-line in flexible manufacturing systems. Some of the other methods are [60]:

- Correlation between surface roughness and cutting vibration to develop an on-line roughness measuring technique.
- Image processing, stray light and laser focus methods [12].
- Roughness measurement with non-contacting inductance pick-up.
- Direct measurement with a stylus (contacting sensor or profilometer).
- Ultrasonic sensing approach [12].

As with TCM systems, roughness monitoring systems can also be divided into direct and indirect approaches. This section concentrates on tool wear and vibration monitoring with relevance to surface roughness monitoring.

1.4.2 Surface roughness analysis and tool wear

The surface roughness of machined components holds direct correlation with the amount of wear on the cutting tool [62,63]. A logical next step is to use the roughness information to control the machining operation as the tool wears. To maintain a certain roughness, the feed and cutting depth must either be increased or decreased to maintain the workpiece quality. For this, relatively simple geometric control systems can be developed, that measure the roughness, calculate an error value, and then change certain machining parameters accordingly.

The ultimate goal is to develop an automated in-process monitoring system that would counteract any troublesome external factors. Process parameters could be varied in-process with an adaptive or geometric control scheme, which would ensure consistent part quality [12].

Bonifacio and Diniz [9] found that vibration of the tool is a reliable way to monitor the growth of surface roughness in finish turning, and can be used to establish the end of tool life for these operations. Flank and groove wear mostly influence surface roughness. Some researchers found that there is increased amplitude of roughness at the beginning stages of cut, a lesser tendency in the middle and again an increasing tendency at the end of tool life. In finish turning, it is important to monitor the surface roughness in order to establish the moment to change the tool.

1.4.3 Vibration monitoring and surface roughness analysis

The average surface roughness of a machined part can be assumed to be the result of the superpositioning of a theoretical profile computed from cutting kinematics, and of the oscillatory profile determined by the relative vibration between the cutting edge and the workpiece [64]. The cutting kinematics are influenced by parameters like speed and feed rate, while the relative vibration between the tool and workpiece are caused by the random resistance against cutting, that causes a stick-slip process between the chip and the tool.

The ideal or theoretical surface profile can be easily calculated from the cutting kinematics. The actual surface profile can be measured, or it can be estimated by measuring the relative vibration between the tool and the workpiece. This makes it possible to determine the surface roughness on-line without interrupting the machining process. However, there are a lot of practical problems involved when working in a realistic machining environment.

One problem is that chatter between the tool and workpiece causes large vibrations that cannot be superimposed on the surface roughness. Another problem is that loose metal parts and other external factors easily distort signals from the sensors. However, the method has been successfully implemented in dry turning with ferrous metals by Jang *et al.* [60]. They suggested that further research be done in this field.

Bonifacio and Diniz [9] did experiments with coated carbide tools in finish turning, measuring in the 0 – 8 kHz range. The vibration was measured on two channels, one in the cutting direction and one in the feed direction. The rms value was used to compare sets of measurements. They also varied the feed and cutting speeds with different experiments. They found that cutting speed had a much larger influence on the tool life than the feed. They also found that both vibration and roughness measurements correspond to a certain amount of tool wear at a given time. They also discovered that an increase of flank wear causes an increase in vibration in a large frequency range (0-8 kHz), despite the fact that some authors state that only changes in some narrow frequency ranges take place. However, this discovery is definitely process dependent.

1.4.4 Parameters used in roughness monitoring

A. Surface Texture

A surface which is nominally smooth and flat will always exhibit some roughness, which may vary from fine to coarse, depending on the finishing operation used. It may also exhibit some waviness, but some surfaces exhibit roughness and waviness, and may also be curved, as shown in figure 1.3 [65].

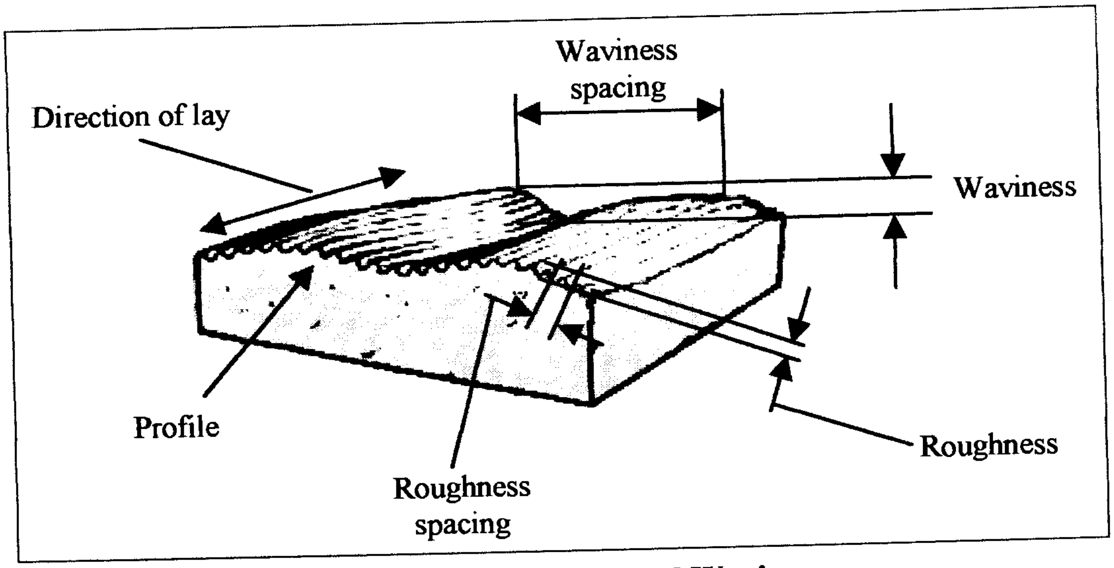

Figure 1.3: Roughness and Waviness

Figure 1.3 illustrates the two components of surface texture, which are:

- Roughness
  The irregularities in the surface texture which are inherent to the production process, but excluding waviness and errors of form.
- Waviness
  This is the component of surface texture upon which roughness is superimposed. Waviness may result from such factors such as machine or workpiece deflections, vibrations, chatter or heat treatment.

Each pattern is characterised by the lay (the principal direction of the predominant surface pattern), the spacing of the principal crests and, in height, its departure from a reference line.

B. Assessment of surface roughness

The standard method for assessing surface texture is based on traversing a stylus across the surface to produce an electrical signal, which can generate the surface profile on a chart or an average reading on a meter. Roughness average, R_a, is defined as the arithmetical average of the profile above and below the reference line throughout the prescribed sampling length. This is illustrated in figure 1.4. Surface roughness values are normally assessed as mean results of several sampling lengths taken consecutively along the surface.

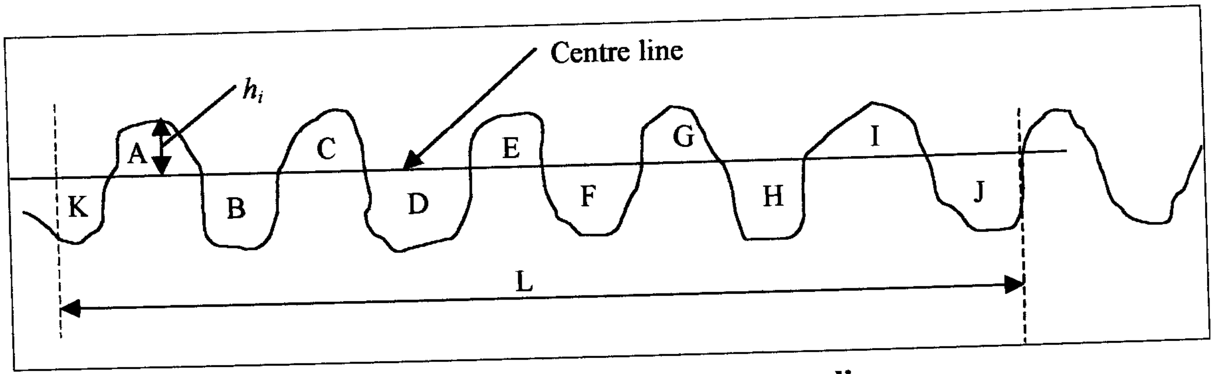

Figure 1.4: Definition of the centre line

Over a length of surface L, the centre line is a line such that the sum of the areas embraced by the surface profile above the line is equal to the sum of those below the line, thus:

$$\text{areas A + C + E + G + I} = \text{areas B + D + F + H + J + K} \tag{1.3}$$

The R_a value is the average height of the profile above and below the centre line [65]:

$$R_a = \frac{h_1 + h_2 + h_3 + ..h_n}{L} = \frac{1}{L}\int_0^L |h| dL \tag{1.4}$$

where h is the height of the profile above or below the centre line at **unit distances** apart. The units of L is not added into the equation - R_a is normally expressed in µm.

R_q is the rms value for R_a:

$$R_q = \sqrt{\frac{1}{L}\int_0^L h^2(x)dx} \tag{1.5}$$

R_{ti} is the peak to valley value for a surface profile.

R_y is the largest R_{ti} value over a length L.

R_{tm} is the mean value of all the R_{ti} values within a length L.

R_v is the maximum depth of a surface profile from the centre line.

R_p is the maximum height of a surface profile from the centre line.

R_{pm} is the mean of R_p, thus

$$R_{pm} = \frac{1}{n}\sum_{i=1}^{n} R_{pi} \tag{1.6}$$

$$\text{where } n = \text{number of off - cuts}$$

These are the basic parameters used for surface roughness assessment. The same type of parameters can also be derived to quantify the waviness of the profile. A W is used instead of an R as a reference to waviness. Depending on the type of operation, some of these parameters will be specified to fall within certain limits. In many instances, the R_a value alone is satisfactory.

1.5 Diamond tools

1.5.1 Introduction

The use of diamond tools for ultra-precision manufacturing have gained much ground in recent years. This includes the use of single-crystal diamonds in the production of optical and magnetic parts such as magnetic discs, laser mirrors, polygon mirrors and copier drums [66]. Artificial diamond tools are also preferred in machining of aluminium, because of diffusion occurring between carbide coated tools and aluminium. This is especially true in the automotive industry, for the manufacturing of pistons and other automotive parts. Diamond tools can also generate outstanding surface quality when used with ultra-precision CNC machines. The overall quality of the product is a function of the tool edge sharpness and the machine stability. When manufacturing a piston, the surface finish must possess certain qualities to ensure long life of the part. When the surface of the piston wears, it must allow grooves for adequate lubrication. This is also the reason why a certain shape of diamond tool is used for the manufacturing of pistons.

It is known that the surface profile is made of repetitive tool passes on the face perpendicular to cutting direction. When using diamond tools, it is generally accepted that the surface is wholly a duplicate of the tool geometry, which is not always the case with other tools. Also, diamond has very little attracting force to other materials, making it more efficient in duplicating its own shape on the target surface. Diamond tools can be resharpened after a certain amount of wear has occurred. This is possible until all the usable diamond material is finished.

1.5.2 Diamond tool wear studies

Choi and Kim [66] researched the single-crystalline diamond tool wear in the manufacturing of hard drives for Personal Computers (PCs). The objective was to provide information on the optimal regrinding time of the diamond tool as well as to minimise material loss by ensuring machining accuracy. A monitoring system was developed using the frequency response from force and acceleration signals. The wear features that were used included mostly the energy within a specific frequency band.

They found that the diamond tool also display five stages of wear, namely the initial, normal, micro-fracture, wholly worn and tool breakage stages. The wear features used to classify the tool wear yielded positive results, and it was found that the dominating wear pattern is micro-chipping, rather than crater wear and flank wear.

Afaghani *et al.* [67] studied the effects of diamond tool grain size in machining SiC-particulate-reinforced epoxy composites. They found that a coarse-grained tool is preferred in cutting the composite because tool wear increases drastically when the composite particle size is increased. They also found that the wear mechanism of the sintered diamond tool involves tearing off of diamond grains, and established an empirical fatigue-like curve for tool wear. This can help to predict tool life for different grains of tool and composite particle size.

Wilson and Marinescu [68] studied the machining of granite cylinders on a lathe using single round Polycrystalline Diamond Compact (PDC) cutters. PDC cutters have found wide acceptance in drilling soft and medium rock formations, and also in the machining of non-ferrous metals. The authors discovered that the wear rate of the diamond tool is not constant when the cutting temperature is constant. Cutter wear rate increases gradually with increased temperature until cutter burnout occurs at a critical temperature. They also established an analytical mathematical model for diamond wear, which correlated reasonably well with the experimental results.

Paul *et al.* [69] studied the chemical aspects of diamond tool wear and proposed a chemical theory of diamond tool wear. They state that some wear is always observed with the diamond cutting of any material. This is because the higher temperatures induced by extended rubbing of hard objects provide enough kinetic energy to break carbon-carbon bonds on the surface of the tool. They also state that there is a lack of experimental data on diamond tool wear in the literature, and that such data could help in providing insight into comparative wear mechanisms for different processes.

Other diamond tool wear studies, of less relevance, include the wear of an Atomic Force Microscopy (AFM) diamond tip sliding against silicon [70], and Aluminium-based Metal Matrix Composites machining with diamond coated tools [71].

1.6 Optimisation of manufacturing process

1.6.1 Introduction

Tool wear studies are regularly included in manufacturing process optimisation studies. For this reason some of the basic concepts regarding process optimisation are discussed in this section. During the optimisation of most machining and manufacturing operations, the objective functions are usually related to economic criteria. Previous attempts to determine the optimal machining parameters can be divided into three main categories [72]:

- Computer Aided Design (CAD) approaches.
- Operations Research (OR) approaches.
- Artificial Intelligence (AI) approaches.

These approaches could be based on an off-line adjustment system, or an on-line Adaptive Control (AC) system. On-line AC systems can divided into two categories:

- Adaptive Control Optimisation (ACO).
- Adaptive Control Constraint (ACC).

1.6.2 Literature Survey

The obvious optimisation problem for a turning operation will have feed and speed as variables, with the aim normally linked to economic criteria. Ermer [73] developed a geometric programming technique to optimise the control variables for minimum cost, subject to constraints such as available horsepower, surface finish and available feeds and speeds. This very early work, one of the first taking constraints into account, did not account for the tool wear constraints. Da, Sadler and Jawahir [74] presented a computer aided methodology for predicting optimum cutting conditions in process planning of turning operations. This also involved the effect of the progressive tool wear on the performance of the machine.

As Da *et al.* also state, most past research on machining optimisation made the assumption that all machining is done with fresh and unworn tools. However, in a 'real' machining process, machining performance vary due to tool wear. Empirical equations, based on earlier research, were used to describe the behaviour of the different variables as well as their dependence on one another. Non-linear programming techniques were used to determine the constrained optimum cutting conditions for a certain tool wear state.

Choudhury *et al.* [75] utilised an adapted version of the Taylor tool life equation (using force measurements as input) to predict the optimum cutting conditions in a turning process. This approached enabled them to predict the optimum conditions with the minimum amount of experiments, given a database of the various material properties. A computer program reads the current machining conditions, determines the tool life from the Taylor equation, and then supplies the optimum parameters using a pre-established optimisation model. Zhou and Wysk [76] proposed a methodology for probabilistic optimisation in batch production, also using the Taylor equation. Their approach included a tool status recording feature (not on-line) to determine a tool wear index. This index plays an important role in the choice of the optimal machining parameters for the next batch.

Yen and Wright [77] proposed an optimisation procedure for adaptive control in machining. A safe working space is determined by the constraints of three different modes of failure. Control variables such as speed and feed rate are optimised for maximum metal removal rate. The gradual development of flank wear was also taken into account to update the optimisation dynamically. An important contribution was the establishment of a model that links the tool failure constraints with the control and state variables. Obikawa *et al.* [78] proposed a tool wear monitoring system integrated with an optimisation system for cutting conditions. The tool wear is estimated by monitoring the AR coefficients representing the power spectrum of the cutting force, and feeding it into two neural networks. The machining parameters are optimised to ensure that a certain amount of components can be manufactured reliably before the end of the tool life is reached.

Jang and Seireg [79] proposed an optimisation procedure by which the machining parameters are optimised for specified surface conditions. Tool failure, tool wear, dimensional accuracy and chip formation are taken into account as constraints with a penalty function formulation. Maximum metal removal rate is achieved in conjunction with specified surface conditions.

1.6.3 Adaptive Control (AC)

Adaptive Control (AC) involves continuous changing in machining conditions by means of an on-line strategy, like the fuzzy-based AC system proposed by Tarng *et al.* [80]. Running an AC system based on one objective might cause an infraction on other constraints. This is why an AC system must be based on different control objectives, in order to optimise the process for the current machining conditions. Combining a range of sensors to interpret measured data can also extend the possibilities of an AC system. This is referred to as so-called intelligent manufacturing [81,82]. The following monitoring and control functions are considered to be significant for such systems [83]:

- Advanced process monitoring, to protect from fatal events, with respect to:
  - tool wear.
  - chipping.
  - tool breakage.
  - collisions.
  - vibrations.
  - motor currents.
- Adaptive Control Optimisation (ACO) with respect to:
  - maximum productivity.
  - maximum production rate.
  - mixed function of productivity and production rate.
- Adaptive Control Constraint (ACC) with respect to:
  - cutting-forces.
  - chatter vibrations.

ACO seek to adjust machining parameters in a direction that will optimise a predefined performance index. The aim of ACC systems is to adjust the machining parameters to their maximum possible values given the constraints of the process.

To implement all of these functions in a single monitoring system for a single machine might be a little ambitious, but simplified versions can be developed, involving only a few variables, such as:

- Advanced process monitoring in accordance with a long term plan.
- ACC of feedrate with respect to cutting-forces.
- ACO of feedrate with respect to maximum productivity.
- In a more sophisticated system, variables such as depth of cut and cutting speed will also be involved.

1.6.4 Approaches for Optimising a Machining Process

The conventional methods for selecting CNC machining conditions, are based on textbooks or the knowledge and experience of the programmer. In most instances, the parameters are selected in a conservative manner, in order to prevent failures such as tool breakage. As a result, the Metal Removal Rate (MRR) is low [72]. An optimisation strategy may consist of one or more of the following approaches:

A. Computer Aided Design (CAD) approaches

This off-line approach use process, tool wear and cutting force models based on prior knowledge gathered from experiments. Based on these models, a computer simulation, using the Numerical Control (NC) code, can estimate the cutting force and tool wear. With these results, the MRR can be optimised without violating the machining constraints. The advantage of this approach is that it is easy to implement and effective for most applications. A disadvantage is the fact that the approach can only be used off-line. CAD approaches can be divided into three sub-categories, namely:

- Machining Process Models.
- Computer Machining Simulation.
- Machining Parameter Optimisation.

B. Operations Research (OR) approaches

The objective of Operations Research (OR) approaches is to minimise global machining cost by considering multiple criteria related to machining, like the policy developed by Jeang [84] and Akturk *et al.* [85]. These methods are used for off-line adjustment due to their computational difficulty. An advantage is the establishment of a reference model that can adjust to changes in the machining parameters. Gopalakrishnan and Al-Khayyal [86] demonstrated a machine parameter selection scheme based on geometric programming for turning, which is a typical OR approach.

C. Artificial Intelligence (AI) approaches

Artificial Intelligence (AI) based methods can be used to optimise a CNC machining process. AI methods can be either ACO or ACC based, or may even be an off-line system. However, an on-line AC system is preferred with AI approaches. AI based methods attempt to automatically optimise machining parameters based on sensor information. Reaction of the control system due to changes in process must be carried out within milliseconds to ensure the reliability of the process. There have been a number of studies on the application of AI techniques in on-line control [87,89]. These can be divided into three categories:

- Neural Networks
- Knowledge-Based Expert Systems (KBES) [90]
- Probabilistic Inference

1.7 Summary of literature

Many concepts from the literature were mentioned in this chapter. One of the main motivations for research is to make a contribution to the literature of the international research community. In order to identify aspects regarding the contribution of this study, table 1.1 was constructed. In this table reference to recent tool wear monitoring studies are made, showing all the relevant information regarding these studies. This information includes the type of tools, material, machining process, signal processing and wear classification methods used. This table is a summary of all the important concepts mentioned in this chapter, and show how previous authors have combined different monitoring methods with different classification strategies. The table is arranged from the oldest to the most recent date of publication.

Table 1.1

Summary of recent and relevant TCM literature

Year	Author(s)	Process	Tool	Material	Monitor	Feature	Classification scheme	Ref.
1986	Rao	Turning	Tungsten carbide	Steel	Vibration Dynamic force	FFT peaks	Trend / threshold	11
1987	Jiang, Zhang, Xu	Turning	Carbide insert	Steel	Vibration	PSD	Trend / threshold	22
1993	Ruiz, Guinea, Barrios	Turning	High-speed steel	Steel	Tempera-ture Force AE	FFT Frequency band energy Standard deviation Skewness Kurtosis min, max, max-min	Quality space' identification methods Distance based classifiers Neural networks Informational entropy considerations	14
1993	Ravindra *et al.*	Turning	Coated carbide	Cast iron	Dynamic force Surface finish Vibration	Force components Surface roughness parameters	Multiple regression (mathematical model) Multiple correlation F statistic Standard error Maximum error	16
1993	Barrios *et al.*	Milling	Carbide insert	Steel	Current Vibration AE	rms Mean Kurtosis	Analysis of variance (ANOVA) Empirical model	18
1994	Bonifacio, Diniz	Finish Turning	Coated carbide	Steel	Vibration	Surface roughness parameters rms	Trend / threshold	9
1995	Zhou, Hong, Rahman	Turning	Carbide inserts	Steel	Dynamic force	Wavelet analysis	Backpropagation neural network (BPNN)	42
1996	Das *et al.*	Turning	Uncoated carbide	Low C-steel	Dynamic force	Force components in three directions	Regression analysis Three layer backpropagation neural network	47
1996	Hong, Rahman, Zhou	Turning	Carbide inserts	Steel	Dynamic force	Wavelet analysis	Backpropagation neural network (BPNN)	95
1996	Das *et al.*	Turning	Uncoated carbide inserts	Low C-steel	Dynamic force	Force components in three directions	Backpropagation neural network (BPNN)	43
1996	Dimla, Lister, Leighton	Turning			Dynamic force Vibration	FFT	Single layer perceptron neural network	39
1996	Li, Elbestawi	Turning	Carbide inserts	Steel	Dynamic force Vibration	Mean Variance rms FFT Frequency band energy	Principal component fuzzy neural network	57
1996	Wu, Du	Turning (chatter) Drilling (wear)	Uncoated carbide Uncoated carbide twist	Steel Cast iron	Vibration	Wavelet analysis with Cross-correlation, Cross-coherence, Correlation coefficient and Power spectrum	Threshold	97
1996	Novak, Wiklund	Turning			Dynamic force Vision system	Force components ratios	Regression models ARIMA models Correlation coefficient	35

table 1.1 continued…

1996	Obikawa *et al.*	Turning	Carbide insert	Steel	Dynamic force	FFT AR coefficients	Neural network	78
1996	Coker, Shin	Milling	Carbide inserts	Aluminium Cast iron	Ultrasonic system	Surface roughness parameters	Analysis of variance (ANOVA) Regession analysis	12
1996	El-Wardany *et al.*	Drilling	High-speed steel-twist	Cast iron	Vibration	Kurtosis Cepstrum analysis Ratio of absolute mean values PSD	Threshold	20
1997	Luetzig *et al.*	End-milling			Simulated data		Kohonen feature maps (SOMs) Radial basis function network (RBFN) Recurrent neural network (RNN)	44
1997	Xiaoli *et al.*	Drilling	High-speed steel-twist	Steel alloy	Vibration	FFT Mean in frequency band	Fuzzy neural network (FNN)	55
1997	Xiaoli *et al.*	Drilling	High-speed steel		AE	Wavelet analysis	Fuzzy neural network (FNN)	96
1997	Dimla, Lister, Leighton	Turning			Static force Dynamic force Vibration	Mean FFT Frequency band energy	Multi-layer perceptron (MLP) neural network	41
1997	Fu, Hope, Javed	Milling		Mild steel	AE Vibration Dynamic force Spindle current	FFT Frequency band energy rms	Fuzzy pattern recognition algorithm	56
1997	Venkatesh *et al.*				Process parameters Force		Artificial neural network (ANN)	40
1997	Chen, Black	End-milling	High-speed steel	Aluminium	Dynamic force	Force components variation	Fuzzy neural network	54
1997	Lou, Lin	Milling	Carbide inserts	Cast iron	AE Dynamic force	rms Mean	Neural network (multilayer backpropagation with Kalman filter)	53
1997	Li, Wong, Nee	Turning	Cubic boron nitride inserts	Inconel	Vibration	Coherence	Threshold	21
1997	Wilkinson *et al.*	Face milling	Various inserts	Steel Stainless steel Aluminium alloy	Surface finish (optical probe)	Spatial frequency domain Analysis of surface roughness Surface roughness parameters	Trend / threshold	61
1997	Abu-Zahra, Nayfeh	Turning	Various carbide inserts	Steel	Ultrasonic sensing	Absolute value of wave form	Trend / threshold	32
1997	Tansel *et al.*	End-milling	High-speed steel	Steel	AE Force	Average values	Trend / threshold	31
1997	Wilson, Marinescu	Turning	Poly-crystalline diamond cutters	Granite	Surface roughness Tempera-ture	Off-line roughness measurement	Analytical model	68
1997	Da, Sadler, Jawahir	Turning	Carbide insert	Steel	Surface roughness Force	Surface roughness parameters Force components ratios New wear index Chip breakability index	Least square model	74
1997	Kurada, Bradley	Turning	Uncoated carbide inserts	Steel	Vision system	Vision parameters	Trend / threshold	34
1997	Wong *et al.*	Turning	Carbide inserts	Steel	Laser system	Surface roughness parameters Laser scatter parameters	Trend / threshold	36
1997	Chou, Evans	Hard turning	Cubic boron nitride inserts	Steel	Surface roughness	Off-line roughness and wear measurement		63
1997	Karthik *et al.*		Carbide inserts		Vision system Stereo imaging	Vision parameters	Trend / threshold	37

table 1.1 continued...

1998	Tsamas, Szecsi	Turning	Carbide inserts	Steel Cast iron Aluminium	Force (inductive trans-ducer)	Force components	Regression models Backpropagation neural network (BPNN)	17
1998	Quan, Zhou, Luo	Turning End-milling	Carbide inserts High-speed steel cutters	Steel	AE Power (Hall-effect sensor)	FFT Frequency band energy	Correlation coefficient Backpropagation neural network (BPNN)	45
1998	Grabec *et al.*	Turning		Steel	Dynamic force AE	FFT	Empirical modeling Class scatter criterion	13
1998	Silva, Reuben, Baker, Wilcox	Turning	Coated carbide inserts	Mild steel	Vibration Sound Strain gauge Current	Absolute deviation Average value Kurtosis Skewness FFT Frequency band energy	Adaptive resonance theory (ART2) neural network Self-organising map (SOM) Taylor tool-life equation	6
1998	Lee, Kim, Lee	Turning	Carbide insert	Steel	Force	Force components ratios Mean Signal to noise ratio	Multilayer perceptron neural network Analysis of variance (ANOVA) ARX model	48
1998	Jemielniak	Turning		Steel	AE	Skewness Kurtosis rms Standard deviation	Threshold	27
1998	Liu, Chen, Anantharaman	Drilling	High-speed steel twist	Stainless steel	Dynamic force	Average thrust / torque Peak thrust / torque rms thrust / torque Integral of thrust / torque vs time	Backpropagation neural network (BPNN)	50
1998	Caiazzo *et al.*	Turning	Carbide insert	Steel	Capacitive sensor	Surface roughness parameters	Trend / threshold	33
1999	Braun, Miller, Schultze	Turning	Carbide insert	Steel Aluminium	Vibration Dynamic force	FRF	Analytical model and verification of model by force measurements	15
1999	Choudhury, Kumar, Ghosh	Turning	High-speed steel	Steel	Dynamic force	Maximum force components	Mathematical model	75
1999	Kuo, Cohen	Turning	Carbide inserts	Steel alloys	Dynamic force Vibration AE	MA parameters ARMA parameters FFT peaks	Radial basis function network (RBFN) Artificial neural network (ANN) Fuzzy modeling Self-organising algorithm	58
1999	Choudhury, Jain, Rao	Turning	High-speed steel	Steel	Photo-electronic sensor	Change in workpiece diameter Surface roughness parameters	Backpropagation neural network (BPNN)	46
1999	Choi, Kim	Ultra-precision turning	Single crystal diamond	Aluminium	Dynamic force Vibration	FFT Frequency band energy	Trend / threshold	66

Table 1.1 is of prime importance because it highlights all the recent research activity in the field of TCM. It also shows how this study fits into the global concept of TCM and where this study has made contributions to the literature. These contributions will be discussed in Chapter 5.

1.8 Scope of the present work

It is apparent from the discussions in this chapter that the literature on TCM systems consist of many concepts that can be combined in numerous ways. These concepts and methods were highlighted in table 1.1. Some of the methods were developed a number of years ago, and have since been implemented in industry. Other methods are fairly new, and still in the development stage. The aim of the present work is to combine some of the successful methods previously proposed for TCM, and to contribute to the literature where possible.

The need for more flexible monitoring systems is evident from all the different approaches proposed by previous authors. It would seem that each manufacturing process requires a very specific monitoring scheme. The aim of the combination of previously developed methods is to design a flexible monitoring system that can adapt to different manufacturing conditions or processes. This monitoring system must be fully automated, requiring only a little human interaction.

The system must have the ability to automatically select the best features for a certain process, depending on the monitoring objective. These features must then be used in an automated classification scheme to interpret the status of the manufacturing process. This classification scheme must be able to train itself, and update its training during manufacturing.

Many neural networks have been developed and tested for TCM up to date, but very few of them implements unsupervised learning that can be automated without human interaction. For this reason, a self-organising neural network, based on unsupervised learning, will be investigated and tested in this study. The testing of the system will commence in a manufacturing plant, with the various random disturbances which is synonymous with a real manufacturing environment. The purpose of implementing the system in a manufacturing environment, is to design a robust and flexible monitoring system which will be valuable to the industry.

Another aim of this study is to investigate a unique type of tool that is used for the manufacture of automotive parts, namely the synthetic diamond tool. Diamond tools were discussed in detail in section 1.5. Very little literature exits on the implementation of monitoring strategies with diamond tools. It is within the scope of this work to investigate the wear modes of these tools, and to investigate the feasibility of the implementation of an automated monitoring strategy for diamond tools.

Again referring to table 1.1, a comparison between previous studies and the scope of this study can be made. Table 1.2 summarise the scope of investigation for this study, from which it can be concluded that this work aims to combine some of the previous methods, and to contribute in terms of the facts mentioned in this section.

Table 1.2

Scope of the present work

Process	***Tool***	***Material***	***Monitor***	***Feature***	***Classification scheme***
Turning	Synthetic diamond Coated carbide	Aluminium Steel	Vibration Dynamic force Surface roughness	FFT Frequency band energy Rms Mean Kurtosis Crest factor Variance Standard deviation Skewness AR coefficients MA coefficients ARMA coefficients Coherence function Surface roughness parameters Wavelet analysis	Self-Organising Map (SOM) Pattern recognition algorithm (investigate)

CHAPTER 2

SIGNAL PROCESSING AND WEAR CLASSIFICATION STRATEGIES

2.1 Introduction

In order to understand the principles of the monitoring strategies proposed in this study, it is necessary to discuss some of the mathematical details regarding the feature extraction and the wear classification strategy. The study focused on features extracted from the time and frequency domains, time series model features, and features extracted from wavelet packet analysis. Furthermore a self-organising neural network were used for decision-making regarding the amount of tool wear. The basic mathematical principles behind each of these aspects in the monitoring strategy are discussed in this chapter.

2.2 Time, model based and frequency domain features

2.2.1 Time domain features

The time domain features are extracted directly from the calibrated time domain signals as recorded by the sensors and analyser. All of these features can be calculated very easily and fast, and can therefore also be used in an on-line monitoring system. The time domain features were: mean, rms, crest factor, variance, skewness, and kurtosis. The choice fell on these features due to information gained from experimentation and the literature. A brief discussion on the chosen features follows [91]:

A. Mean

The mean value of a function $x(t)$ over an interval T is

$$\bar{x} = \frac{\int_0^T x(t)dt}{T} \tag{2.1}$$

B. Root mean square (rms)

The rms value of a function $x(t)$ over an interval of T is

$$X_{rms} = \sqrt{\frac{\int_0^T x(t)^2 dt}{T}} \tag{2.2}$$

C. Crest factor

The crest factor is the ratio of the peak level to the rms level

$$CF = \frac{X_{max}}{X_{rms}} \tag{2.3}$$

D. Variance

The variance is the mean square deviation about the mean

$$\sigma^2 = \frac{1}{T}\int_0^T [x(t) - \bar{x}]^2 dt \tag{2.4}$$

E. Skewness

The skewness is the third statistical moment of a distribution

$$S = \frac{1}{\sigma^3 T}\int_0^T x^3 dt \tag{2.5}$$

F. Kurtosis

The kurtosis is the fourth statistical moment of a distribution

$$K = \frac{1}{\sigma^4 T}\int_0^T x^4 dt \tag{2.6}$$

2.2.2 Time series model based features

Time series models can also be used to monitor a process, where the model coefficients are used as features. The model coefficients represent the characteristic behaviour of the signal. Depending on the order of the model, a number of model coefficients can be chosen. Normally only the first model coefficient, or sometimes the first three to four model coefficients are chosen, because they are most descriptive of the signal [28,58,78]. Higher coefficients can actually become descriptive of noise within the signal, and therefore they are not preferred as wear monitoring features.

For the purpose of this study, the first coefficients from the Auto Regressive (AR) model, Moving Average (MA) model, and the Auto Regressive Moving Average (ARMA) model, were used as features for tool wear estimation. The models are calculated directly from the calibrated time signals recorded by the sensors and analyser. A brief discussion of each of the models follows [92-94]:

A. AR model

In a p-th order AR model for a time series $x(n)$, where n is the discrete time index, the current value of the measurement is expressed as a linear combination of p previous values:

$$x(n) = a_1 x(n-1) + a_2 x(n-2) + \ldots + a_p x(n-p) \tag{2.7}$$

where $a_1, a_2 \ldots a_p$ are the AR coefficients. The first AR coefficient was chosen as a feature.

B. MA model

In a q-th order MA model, the current measurement is expressed as a linear combination of q previous values from a sequence of independent identically distributed (i.d.d.) random variables with a certain probability density function.

$$x(n) = b_1 u(n-1) + b_2 u(n-2) + \ldots + b_q u(n-q) \tag{2.8}$$

where $b_1, b_2 \ldots b_q$ are the MA coefficients and $u(n)$ is assumed to be an i.d.d. sequence. The first MA coefficient was chosen as a feature.

C. ARMA model

The ARMA model is a combination of the above two models:

$$x(n) = -\sum_{k=1}^{p} a_k (x(n-k)) + \sum_{k=1}^{q} b_k (u(n-k)) \tag{2.9}$$

The first two coefficients from this model were chosen as features.

2.2.3 Frequency domain features

The spectral energy in a certain frequency band is one of the most effective features that can be used in a monitoring system. The spectral energy in the frequency band around the natural frequency of the tool and tool holder system is sensitive to tool wear due to the loss of material at the tool tip. This loss of material can have two influences on the chosen frequency band energy:

- The first is an increase of energy due to excessive vibration caused by the worn tool. The worn tool causes the machining process to change from smooth cutting to an irregular breakaway process, which causes the normal vibration amplitudes to increase. This is especially true for normal flank wear situations, which will cause the vibration amplitudes over a wide frequency range to increase.

- The second scenario is a decrease of spectral energy, caused by the fact that the natural frequency of the tool and tool holder system shifts. This is caused by failure modes such as crater wear, where the cutting process remains smooth and within tolerance, but the wear causes a change in the dynamic characteristics of the tool and tool holder system. The natural frequency shifts a little and the spectral energy in the chosen band decreases.

The calculation of the frequency band energy is based on the Power Spectral Density (PSD) function, which is very common in vibration analysis. The energy in the frequency band can be expressed as [22]:

$$\psi_{xb}^{2} = \int_{fl}^{fh} S_{x}(f)df \tag{2.10}$$

with $S_x(f)$ the one-sided PSD function and fl and fh chosen to reflect the energy in the regions of interest.

2.3 Wavelet analysis

2.3.1 Introduction

The wavelet transform is a relatively new method of signal processing that has been applied to many engineering studies with great success. Recent studies also proved that wavelet analysis could be utilised for monitoring of machining processes [95-97]. The success of the wavelet transform is generally attributed to the natural shape of the wavelet, which is more descriptive of most natural processes than the sine function used in Fourier analysis. Signals with sharp and sudden changes might be better analyzed with an irregular wavelet than with a smooth sinusoid.

Wavelet analysis is capable of revealing aspects of data that other signal analysis techniques miss, like trends, breakdown points, discontinuities in higher derivatives, and self-similarity [98]. In this study, wavelet packet analysis was used to generate features that may show consistent trends towards tool wear. In this section, the basic principles of wavelet analysis will be discussed, as well as the principle of wavelet packet analysis used in the study.

2.3.2 Wavelet analysis background

Fourier analysis breaks down a signal into constituent sinusoids of different frequencies, which transforms our view of the signal from the time to the frequency domain. The drawback of Fourier analysis is that the time information is lost, which may be important if the signal contains non-stationary characteristics. This drawback may be overcome by the Short-Time Fourier Transform (STFT), but is of limited precision and not very flexible. These methods are based on windowing the signal and analysing each short time window separately, from which the signal can be mapped onto a two-dimensional display of time and frequency [98].

To overcome the limitations of the STFT, wavelet analysis are based on a windowing technique with variable-sized regions. Wavelet analysis allows the use of long time intervals where more precise low frequency information is desirable and shorter regions for high frequency information. A wavelet is a sometimes irregular and asymmetric waveform of effectively limited duration that has an average value of zero. A variety of wavelets exist, and an analyst can choose the wavelet that suits his application best. A typical wavelet function, Daubechies (db) 10, named after one of greatest wavelet researchers, is shown in figure 2.1.

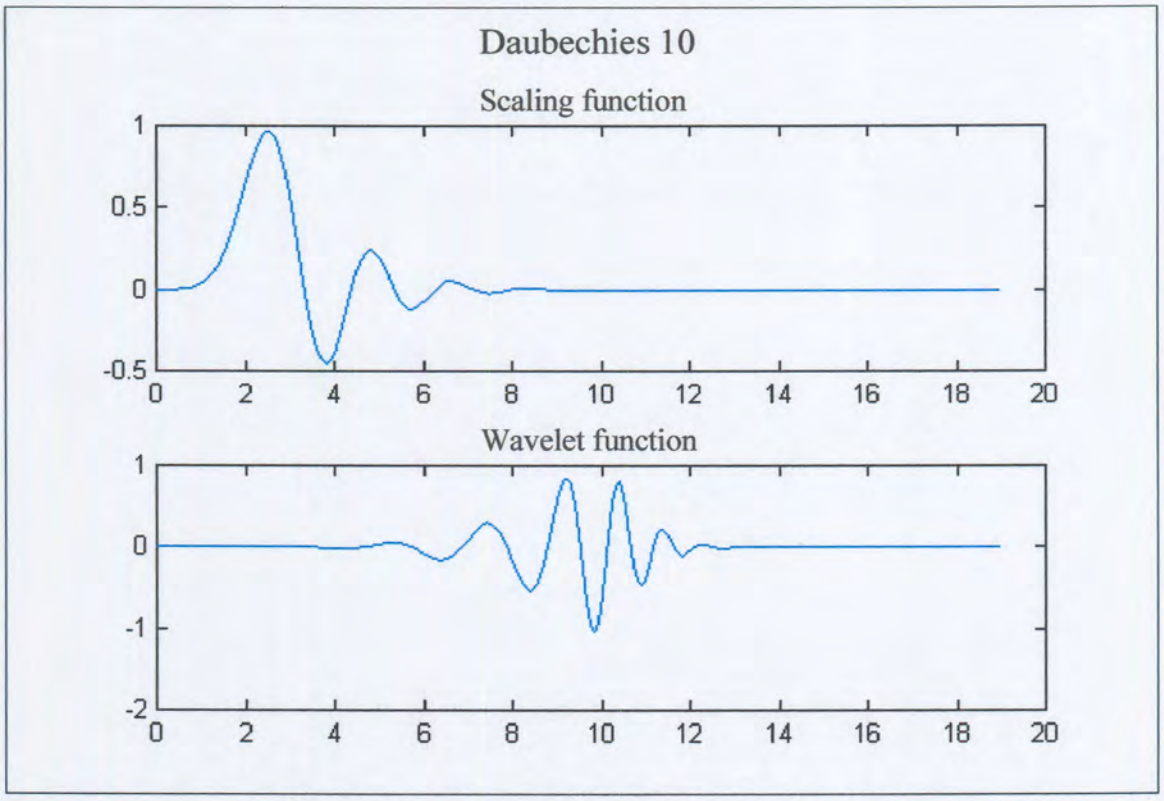

Figure 2.1: Typical wavelet function: db10

Similar to Fourier analysis, wavelet analysis is the breaking up of a signal into shifted and scaled versions of the original wavelet. The Continuous Wavelet Transform (CWT) is defined as the sum over all time of the signal multiplied by scaled and shifted versions of the wavelet function ψ [98]:

$$C(scale, position) = \int_{-\infty}^{\infty} f(t)\psi(scale, position, t)dt \qquad (2.11)$$

The result of the CWT is many wavelet coefficients C, which are functions of scale and position.

2.3.3 Scaling and shifting

Scaling a wavelet means stretching or compressing it, which is denoted by the scale factor a. The smaller the scale factor, the more "compressed" the wavelet, therefore the scale factor is related to the frequency of the signal. In wavelet analysis the low and high frequency contents of the signal are referred to as Approximations (A) and Details (D), respectively.

- Low scale / Compressed wavelet / High frequency / Details.
- High scale / Stretched wavelet / Low frequency / Approximations.

Shifting a wavelet simply means delaying or hastening its onset. For example, delaying wavelet function $\psi(t)$ by k will be represented by $\psi(t-k)$ [98].

2.3.4 The Discrete Wavelet Transform (DWT)

If the scales and positions are chosen based on powers of two, the analyses are much more efficient and just as accurate. This is called the Discrete Wavelet Transform (DWT). An efficient way to implement the DWT is by using filters. The filtering process is actually very complex, and will only be discussed in principle. At its most basic level, the filtering process can be illustrated as shown in figure 2.2 [98].

The original signal, S, pass through two complementary filters to separate the approximations and the details. This causes computation to end up with twice the amount of data points of the original signal. To correct this, the signals are downsampled, and the aliasing caused by the downsampling is accounted for later in the process. The whole process, including downsampling, produces the DWT coefficients as diagrammatically illustrated in figure 2.3 [98].

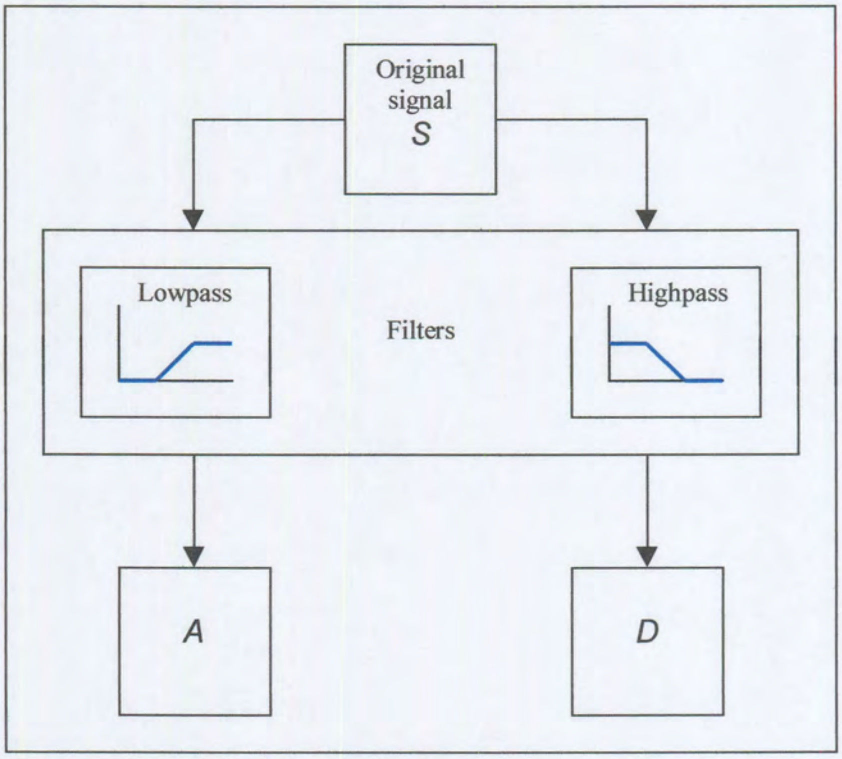

Figure 2.2: DWT at its most basic level, using filters

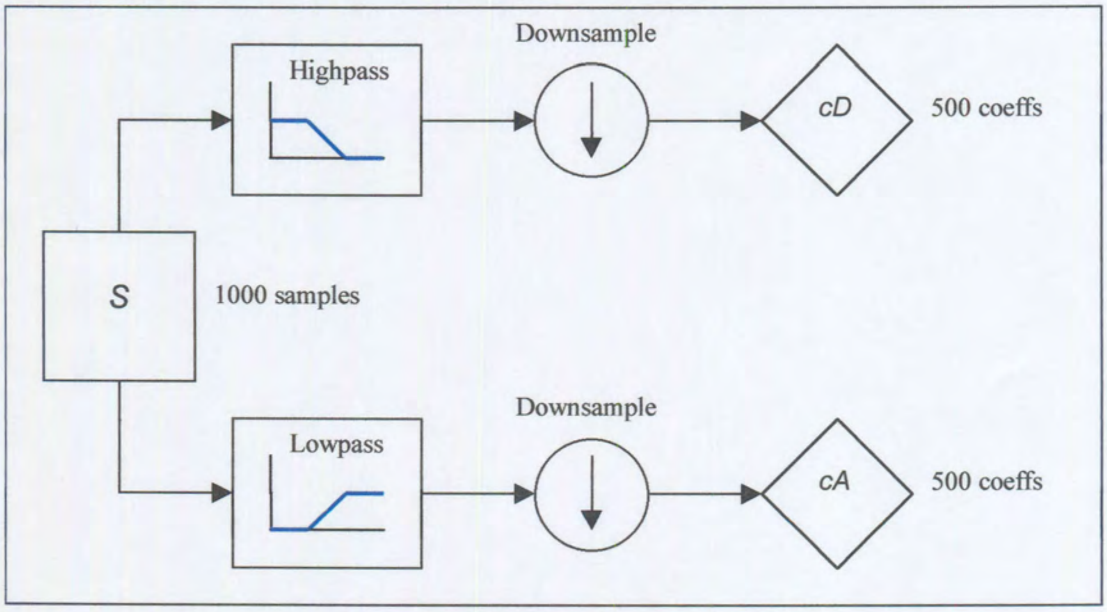

Figure 2.3: DWT with downsampling

2.3.5 Multiple-Level Decomposition and Reconstruction

The decomposition process can be iterated, with successive approximations being decomposed in turn, so that one signal is broken down into many lower-resolution components. This is called the wavelet decomposition tree, which in theory can be calculated to an infinite level, but in practice can only continue until the details consist of a single data point. In most cases, the optimal level of decomposition can be calculated based on an energy approach, such as entropy. The wavelet decomposition tree, as shown in figure 2.4, illustrates the multiple-level decomposition diagrammatically [98].

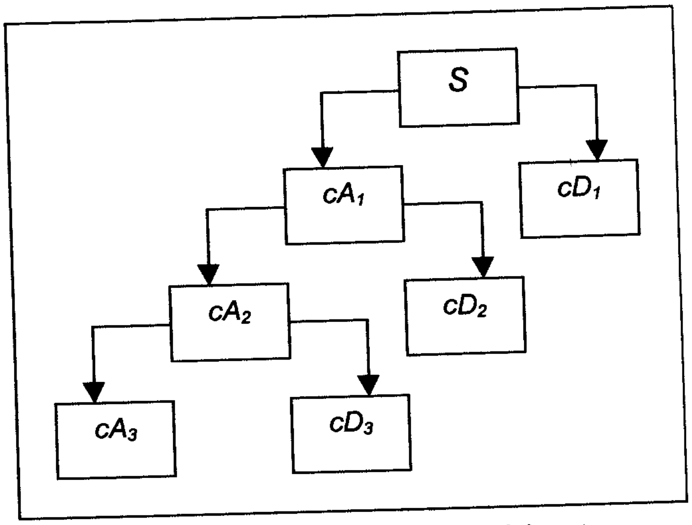

Figure 2.4: Wavelet decomposition tree

The wavelet decomposition tree can now be used to reconstruct the original signal, which is called the Inverse Discrete Wavelet Transform (IDWT). The IDWT process consists of upsampling and filtering. A specific choice of filters for IDWT will cause the effect of the previously mentioned aliasing to 'cancel out'. During the IDWT, the Approximations and Details are reconstructed with the wavelet coefficients, as illustrated in figure 2.5 [98].

The original signal can now be reconstructed with a number of combinations from the Approximations and Details on the decomposition tree, for example:

$$\begin{aligned} S &= A_1 + D_1 \\ &= A_2 + D_2 + D_1 \\ &= A_3 + D_3 + D_2 + D_1 \end{aligned} \tag{2.12}$$

The wavelet tree with reconstructed components is illustrated in figure 2.6 [98].

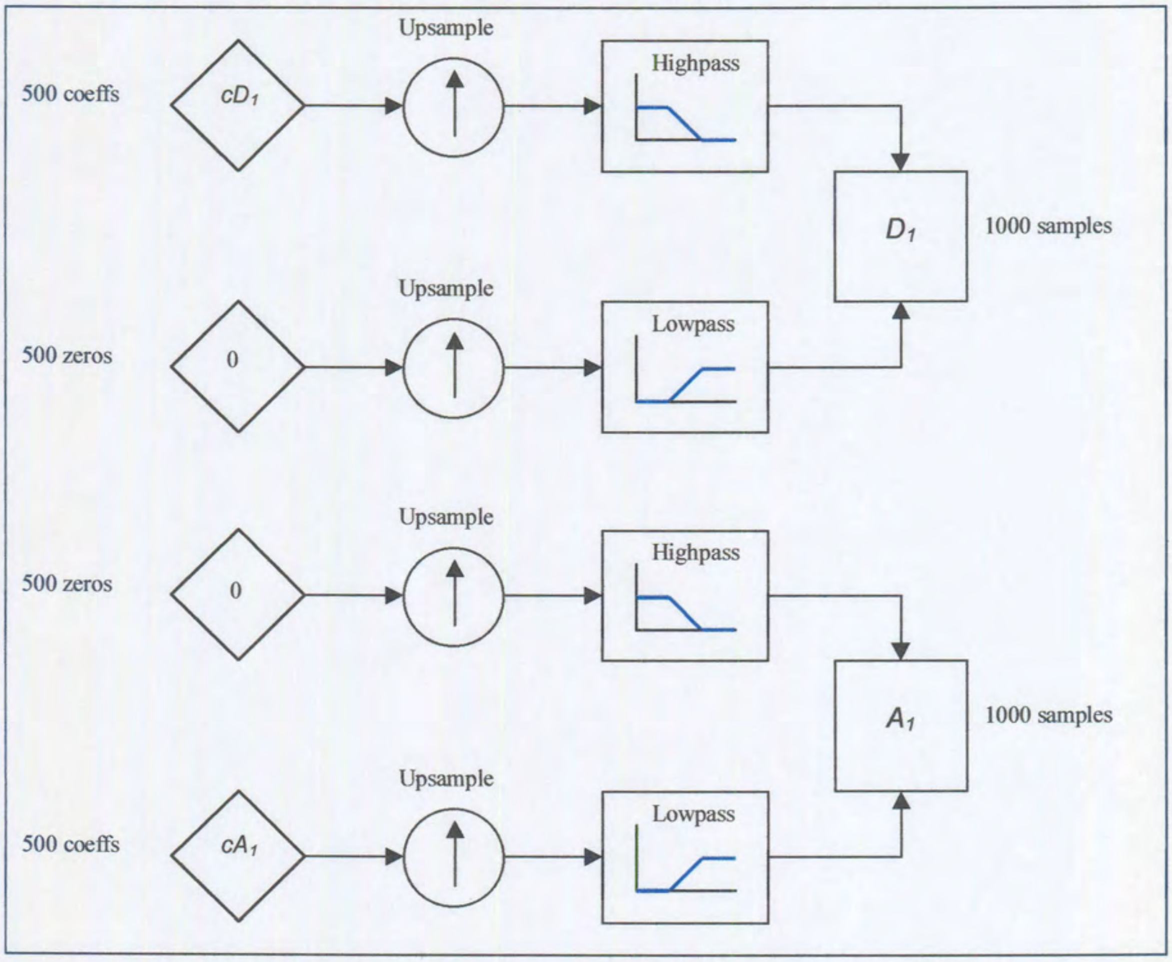

Figure 2.5: Reconstruction of Approximations and Details

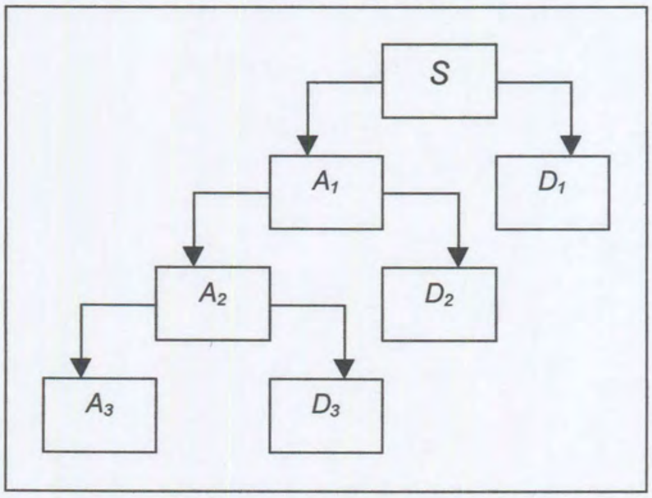

Figure 2.6: Wavelet tree with reconstructed Approximations and Details

2.3.6 Wavelet Packet Analysis

The wavelet packet method offers a wider range of possibilities for signal analysis. With normal wavelet analysis, only the approximations are split in every step. In wavelet packet analysis, the details as well as the approximations are split in every step, as illustrated in figure 2.7 [98]. The signal can be reconstructed using any number and combination of packets on the wavelet packet decomposition tree, for example:

$$S = A_1 + AAD_3 + DAD_3 + DD_2 \tag{2.13}$$

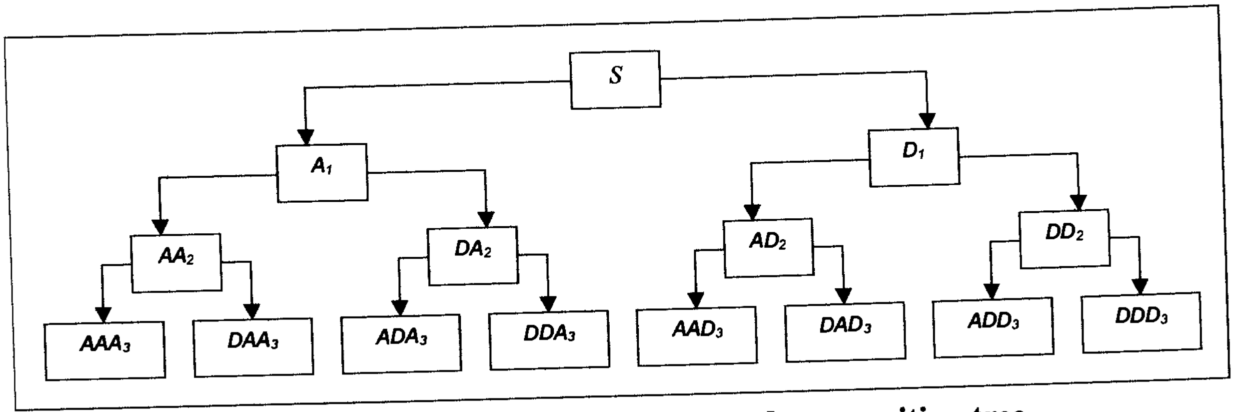

Figure 2.7: Third order wavelet packet decomposition tree

Choosing one out of all these possible encodings presents an interesting problem. An entropy-based criterion can be used to select the most suitable decomposition of a given signal. The entropy is an indication of the information gained by performing each split. A number of entropy types exist, like Shannon, Threshold, Norm, Log energy and SURE (Stein's Unbiased Risk Estimate). In this study, the Shannon entropy formula was used, which is a non-normalized entropy involving the logarithm of the squared value of each signal sample — or, more formally [98]:

$$E = -\sum_i s_i^2 \log(s_i^2) \tag{2.14}$$

The wavelet packets with the highest entropy contain the most information regarding the process. By neglecting the packets with low entropy values during signal reconstruction, the signal can be de-noised or compressed effectively. This is also the reason why the packets with high entropy values were chosen for feature extraction. This ensures that only the most significant information from the signal is extracted, and any changes in the signal due to tool wear can be identified with ease. The manner in which features were extracted from wavelet packet analysis will be discussed in a following chapter.

2.4 The Self-Organising Map (SOM)

2.4.1 Introduction

The Self-Organising Map (SOM), developed by Teuvo Kohonen [99], is a fairly new and effective software tool for data analysis. The SOM has been implemented successfully in numerous applications, in fields such as process analysis, machine perception, control and communication [6,100-103].

The SOM implements the orderly mapping of high-dimensional data onto a regular low-dimensional grid. Thereby the SOM is able to identify hidden relationships between high-dimensional data into simple geometric relationships that can be displayed on a simple figure [104]. The SOM can generally be described as a neural network with self-organising capabilities. Most neural networks require information and interaction from the user for classification. The training of the SOM is based on unsupervised learning, which means that the data is automatically arranged without human interaction. Although the SOM was originally intended as a data visualisation tool, it can be used for data classification as well. The SOM automatically arranges the data on a two dimensional grid of neurones where similar observations are placed close to one another and dissimilar ones further away. If the classes of some of the observations are known, certain regions on the grid could be allocated for these classes.

2.4.2 Computation of the SOM

A. Structure of the SOM

A SOM is formed of neurones located usually on a 2-dimensional grid. Higher dimensional grids can also be used, but their visualisation is very problematic. Each neurone i of the SOM is represented by an n-dimensional weight or reference vector $\boldsymbol{m}_i = [m_{i1}\ m_{i2}\ ...\ m_{i}]$, where n is equal to the dimension of the input vectors. The map shape is usually rectangular, but other shapes have also been used successfully. The number of neurones is set before the training phase commences. The number of neurones affects the accuracy and the generalisation capability of the SOM. As the size of the map increases, the training phase becomes very time consuming.

B. Neighbourhood relation

The neurones on the map are connected to adjacent neurones by a neighbourhood relationship. Immediate neighbours belong to the 1-neighbourhood N_{i1} of the neurone i. In the 2-dimensional case the neurones of the map can be arranged either on a rectangular or a hexagonal lattice. Neighbourhoods of different sizes in rectangular and hexagonal lattices are illustrated in figure 2.8 [105].

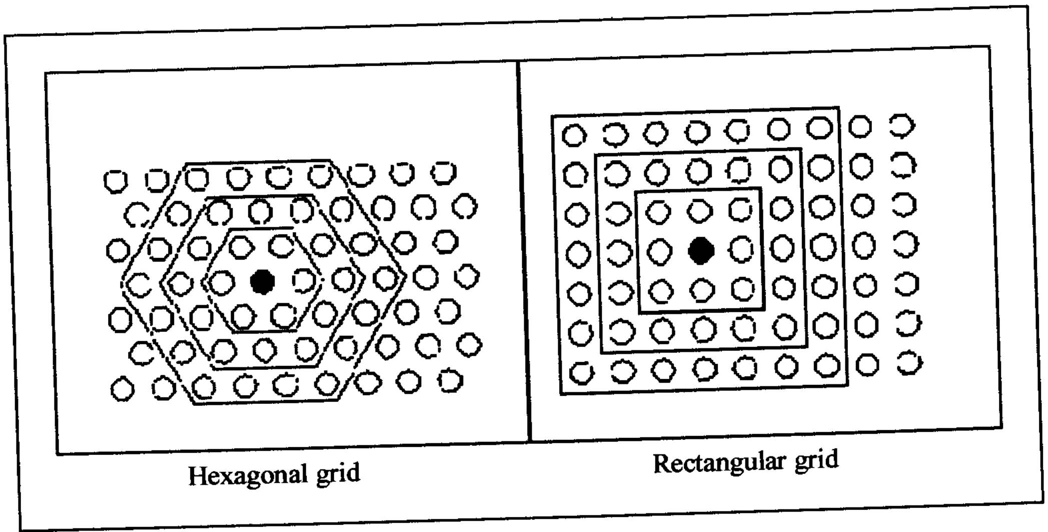

Figure 2.8: Neighbourhood structures

C. Initialisation

Before the training phase initial values are given to the weight vectors. The SOM is robust regarding the initialisation, but a proper initialisation allows the algorithm to converge faster to a reliable solution. Typically one of the three following initialisation procedures are used [105]:

- Random initialisation, whereby the initial values of the weight vectors are selected randomly.
- Sample initialisation, whereby the initial values of the weight vectors are selected based on samples from the training data.
- Linear initialisation, whereby the initial values of the weight vectors are generated linearly from the lowest to the highest value of the training data.

D. Training the SOM

The computation of the SOM is a nonparametric, recursive regression process. In each training step, one sample vector $\boldsymbol{x}$ from the input data set is chosen randomly and a similarity measure is calculated between it and all the weight vectors of the map. The Best-Matching Unit (BMU), denoted as c, is the unit whose weight vector has the greatest similarity with the input sample $\boldsymbol{x}_i$. The similarity is usually defined by means of a distance measure, typically Euclidian distance. Formally the BMU is defined as the neurone for which [99]:

$$\forall i,\quad \|\boldsymbol{x}(t)-\boldsymbol{m}_c(t)\| \le \|\boldsymbol{x}(t)-\boldsymbol{m}_i(t)\| \tag{2.15}$$

which means that $\boldsymbol{m}_c(t)$ is the model that matches best with $\boldsymbol{x}(t)$. This is the Best Matching Unit (BMU).

After finding the BMU, the weight vectors of the SOM are updated. The weight vectors of the BMU and its neighbours are moved closer to the input vector in the input space. This adaptation procedure stretches the BMU and its neighbours towards the sample vector. This is illustrated in figure 2.9, where the input vector given to the network is marked by an x [105]. The SOM update rule for the weight vector of the unit i is:

$$\boldsymbol{m}_i(t+1) = \boldsymbol{m}_i(t) + h_{c(x),i}\left(\boldsymbol{x}(t) - \boldsymbol{m}_i(t)\right) \tag{2.16}$$

where t is the index of the learning step, and learning is performed recursively for each presentation of a sample of $\boldsymbol{x}$, denoted $\boldsymbol{x}(t)$. The scalar multiplier $h_{c(x),i}$ is called the neighbourhood function, which causes similar observations to be placed in the same region on the map [99].

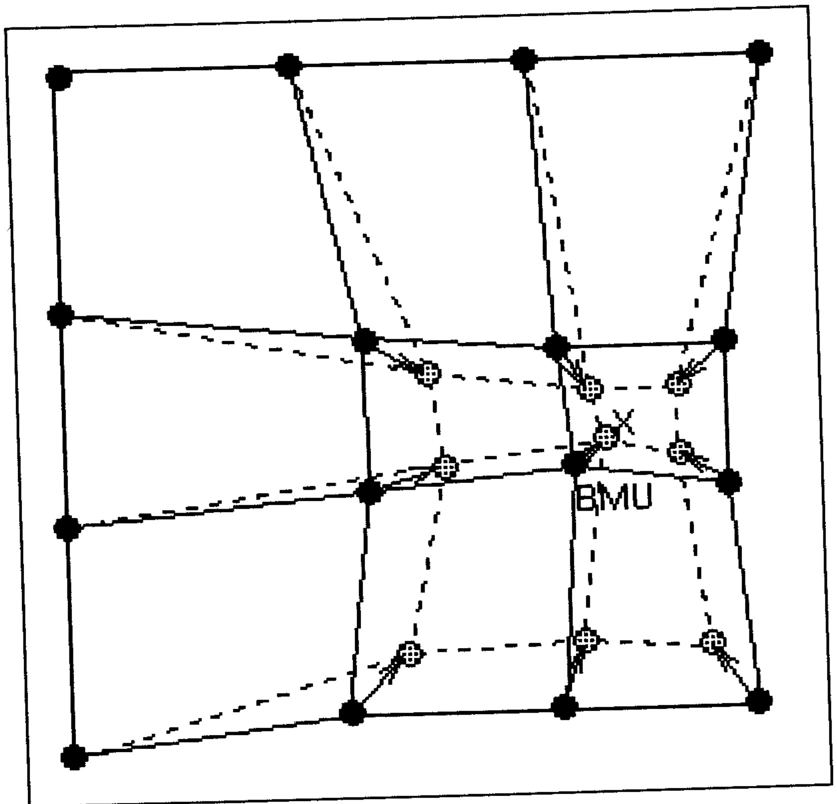

Figure 2.9: Updating the SOM in each learning step

E. Neighbourhood function

The neighbourhood function is a non-increasing function of time and of the distance of unit i from the winner unit c. It defines the region of influence that the input sample has on the SOM. The function is formed of two parts: the neighbourhood function $h(d,t)$ and the learning rate function $\alpha(t)$:

$$h_{ci}(t) = h\left(\|\boldsymbol{r}_c - \boldsymbol{r}_i\| ,t \right) \alpha(t) \tag{2.17}$$

where $\boldsymbol{r}_i$ is the location of unit i on the map grid.

The simplest neighbourhood function is the bubble: it is constant over the whole neighbourhood of the winner unit and zero elsewhere. Another is the Gaussian neighbourhood function. It gives slightly better results, but is computationally somewhat heavier. Usually the neighbourhood radius is bigger at first and is decreased linearly to one during the training. Figure 2.10 displays the two common neighbourhood functions [105].

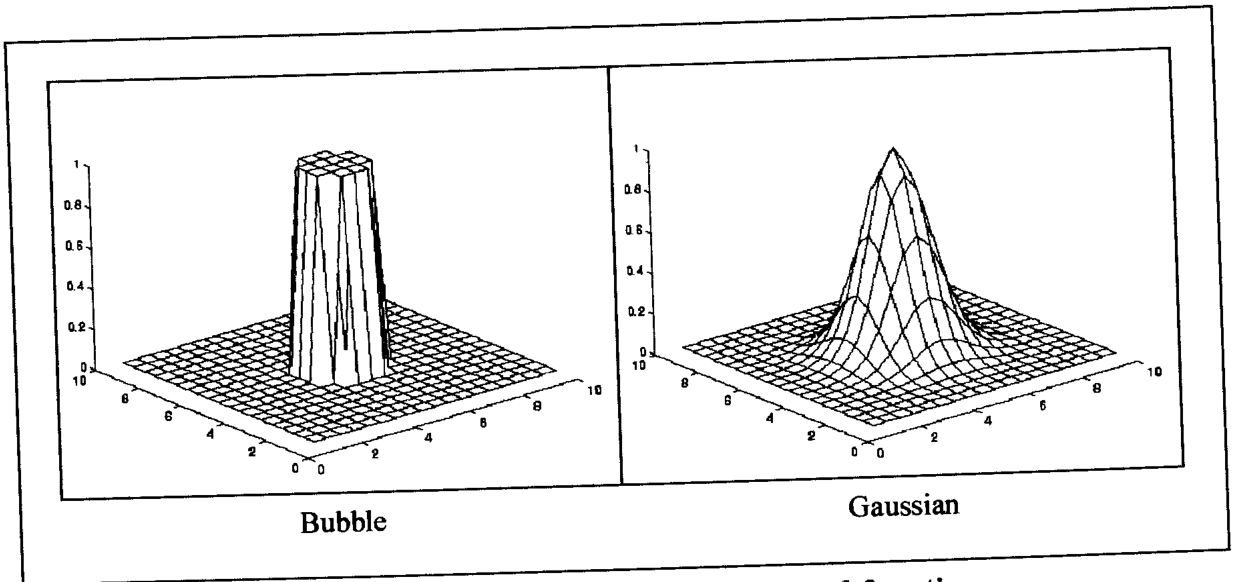

Figure 2.10: Two common neighbourhood functions

F. Learning rate

The learning rate $\alpha(t)$ is a decreasing function of time. Two commonly used forms are a linear function and a function inversely proportional to time, such as:

$$\alpha(t) = \frac{A}{(t+B)} \tag{2.18}$$

where A and B are some suitably selected constants. Use of this function type ensures that all input samples have approximately equal influence on the training result.

G. Training phases

The training is usually performed in two phases. In the first phase, relatively large initial α values and neighbourhood radii are used. In the second phase both the α values and the neighbourhood radii are small right from the beginning. This procedure corresponds to first tuning the SOM approximately to the same space as the input data and then fine-tuning the map. If the linear initialisation procedure is used, the first training phase can be skipped. There are several rules-of-thumb, found through experiments, for choosing suitable values.

H. Batch-algorithm

Another variant of the basic SOM is the batch algorithm. In it, the whole training set is gone through at once and only after this the map is updated with the net effect of all the samples. The algorithm converges usually after a couple of iterations, and is much faster to calculate in MATLAB than the normal sequential algorithm [105].

2.4.3 Examples of SOMs

The SOM is best explained with simple examples. Two examples are discussed here in order to clarify the use of SOMs in subsequent chapters. For more information on SOMs, see references [104] and [105].

A. Speech data

The SOM in figure 2.11 was calculated with speech data (Finnish) [105]. The model vectors are shown on each neurone. Note that similar patterns are arranged close to one another on the map. This technique can be used for voice or word recognition.

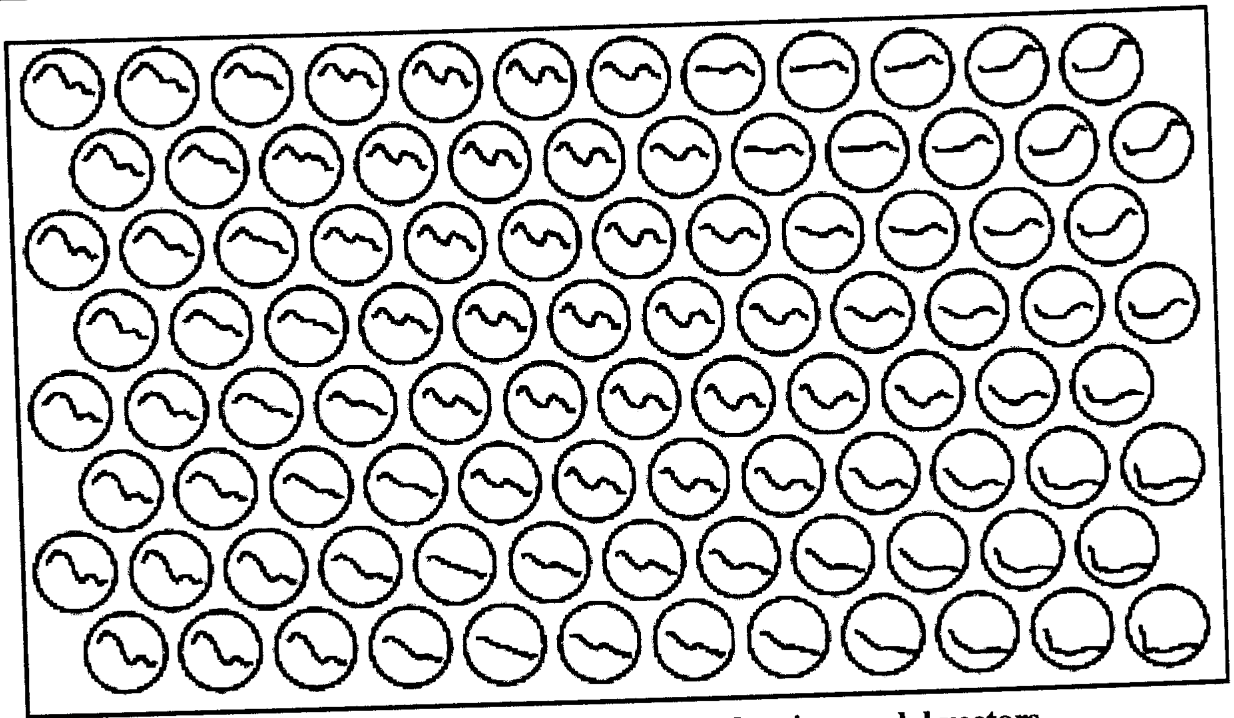

Figure 2.11: SOM with speech data showing model vectors

B. Simple 2-dimensional scenario

The principles of a SOM can easily be explained by considering a 2-dimensional case. Say, for instance, that a data set exists which clearly displays two clusters, as shown in figure 2.12. The one cluster may correspond to an error (*err*) situation, and the other to an acceptable (*OK*) region, for example:

$$\begin{aligned} W &= [x \;\; y] \\ W &= [0.3 \;\; 0.3] - err \\ W &= [0.7 \;\; 0.7] - OK \end{aligned} \tag{2.19}$$

Figure 2.13 shows the SOM after linear initialisation of the model vectors, on a rectangular grid.

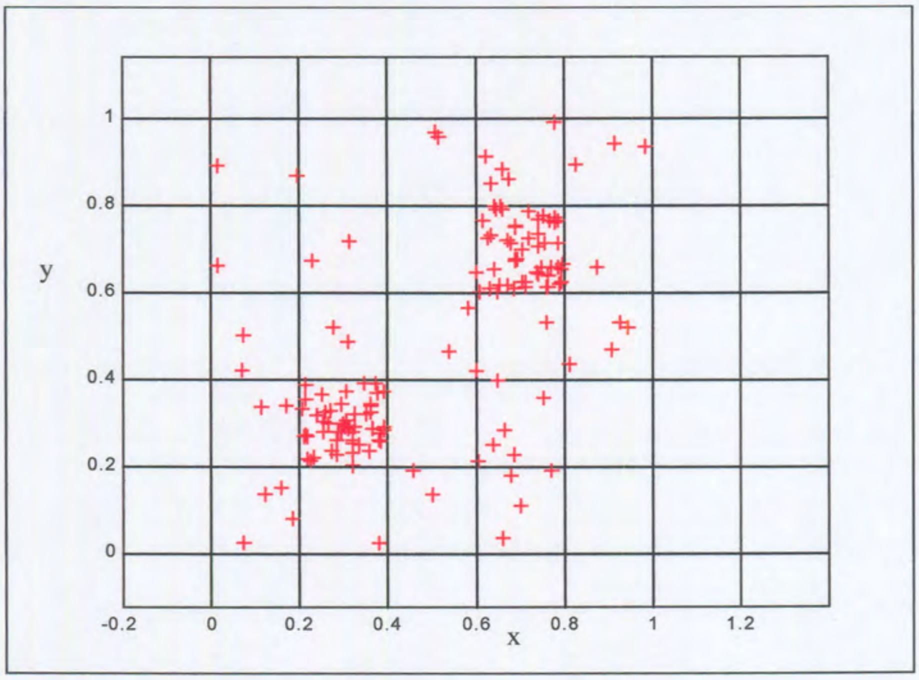

Figure 2.12: Data with two clusters

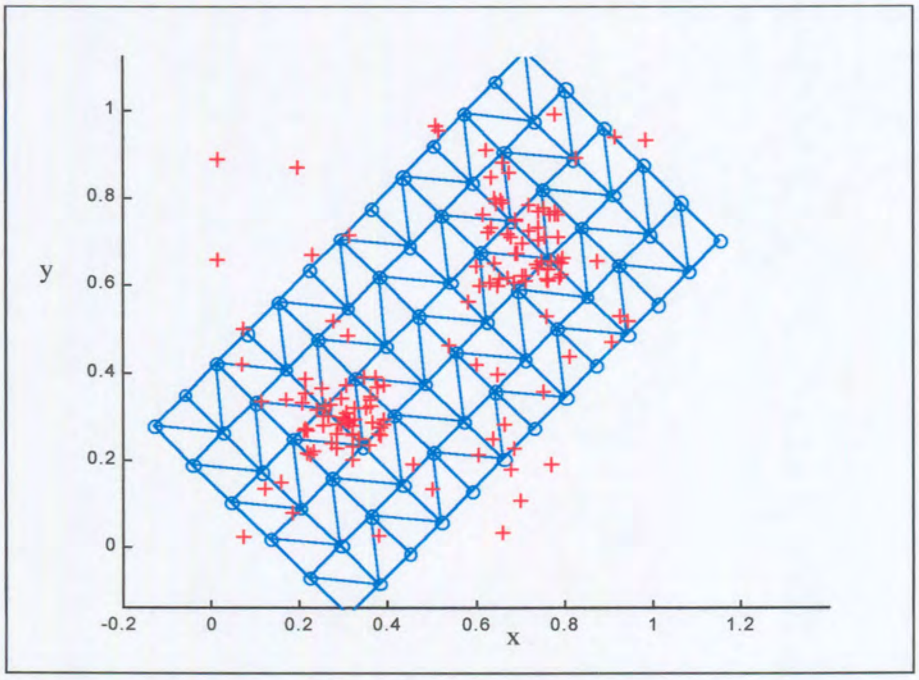

Figure 2.13: Grid with linear initialisation of model vectors

Figure 2.14 shows the SOM after training, which resembles a 'net' folding over the 'cloud' of data. The neurones move closer to one another where the data is dense.

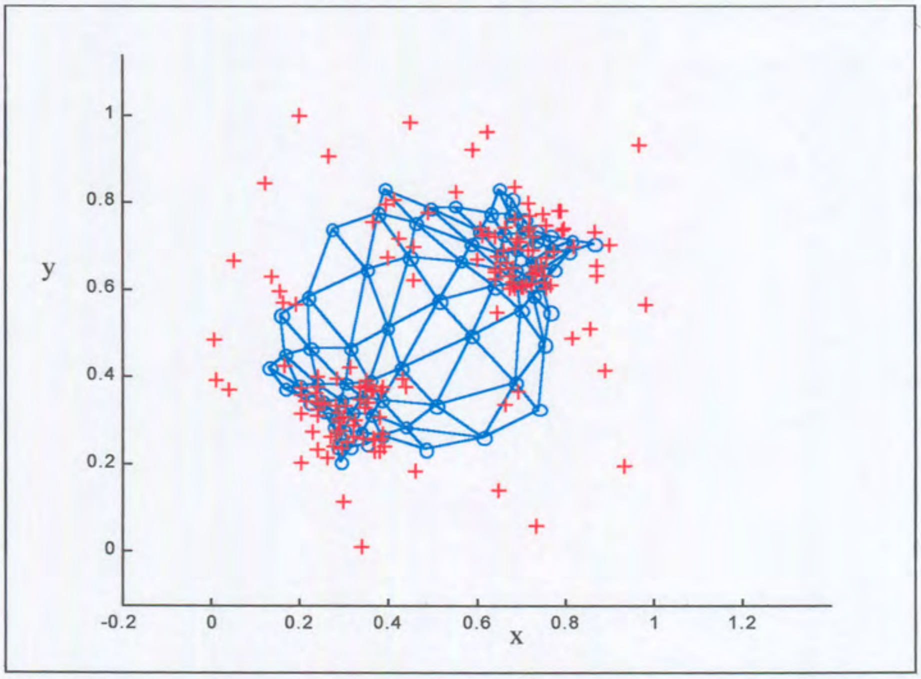

Figure 2.14: Grid after training

Figure 2.15 shows the SOM for variables x and y. Note that the SOM is only one entity, but a picture in the direction of each variable (dimension) can be shown. Also note that the colours of the neurones are an indication of the value of the variable, as shown on the colourmap axis on the figure. The labels of the training data are also shown in figure 2.15, and it is clear that the *'err'* and *'OK'* regions have been identified. Figure 2.16 shows the BMUs for a test data set:

$$
\begin{aligned}
W = [\ & 0.3\ \ 0.3 \quad (err) \\
& 0.5\ \ 0.5 \\
& 0.7\ \ 0.7] \quad (OK)
\end{aligned}
\tag{2.20}
$$

The three BMUs for this test data, have each been marked on figure 2.16. A trajectory, showing how the test data moves through the SOM, is also shown in figure 2.16.

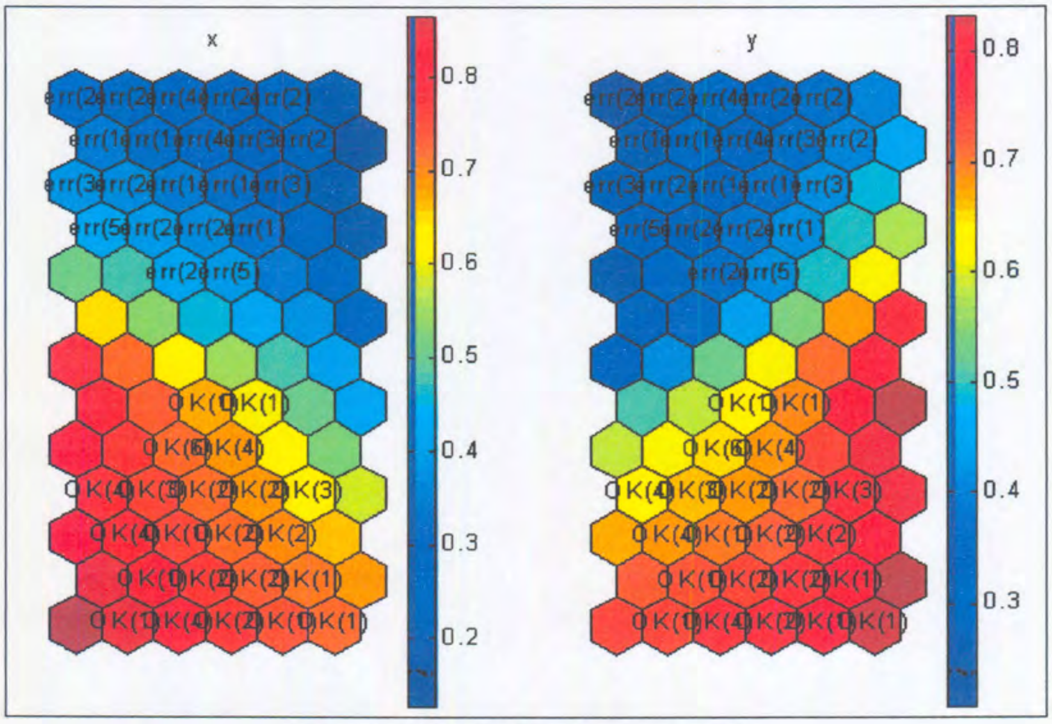

Figure 2.15: SOM with data labels

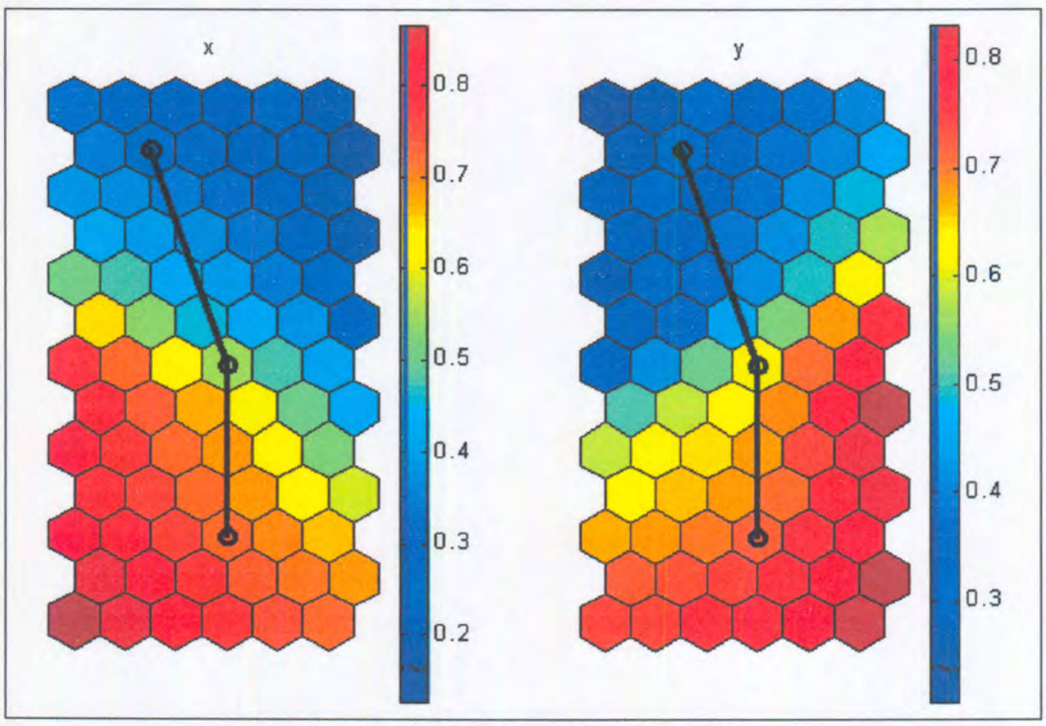

Figure 2.16: BMUs for test data

CHAPTER 3

WEAR MONITORING OF A COATED CARBIDE INSERT IN TURNING

3.1 Introduction

Before attempting to implement some of the monitoring strategies discussed in previous chapters in a manufacturing plant, experiments under controlled laboratory conditions were conducted. The reason for this is to determine if vibration monitoring is suitable for tool wear monitoring, and to solve some of the practical problems that may occur during experimentation. This may be considered as a first case study to prepare for further testing in a manufacturing plant.

3.2 Experimental conditions

Experiments were carried out on a 2-axis CNC, with a coated carbide tool insert. EN24 (BS970 817M40) steel rods with a 20 mm diameter were used as the workpiece material. Machining with 0.5 mm/rev feed at 840 rpm accelerated the tool wear. The machine vibration was measured with two 10 mV/g PCB accelerometers, coupled to amplifiers and a Diagnostic Instruments PL202 real time FFT analyser. The measured acceleration signals were then carried over to a PC for further processing in MATLAB. A bandwidth of 0-5 kHz was considered. To prevent aliasing, the signals were sampled at 12.8 kHz, with 4096 points per 0.32s time interval, or 1600 frequency lines spread over the 5 kHz bandwidth.

Care was taken to ensure the safety of the accelerometers against cutting fluid and chips breaking away from the workpiece. The chips are also very hot and their sharp edges can easily damage the thin sensor wires. A sensor can also be permanently damaged if any cutting fluid penetrates it. This is one of the main problems with vibration monitoring in a manufacturing environment – measurement close to the machining process is virtually impossible without sacrificing the safety of the equipment.

The recorded signals were examined in the frequency as well as the time domains. Three different states of tool wear were identified, using features extracted from the recorded signals. The experimental parameters are summarised in Table 3.1. Figure 3.1 shows a schematic of the experimental setup.

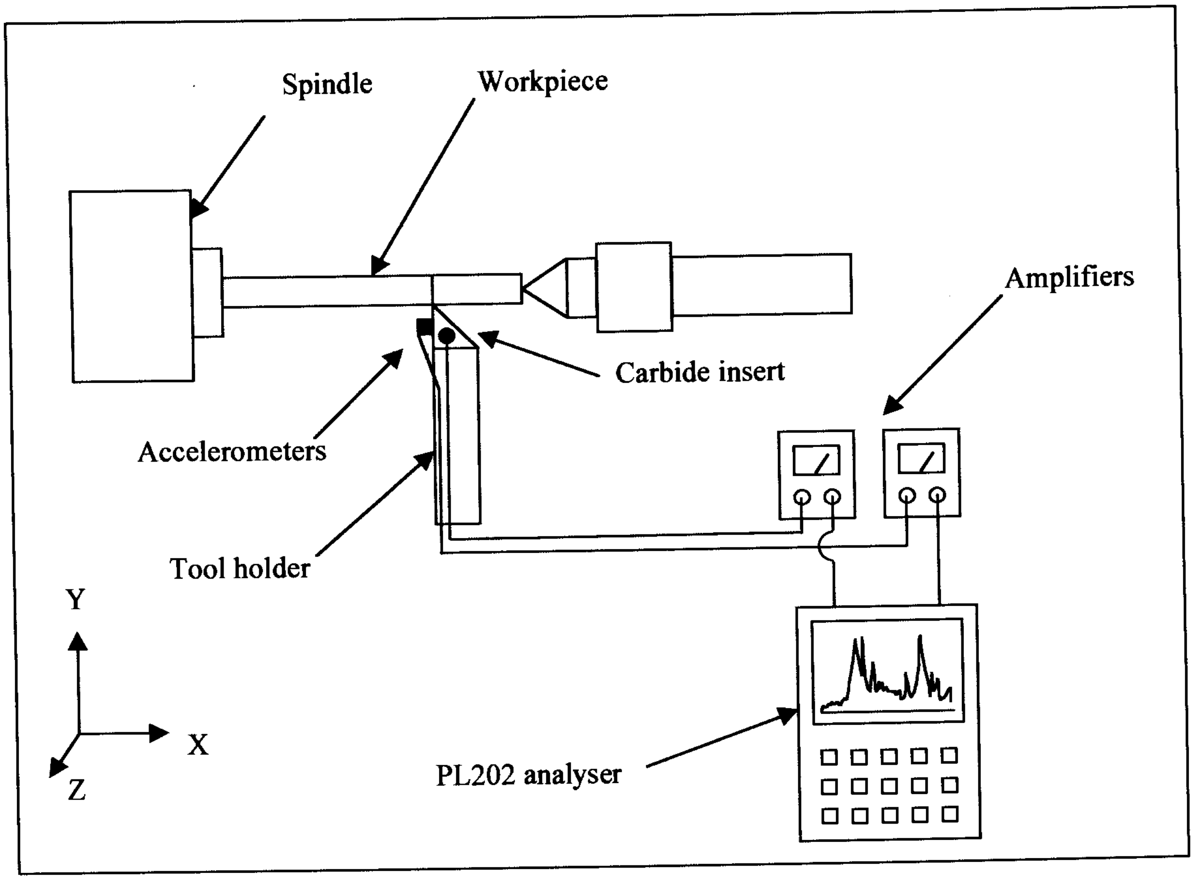

Figure 3.1: Schematic of experimental setup

Table 3.1
Experimental parameters

Lathe	Colchester CNC-2000L
Workpiece	EN24 (BS970 817M40) 20 mm diameter
Holder type	ISCNR model MTJNR-2020k-16W
Insert type	Coated Carbide, Seco model TNMG 160404-M5 P200
Feed rate	0.5 mm/rev
Speed	840 rpm
Sensors	Accelerometers: PCB model 353B17
Amplifiers	PCB model 480E09 ICP
Data acquisition	Diagnostic Instruments PL202 Pentium PC, Matlab 5.1

3.3 Experimental results

Three different states of tool wear were identified. The three different states are:

1. New tool (N - 1)
2. Medium wear (M - 2)
3. Severe wear (S - 3)

A typical signal that was recorded during the 'new tool' state is shown in figure 3.2. Channel 1 is the vibration signal in the Z-direction and channel 2 is the signal in the X-direction.

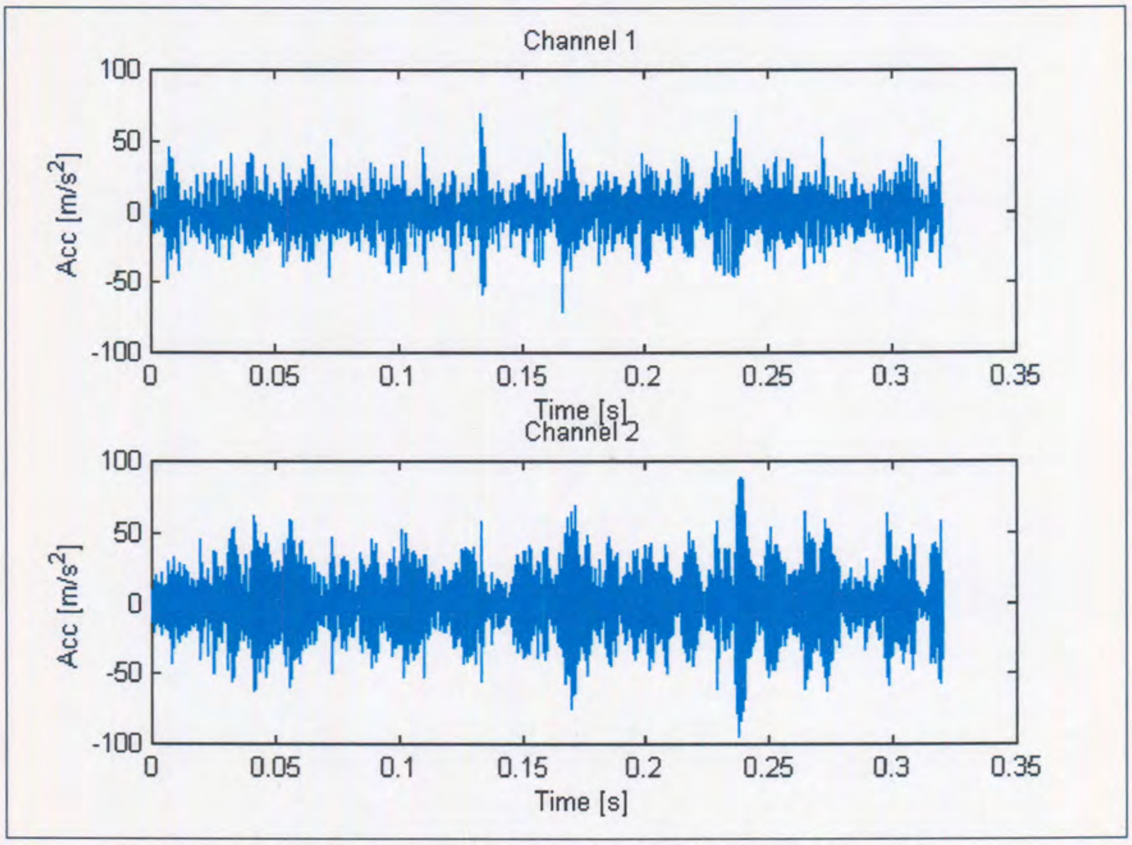

Figure 3.2: Typical time signal recorded by PL202 analyser

3.3.1 Frequency domain analysis

The frequency spectra for the three different states of tool wear are shown in figures 3.3 & 3.4. The spectra were calculated by processing the calibrated time signals from the PL202 analyser. The time signals were divided into overlapping sections, windowed, and then the FFT was taken. The average of many such FFTs were used to determine the average spectrum for each intensity of tool wear.

It is clear from these figures what influence tool wear has on the frequency response. The amplitudes at the peaks become much greater with increasing tool wear. The peak around 1 kHz corresponds with the first natural frequency of the tool assembly (proven in a different case study). The reason for this increase is the fact that with a worn tool, the workpiece material is torn away from the workpiece, instead of cleanly cut. This causes the vibration to increase excessively between the tool tip and the workpiece, and therefore causes the larger amplitudes at the natural frequency. This is not the case with all types of tool failure modes. The dominant failure mode in this case is flank wear, which causes vibration amplitudes to increase.

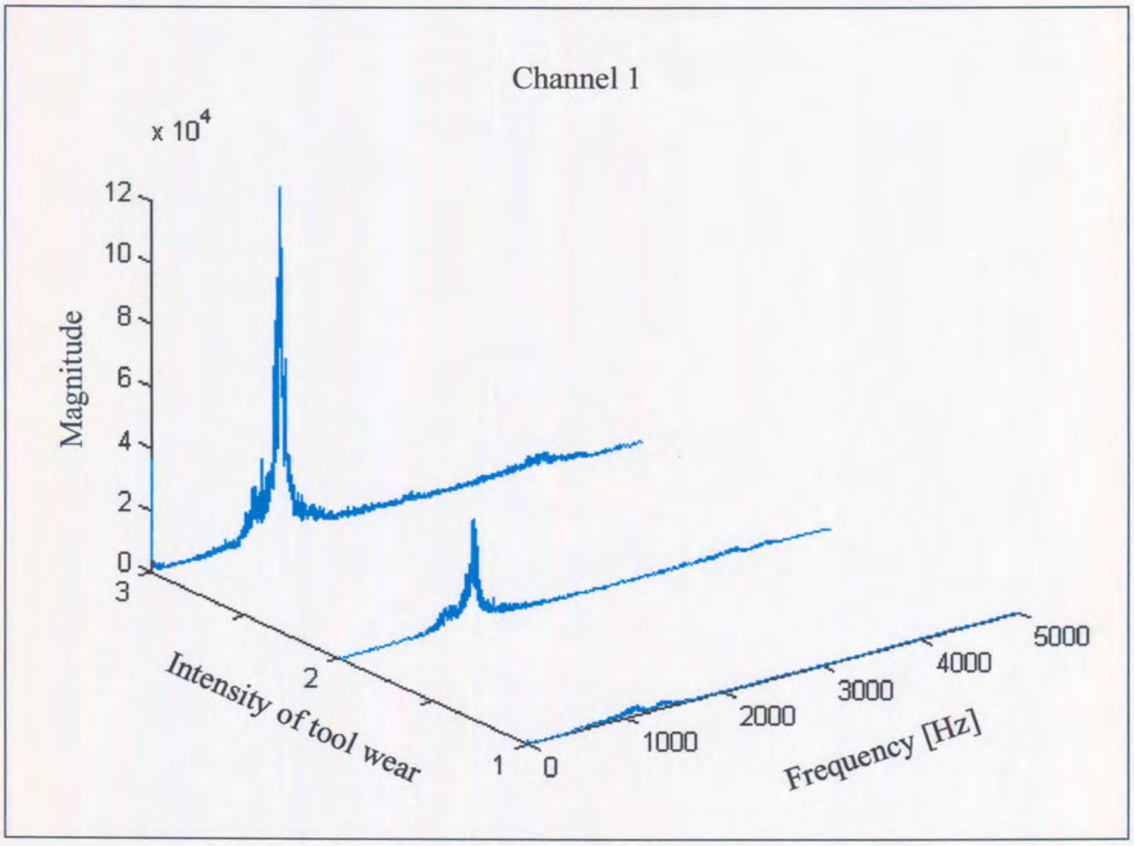

Figure 3.3: Response at different tool wear states – channel 1

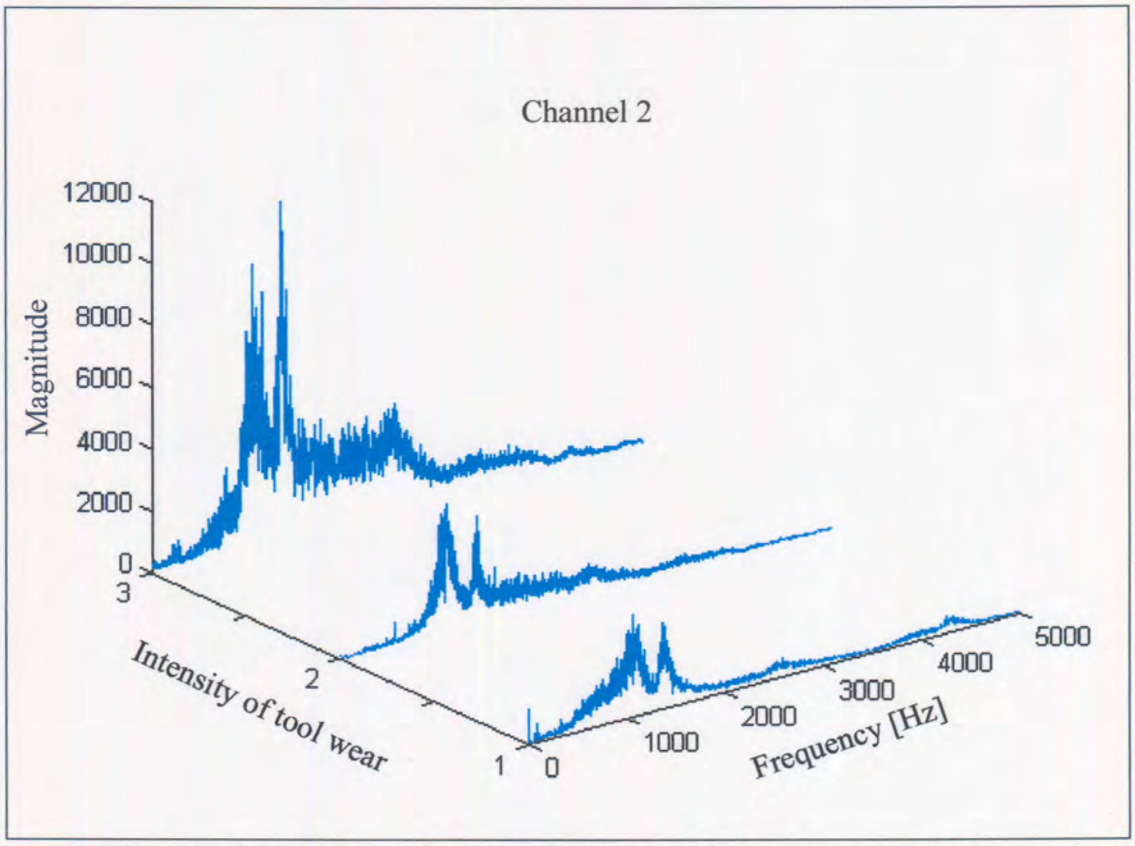

Figure 3.4: Response at different tool wear states – channel 2

3.3.2 Time domain analysis

The objective of the time domain analysis was to determine if any characteristics or features from the time signal change dramatically with increasing tool wear. If a given feature trends with increasing tool wear, it can be utilised to predict tool wear at any given time. Typical features that can be extracted from each time signal are rms, kurtosis, variance, skewness, standard deviation, and crest factor. The same signals from which the above FFTs were derived, were used to obtain the features. The following figures (3.6; 3.7; 3.8) contain two lines, corresponding to channel 1 and channel 2. The figures are also divided in three sections with a vertical green line. The three sections represent the data recorded from a new tool, medium worn tool and severely worn tool. Note that the x-axis is not a time scale, but the measurement number.

It can be seen from the figures that that all features are definitely influenced by tool wear to some extent. Some of the features were, however, more influenced by the tool wear than others. There was also good correlation between the data from the two respective channels.

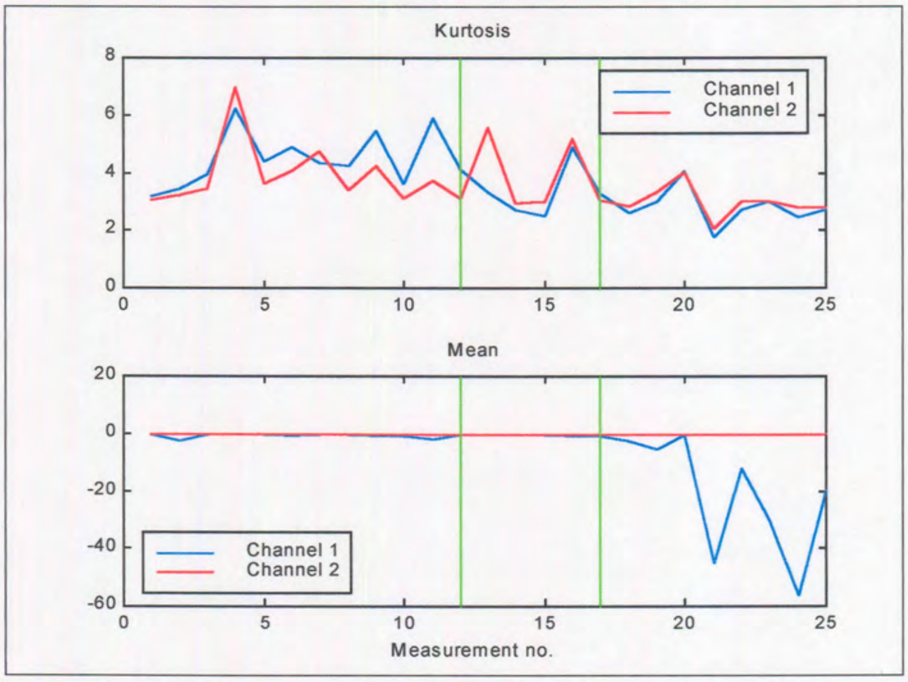

Figure 3.6: Kurtosis and mean of time signals with increasing tool wear

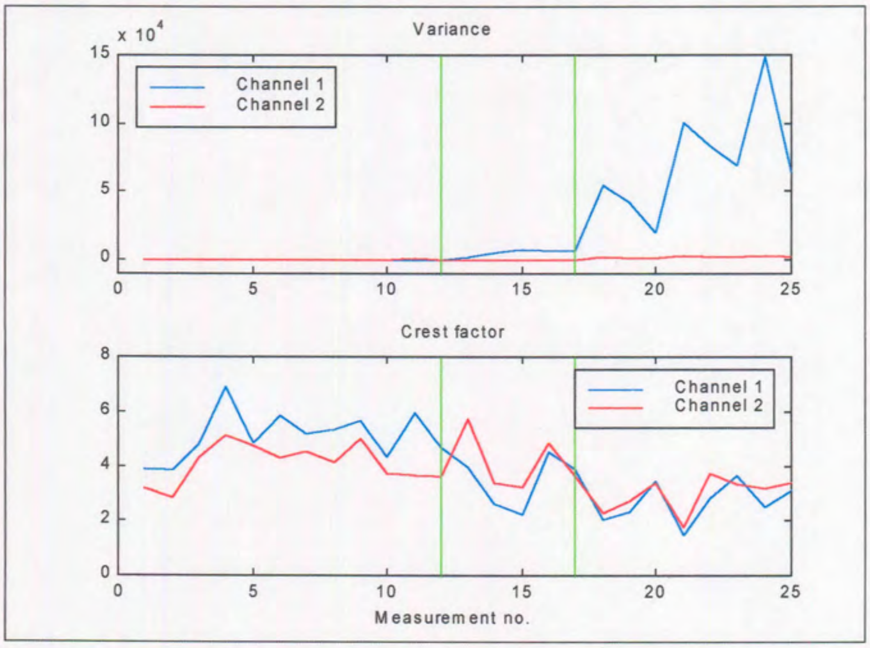

Figure 3.7: Variance and crest factor of time signals with increasing tool wear

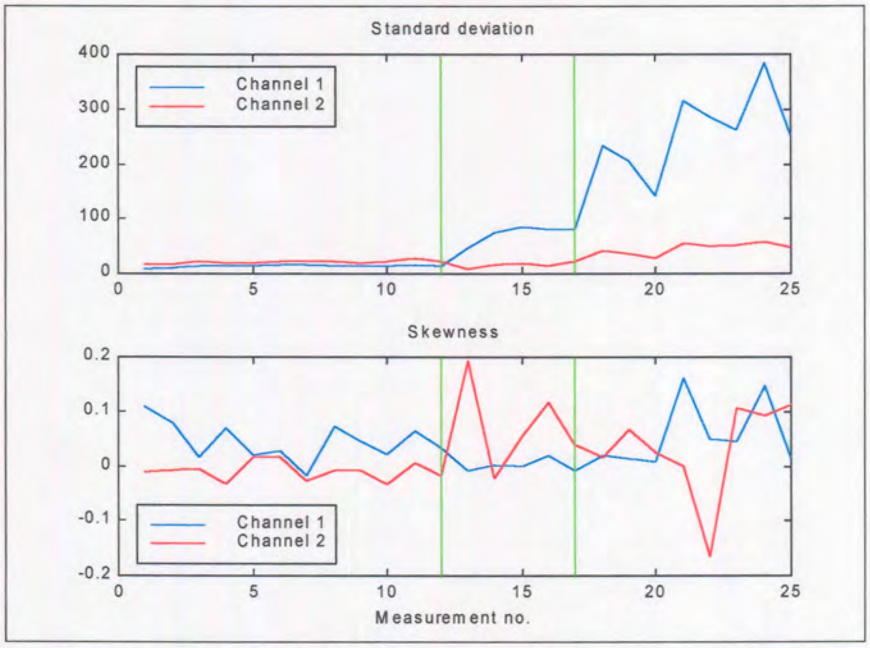

Figure 3.8: Standard deviation and skewness of time signals with increasing tool wear

3.3.3 Conclusion

The purpose of this investigation was to determine if vibration monitoring is fit to identify tool wear. The answer is a very definite yes. Accelerometers coupled to the PL202 FFT analyser were used for this purpose. Data from the time as well as from the frequency domains are useful for predicting tool wear.

The next step will be to identify values of the chosen features that correspond to a certain amount of tool wear. A very simple decision making technique is of course the 'trending' of the features that was described earlier. When a certain feature, or a set of features, reaches certain set limits, an estimation of the tool condition may be derived. These trends in the features are indicative of deteriorating tool condition. The difficulty with this method is to determine the correct threshold value for each feature. For the purpose of this investigation, the Self-Organising Map (SOM), as discussed in Chapter 2, was used to automatically classify the tool wear states from the given features, and to identify possible hidden relationships between the features.

3.4 Wear classification

3.4.1 Introduction

As was stated in Chapter 2, the Self-Organising Map is a type of neural network which can automatically identify classes in data without human interference. With most neural networks, the user of the network specifies the output, and the network models the system to reach the specified output. The SOM arrange the given data in a network of neurones where similar neurones are placed close to one another on the map [99].

The normal practice with neural networks is that the number of observations (measurements) must be ten times the number of features to train the network. In this case, it was not possible because only 25 observations were obtained. However, this does not mean the results will be faulty. It only means that more observations will be needed to train the network more accurately.

3.4.2 SOM with given features

For the purpose of this case study, the usefulness of the SOM to distinguish between data taken from a new and worn tool was investigated. Figure 3.9, 3.10 and 3.11 shows the result of feeding the calculated features from both channels into a 12 x 8 SOM. Figure 3.11 shows one of the features with labels from the original training data.

Each observation was labelled 'new', 'med' or 'sev'. After the map was trained, a simple command can determine to which neurone a specific observation corresponds best. This is referred to as the Best-Matching Unit (BMU). The number of BMUs on each neurone, as well as the label of these hits, can be plotted directly onto the SOM. This gives an idea of which regions on the map correspond to new tools, and which regions correspond to worn tools. When a new observation is made, the SOM can easily calculate the BMU and use the new observation to update the map.

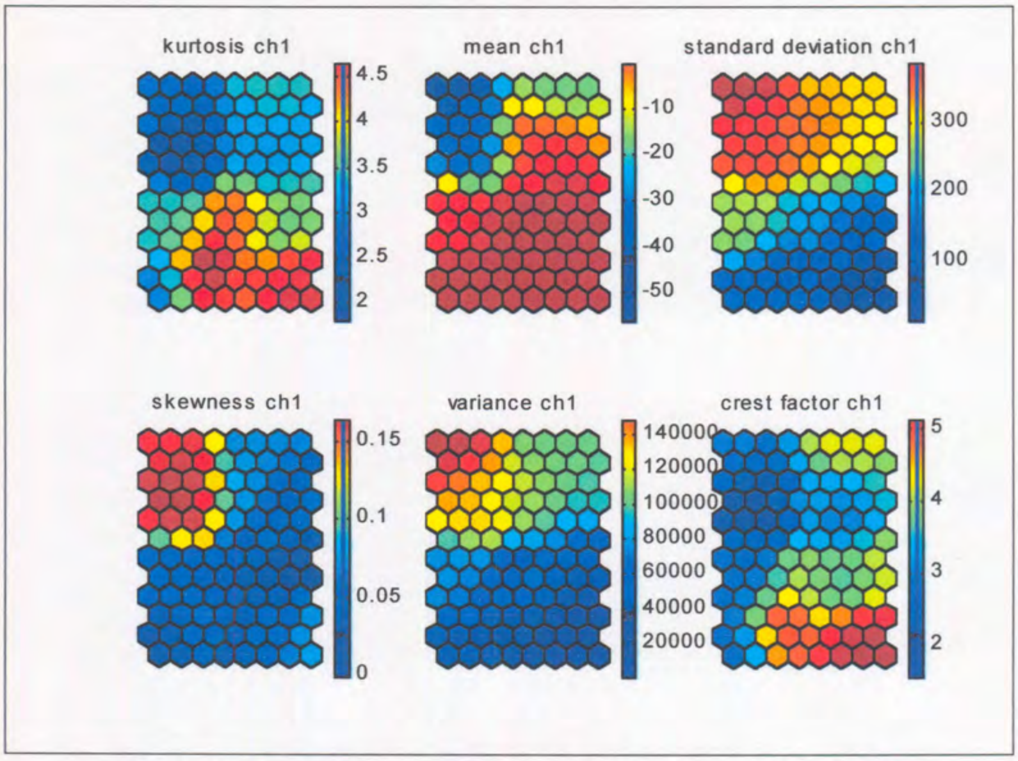

Figure 3.9: Self-Organising Map, features from channel 1

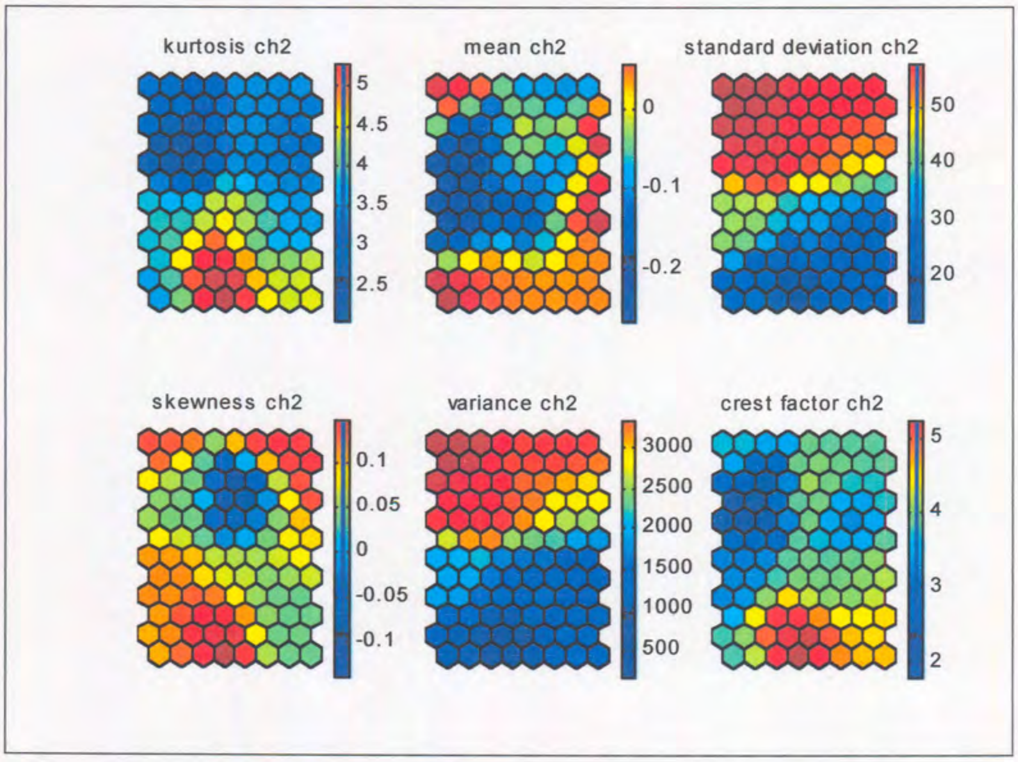

Figure 3.10: Self-Organising Map, features from channel 2

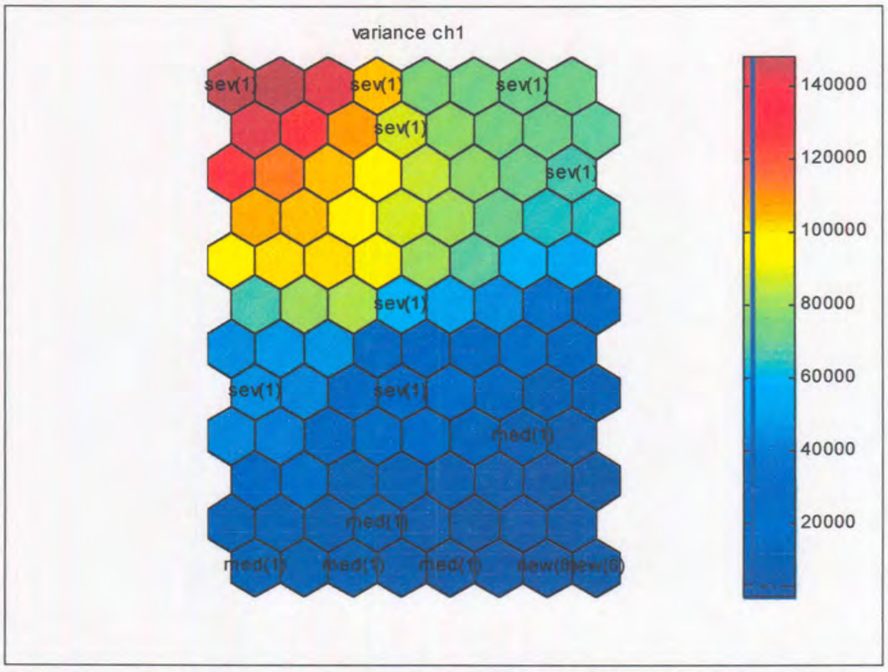

Figure 3.11: Self-Organising Map with labels from training data

3.4.3 SOM with thresholded features

A further advantage of the SOM is that it can handle discrete variables. For instance, if the threshold value for each feature is known, one can easily threshold the value to 0 for normal conditions, or 1 if the threshold value is exceeded. An advantage of this approach is that a new variable can be defined, namely the intersection between the thresholded variables. The intersection value for each observation is the sum of all the variables for the observation. This enables the definition of a single variable that can combine all information supplied by features. Figures 3.12, 3.13 and 3.14 show the thresholded features.

The concept of thresholding and using discrete variables with the SOM was also proposed by *Cser et al.* [103] for improving the geometric quality parameters for hot-rolled strips. They also proposed the definition of the intersection variable, which can show how certain values of the quality parameters directly influence the process. To the author's knowledge, this is a fairly new approach of utilising the SOM.

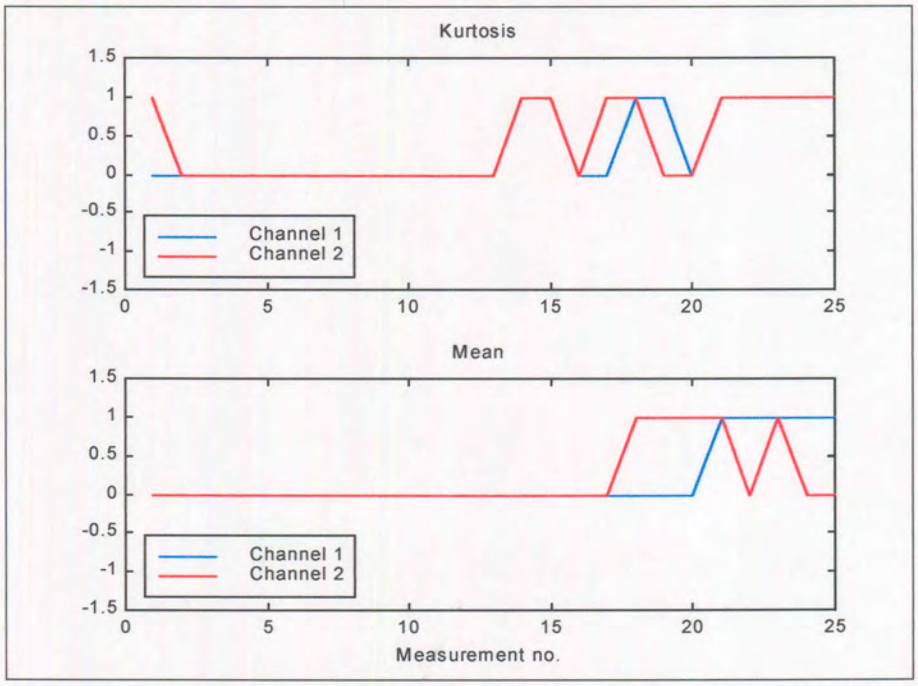

Figure 3.12: Thresholded values of kurtosis and mean with increasing tool wear

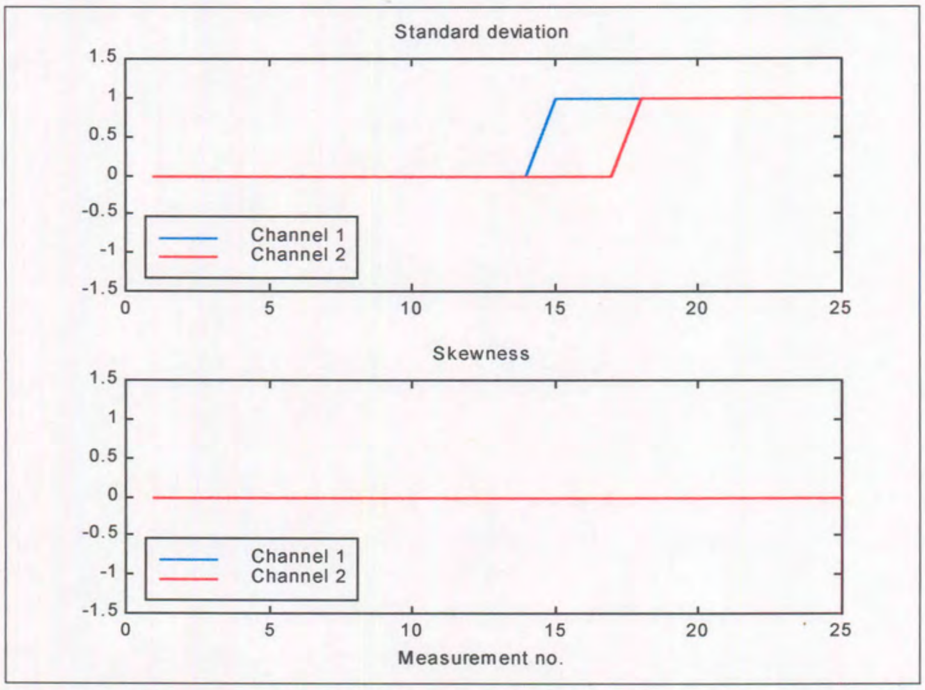

Figure 3.13: Thresholded values of standard deviation and skewness with increasing tool wear

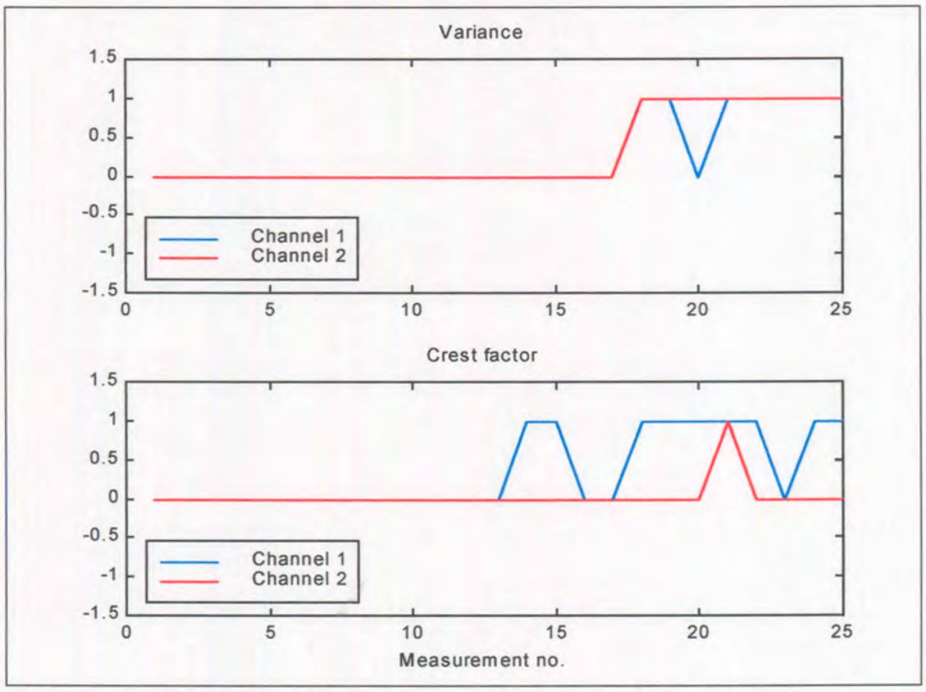

Figure 3.14: Thresholded values of variance and crest factor with increasing tool wear

It is clear from these figures of the thresholded features that some of the features are less sensitive to tool wear than others. For instance, skewness could not provide any information regarding tool wear. Kurtosis and crest factor provided data which shows ones and zeros in the severe wear region. This proves that although these features are influenced by tool wear, they are not sensitive enough to base decision making process on them alone. Variance, mean and standard deviation on channel 1 proved to be the best features for tool wear identification.

Figures 3.15 and 3.16 display the SOMs for the thresholded values of the variables. Note that each map is divided into basically two regions, a zero and a one region, corresponding to an acceptable and an unacceptable region. Figure 3.17 shows the intersection variable discussed earlier, together with the labels and BMUs on each neurone. All the features from both channels were used to calculate the intersection variable. This figure shows that the SOM divided the data in a blue region in the upper right hand corner corresponding to new tools, a light blue section corresponding to medium worn tools and a yellow, orange and red region corresponding to severely worn tools.

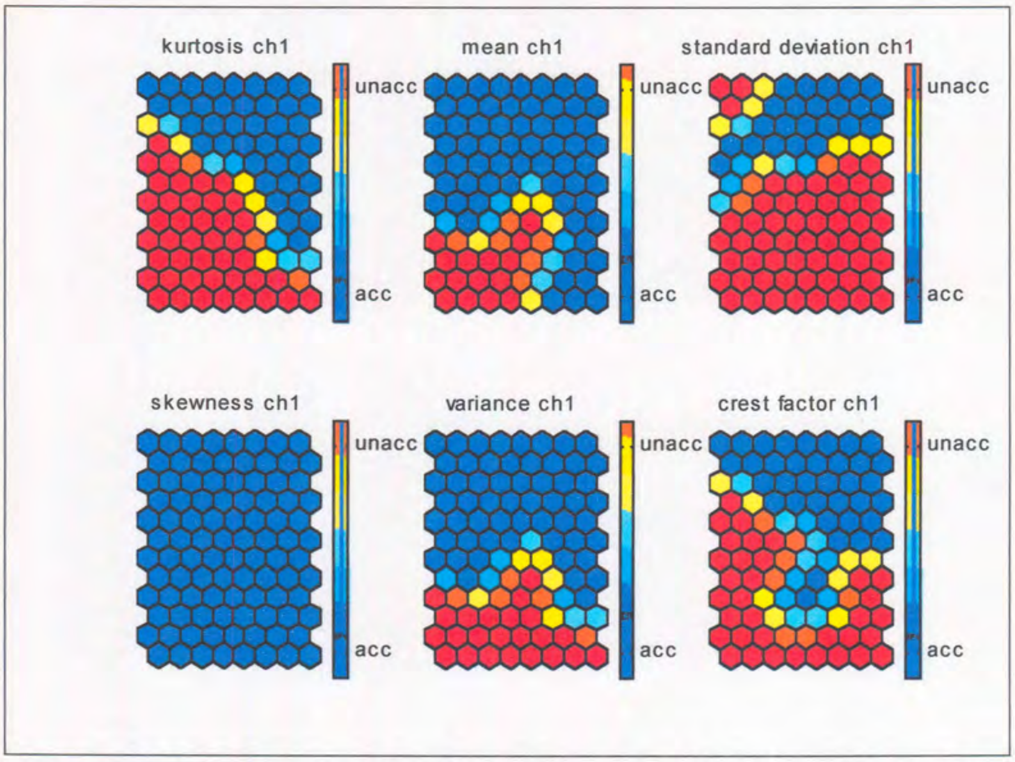

Figure 3.15: Self-Organising Map of thresholded features - channel 1

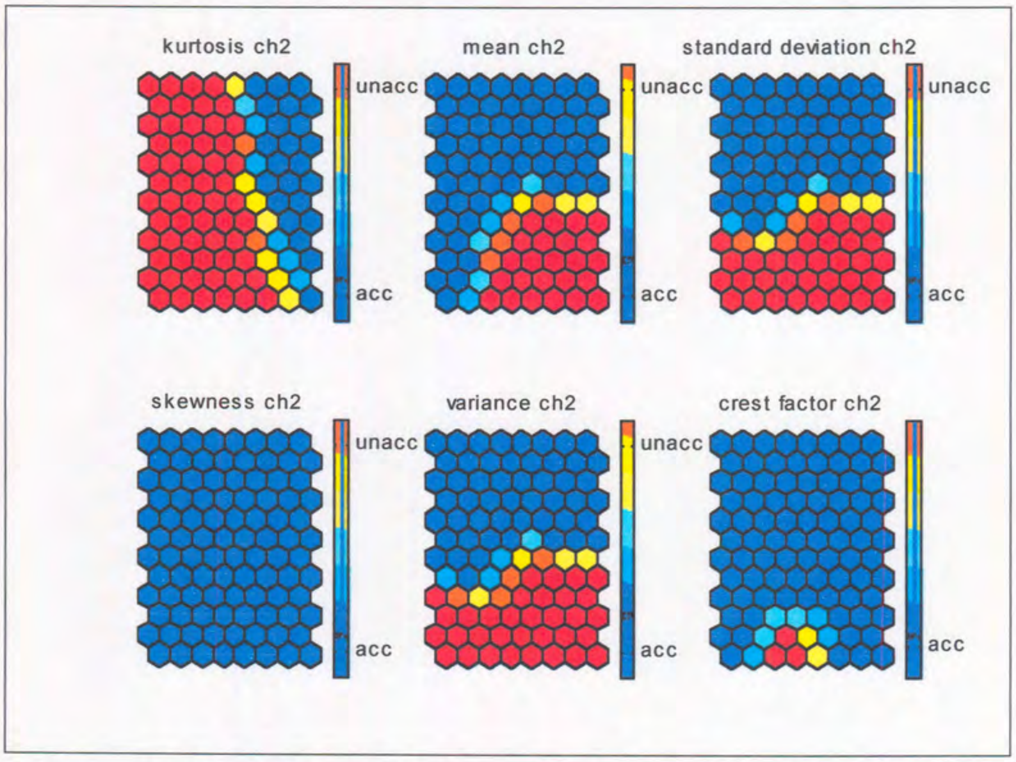

Figure 3.16: Self-Organising Map of thresholded features - channel 2

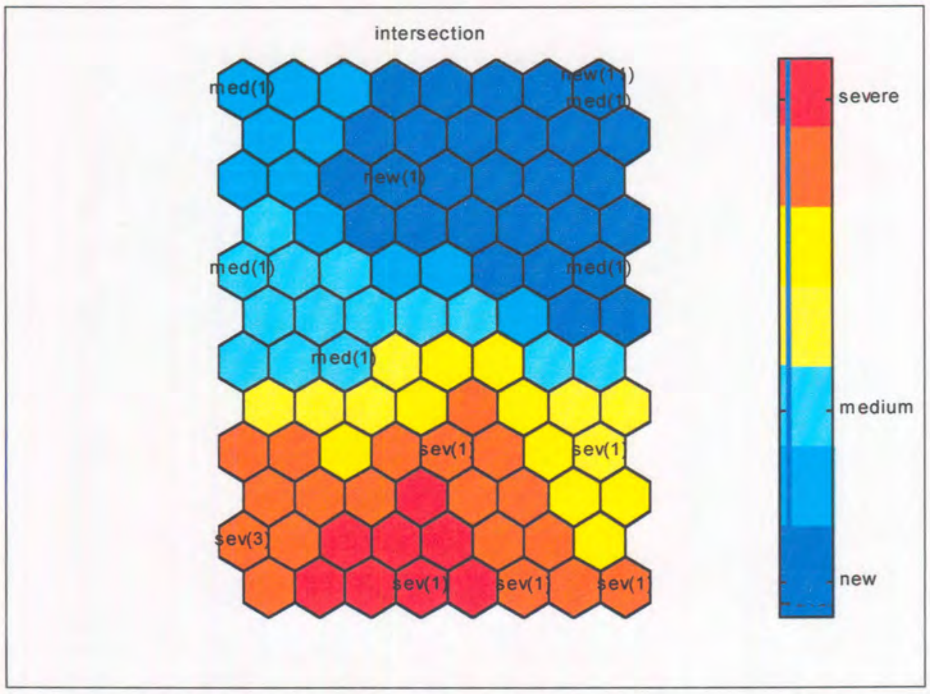

Figure 3.17: Self-Organising Map of intersection of features - both channels

3.4.4 Conclusion

The purpose of this investigation was to determine if the Self-Organising Map could be used to identify classes in tool wear data. It was shown that the SOM can be used not only to classify the tool wear data correctly, but it can also handle discrete values of the variables that may be very useful if threshold values for the variables are known. This is a relatively new approach of utilising the SOM, which can be used to determine which regions on the map can be allocated for certain conditions.

The SOM is also useful to identify hidden characteristics within the data, such as the sensitivity of a certain feature regarding the objective of the investigation. The reason why the SOM is more fit for the purpose for this study, is the fact that the ideal 'output' of the system is unknown. The final conclusion is that the SOM is fit for data analysis for future case studies.

CHAPTER 4

MONITORING OF THE SYNTHETIC DIAMOND TOOL WEAR IN A MANUFACTURING PROCESS

4.1 Introduction

One of the main focuses of this project was to do research which would directly benefit the South African manufacturing industry. The need for a monitoring strategy on machine tools in the South African manufacturing industry was investigated through discussions with various companies and experts in the field. Different companies experience different machine monitoring needs, but a common need in most cases is the identification of tool wear and breakage. Federal Mogul (Pty) Ltd (formerly AE Goetze (Pty) Ltd) indicated that it would co-operate in the research and development of a system that would monitor the wear of synthetic diamond tools. These diamond tools are very expensive and the company has to optimise its use of these tools. Federal Mogul (FM) manufactures automotive pistons for various vehicle manufacturers. The pistons are precision machined from aluminium casts.

Up to date, FM monitored the wear of the synthetic diamond tools based on the following:

- The number of machined components.
- If regular offset changes have to be made, it is an indication of volumetric loss at the tool tip. This is an indication of wear.
- Surface roughness, which is only done once a day for this specific process.
- A built-in monitoring option in the machine monitors the spindle current. The operators found that this is not satisfactory, because the alarm levels are not sensitive enough. It was found that it is only helpful to monitor tool breakage in some instances.

None of these methods could give the operator an indication of the residual tool life. The result of this strategy is that all tools are replaced at the start of the manufacturing of a new batch of components. The amount of components in a batch depends on the order from the vehicle manufacturers. The pro-active replacement of tools minimise down time on the machine, because the machine has to be set for the current component at the start of each new batch. The end result is the waste of many acceptable tool tips. FM also found that their tools followed the so-called 'bathtub curve' behaviour. This means that the tool goes through an initial rapid wear stage, a normal wear stage and a final rapid wear stage before breakage. This 'bathtub' phenomenon also had to be investigated.

4.2 Monitoring system

4.2.1 Introduction

In order to identify the diamond tool wear in a real manufacturing process, a monitoring strategy was devised using three sensors, located near the diamond tip on the tool holder. The sensors consisted of the following:

- Piezo strain sensor in the X-direction (direction of feed force).
- Piezo strain sensor in the Y-direction (direction of thrust force).
- Accelerometer in the Z-direction.

The reason for the choice of three sensors is to record as much as possible data from the process. This will enable the generation of a large number of features which may be used with the SOM to identify the stages of tool wear. A large number of features may be required due to the fact that the influence on the machine vibration and wear mode of the synthetic diamond tool is unknown.

The synthetic diamond tool is commonly referred to as Syndite in the industry. The reason for the use of the Syndite tip is due to the fact that normal tool tips can diffuse with aluminium, and because the Syndite tip lasts longer it is also more economical. However, the Syndite tips are still very expensive, and the company would prefer to utilise each tip to its full extent without wasting parts, and with minimum down time of the machines. The Syndite tip can be re-sharpened five to six times before it is scrapped. If a tip breaks due to extensive wear, a tool that still could have been resharpened a few times is wasted.

The process from which measurements were obtained, consisted of quick metal removal before the final finishing of the component commences. Because FM manufactures a large variety of pistons, it was decided to design a robust monitoring system that can adjust to changes in the process. During the measurement phase, only one type of component was manufactured, but the operator was allowed to change the feed rate randomly (using the manual override button) within certain set limits. The feed rate has a large impact on the subsequent vibration, which forced the implementation of a robust monitoring system. A robust monitoring system can later be adjusted to monitor the tools when manufacturing other parts as well. An Analysis of Variance (ANOVA) was carried out to ensure that the disturbances in the recorded data are truly randomly distributed.

4.2.2 Experimental setup

Figure 4.1 display schematic details of the experimental setup. It is very important to ensure that the sensors are well isolated against cutting fluid and chips, without disturbing the dynamics of the cutting process too much. Furthermore, measurements have to be made as close as possible to the physical cutting process, because, as mentioned in previous chapters, tool wear causes very small changes in a process with a very wide dynamic range. Another problem with the placement of the sensors was a limitation on the amount of available space on the tool holder. Due to the fact that this is a precision process, any deflection of the tip is undesirable. Therefore, the holder is clamped on all four sides, very close to the tool tip. For this reason, only three sensors were used, instead of four as was originally intended.

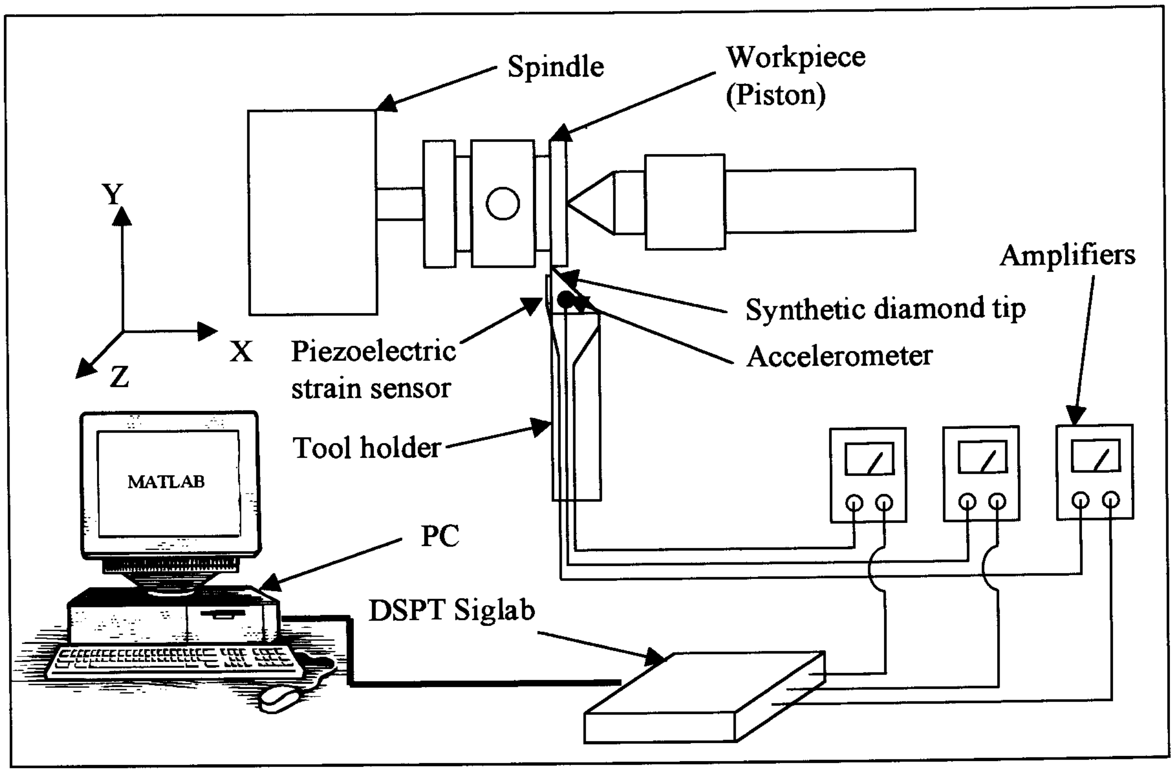

Figure 4.1: Schematic of experimental setup

Another problem that was encountered was with the isolation of the sensor wires. The specific machine chosen for monitoring is a 4-axis CNC, with two turrets machining simultaneously. Each turret is capable of holding four tools. The turret indexes between tools regularly during a cycle, resulting in the risk of breaking a sensor wire. These practical problems were overcome by isolating the sensors with various substances, like nitrile varnish, rubber and silicon. The sensor wires were housed in plastic pipes, sealed with silicon. Furthermore, the operator was instructed to program the machine in such a manner as to prevent the turret to rotate through 360 degrees. Figures 4.2 to 4.9 display details of the complete experimental setup.

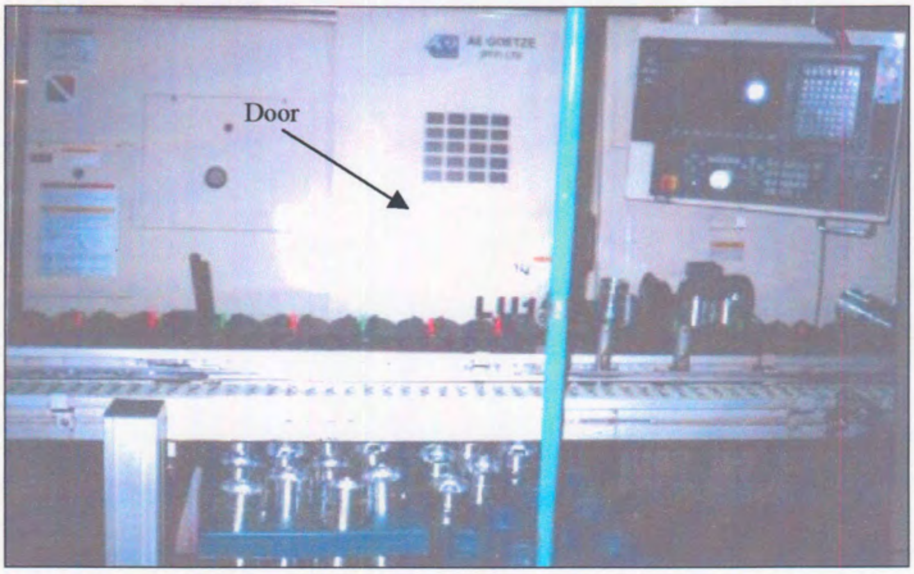

Figure 4.2: Machine used for experiments, in operation with door closed

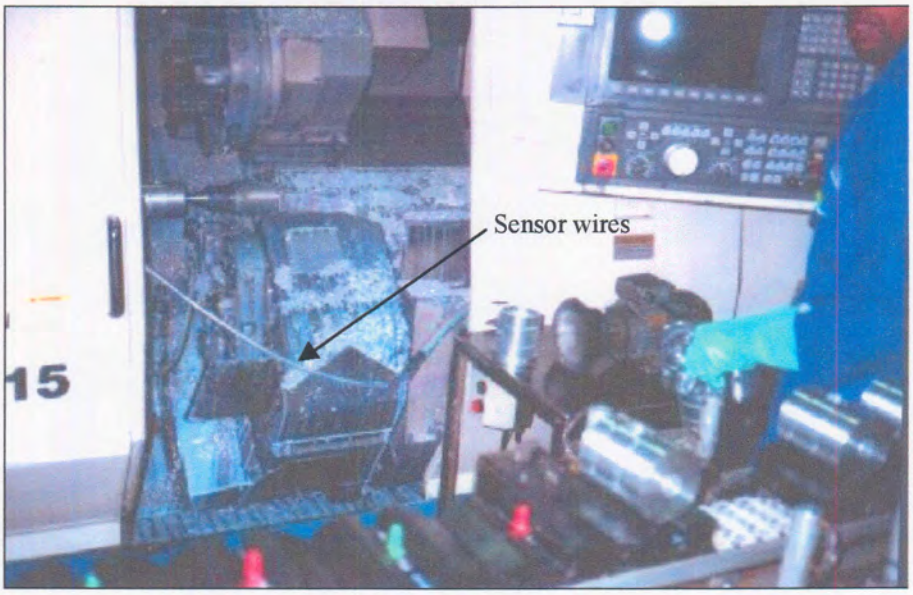

Figure 4.3: Machine with sensor wires in plastic tube visible

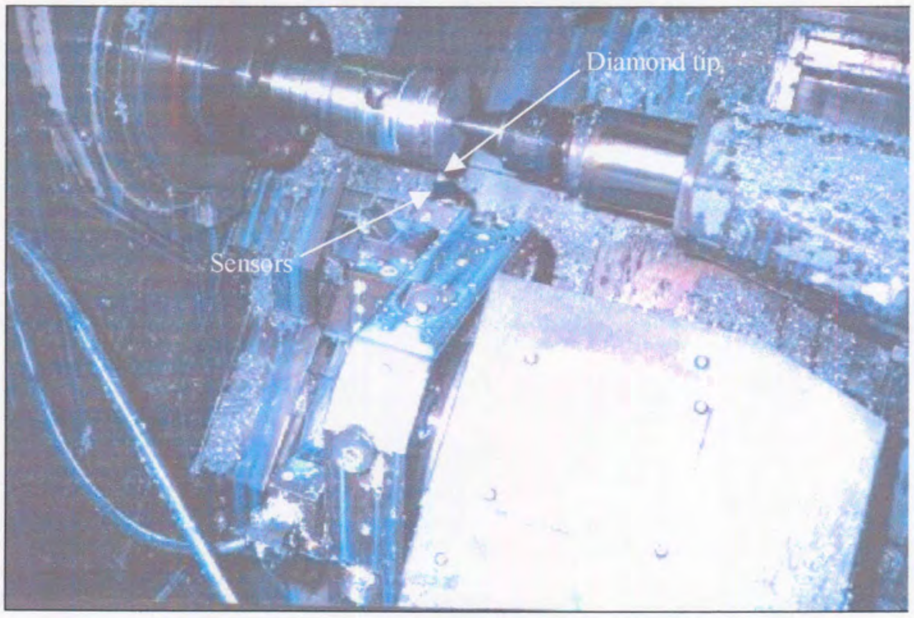

Figure 4.4: Part before machining, with diamond tip and mounting of sensors and wires visible

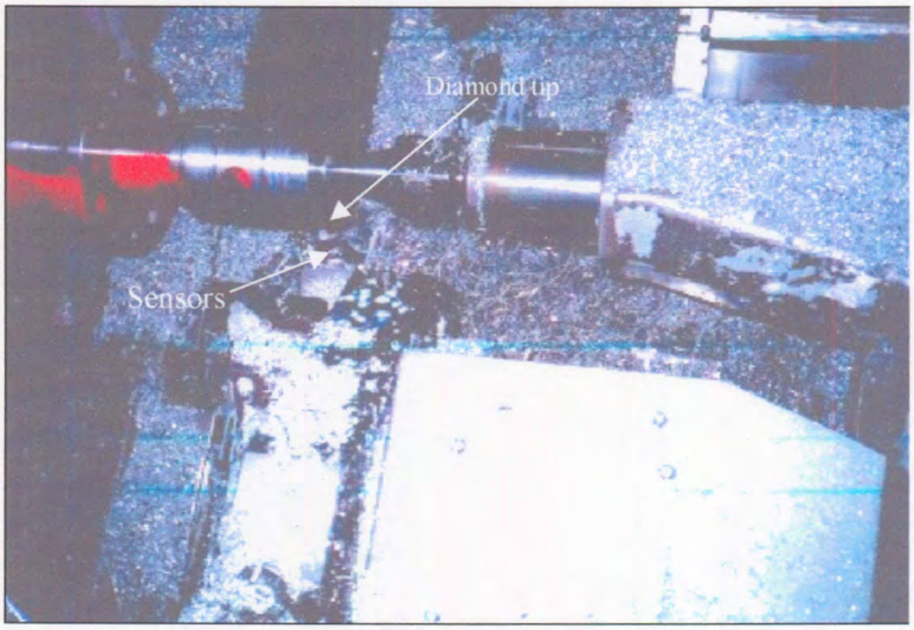

Figure 4.5: Part after machining, with sensor mounting on diamond tip visible

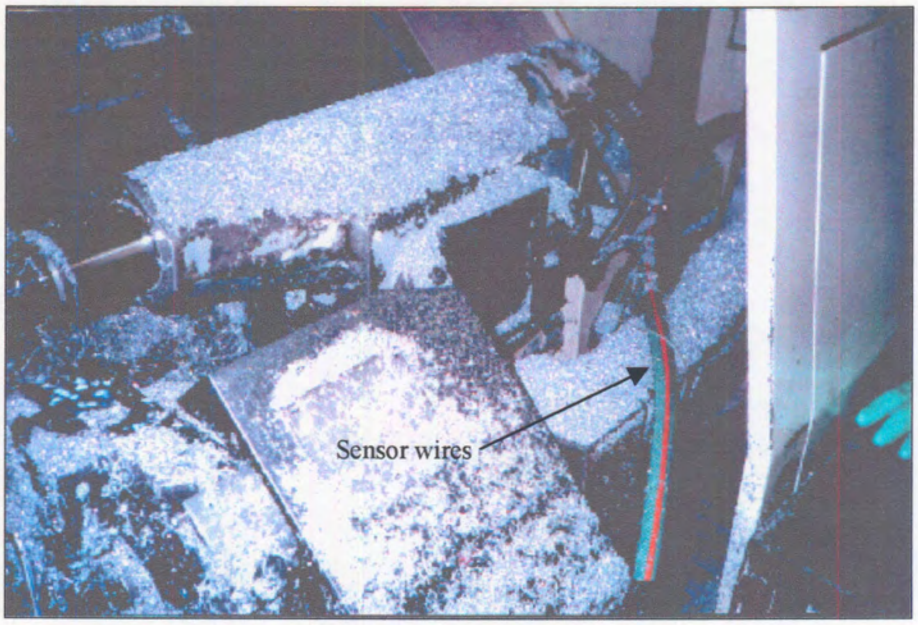

Figure 4.6: Mounting of sensor wires inside machine

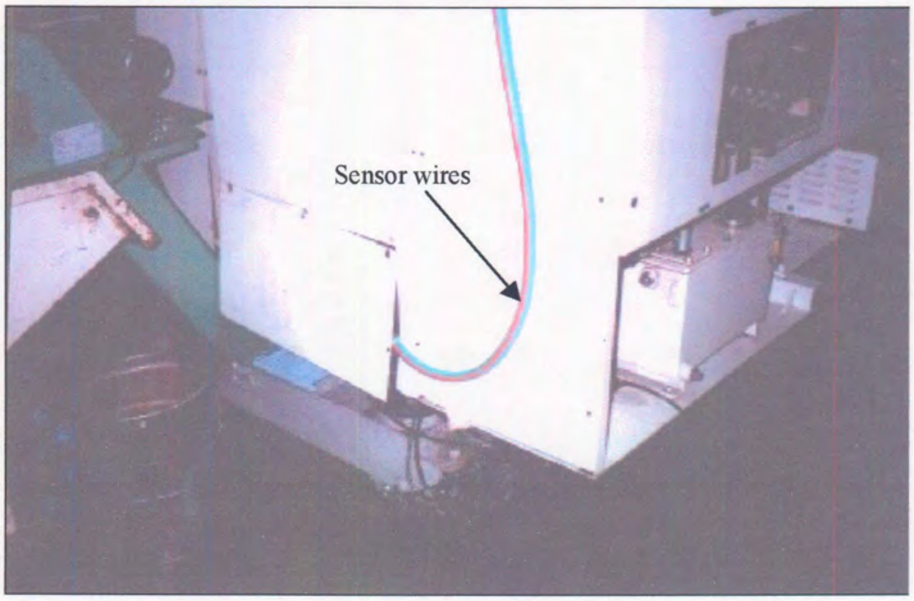

Figure 4.7: Exit of sensor wires from machine

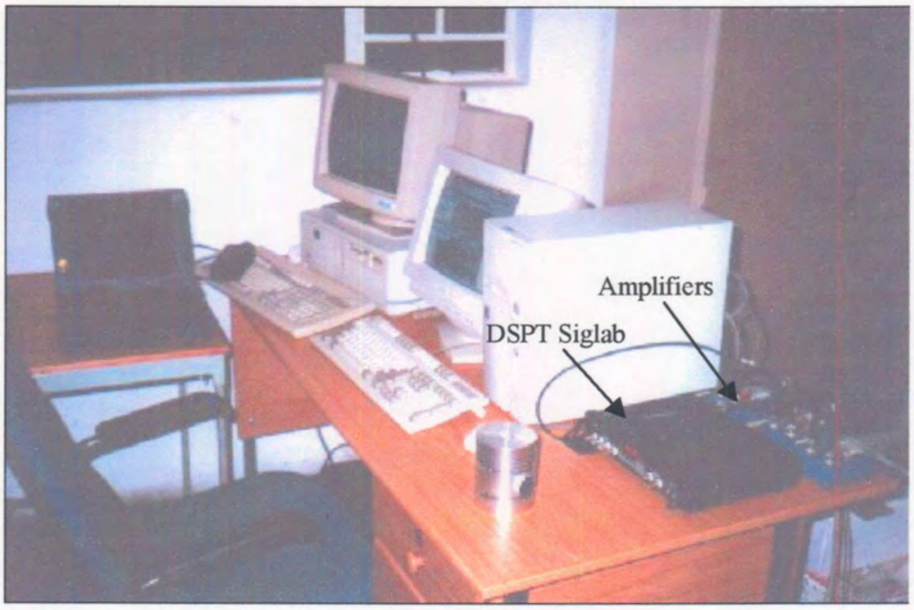

Figure 4.8: Amplifiers, DSPT Siglab and PC for data recording

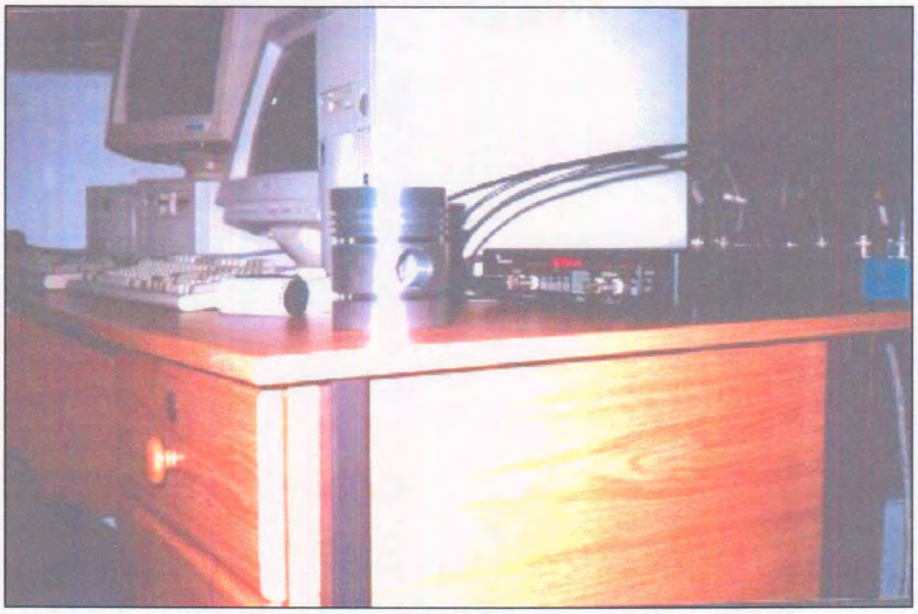

Figure 4.9: Example of part after machining, as used for surface roughness analysis

4.2.3 Experimental parameters

Table 4.1 summarise the cutting parameters and instrumentation. The DSPT Siglab was used to record a ten-second time signal on all three channels, sampled at 25.6 kHz. The Siglab, driven from the MATLAB environment, automatically filters the signals against aliasing and then stores the signals in MATLAB format on the PC. All data processing were done in the MATLAB environment.

Table 4.1
Experimental parameters

Lathe	Okuma LU 15
Workpiece	Aluminium
Holder type	Sandvic SDJCR 2020k11
Insert type	Synthetic diamond (Syndite)
Feed rate	0.5mm/rev ± 10%
Speed	3600 rpm
Sensors	Accelerometer: PCB model U353B65 strain sensors: PCB model 740B02
Amplifiers	PCB model 480E09 ICP
Data acquisition	DSPT Siglab model 20 – 42 Pentium PC, Matlab 5.1

Measurements were taken on an hourly basis, and three samples were recorded in each instance. This ensured that three data sets were available for data processing with a neural network. Two sets can be used for training a network, and the third for testing the network. Approximately fifty components are manufactured in one hour, although this number varies quite a lot. The experiment ran over six days, during which approximately 2300 components were manufactured. Ninety-nine samples were taken, which resulted in thirty-three samples in each data set. The total amount of recorded data occupied 600Mb of hard disk space.

4.3 Signal processing

4.3.1 Introduction

As discussed earlier, a number of different signal characteristics have been used by previous authors to identify tool wear. Some characteristics will, however, not yield satisfactory results in all instances. Many signal processing techniques have proven themselves to be very accurate in monitoring tool wear in a turning process. However, much of the previous work focused on laboratory experiments, with dry turning and normal carbide / tungsten tool tips. Very little work investigated the implementation of such a system in a real manufacturing environment. Furthermore, only a few references were found dealing with diamond tips, which do not display the same behaviour as carbide coated tools [66-71].

The focus of the signal processing is to extract features from the recorded signals, and automatically select the features that display a consistent trend towards tool wear. To increase the reliability of the tool wear monitoring system, a monitoring strategy was devised based on features extracted from the time and frequency domains, as well as features extracted from time series models and wavelet packet analysis.

4.3.2 Single observation

A typical time signal, or single observation, is shown in figure 4.10. Each observation consisted of a ten-second time signal on three channels, sampled at 25,6 kHz. The signals were also filtered before feature extraction, allowing the 10 Hz - 10 kHz frequency band to pass. Three sets of data were collected with the aim to train and test a neural network based monitoring strategy.

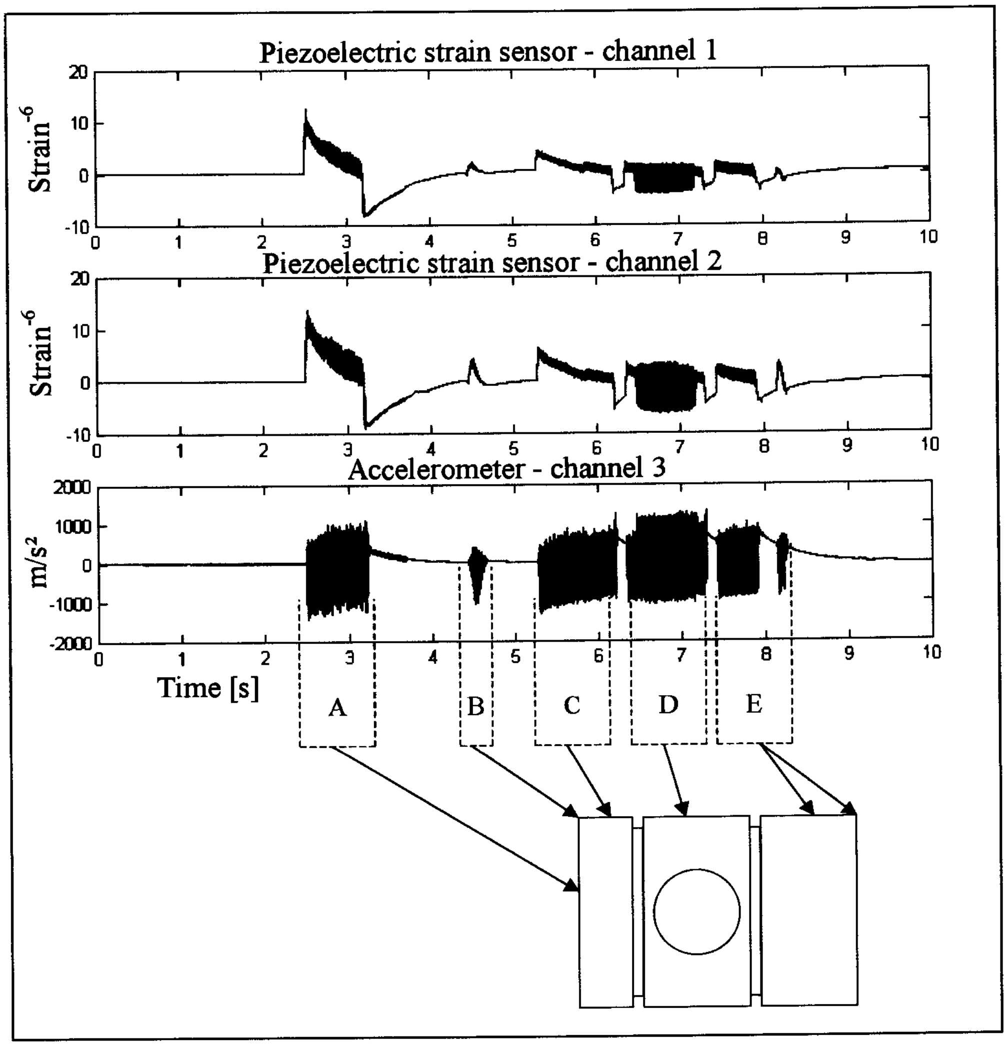

Figure 4.10: Typical observation showing five parts of signal

As can be seen, the signal consists of five distinctive parts, labelled A, B, C, D and E. Each of these parts correspond to a certain cut on the workpiece, schematically shown on the figure. The signal contains 256 000 data points, which is too many too analyse effectively at once, especially if the ultimate goal is to devise an on-line system. Therefore the signal was broken up into the shown parts, by an automatic triggering algorithm in MATLAB. Certain parts of the signal may contain more information on the progressive tool wear, and it is also possible that the different cuts may cause different failure modes to be dominant. Breaking the signal can expose such behaviour. The breaking of the signal also enables the generation of more features, as will be shown later in this chapter.

4.3.3 Feature extraction

After the signal was broken up in the five parts, the feature extraction program starts analysing the data, treating each part as a separate signal. The following time domain features were extracted from each of the parts: mean, rms, crest factor, variance, skewness and kurtosis. Furthermore, coefficients from time series models were used as features, in this case: AR coefficients, MA coefficients and ARMA coefficients. The mathematical principles of these features and models were discussed in Chapter 2.

The most common frequency domain characteristic found in the literature is the spectral energy around the first natural frequency of the tool-workpiece system. It was established that the first natural frequency for this system lies at about 5 kHz. The spectral energy in the 5 kHz region was taken as a feature. However, some authors also found that useful information about the process can be found in the 'low' frequency domain. Investigations proved that the spectral energy between 100 - 1000 Hz also displays a significant trend towards tool wear. Therefore, this was also taken as a feature.

Li *et al.* [21] also found that the coherence function between two crossed accelerations is very useful to identify tool wear. In this study, the coherence between the two dynamic force signals in the 5 kHz frequency band was taken as another feature. However, the coherence function did not yield satisfactory results. This may be due to the fact that the dynamic forces in the two directions are too closely related. The principle of calculation of the frequency band energy was discussed in Chapter 2. Figures 4.11 to 4.15 display parts of the signal and their PSDs, with the signals filtered with a bandpass filter of 1-10 kHz, in order to display the activity at 5 kHz clearly.

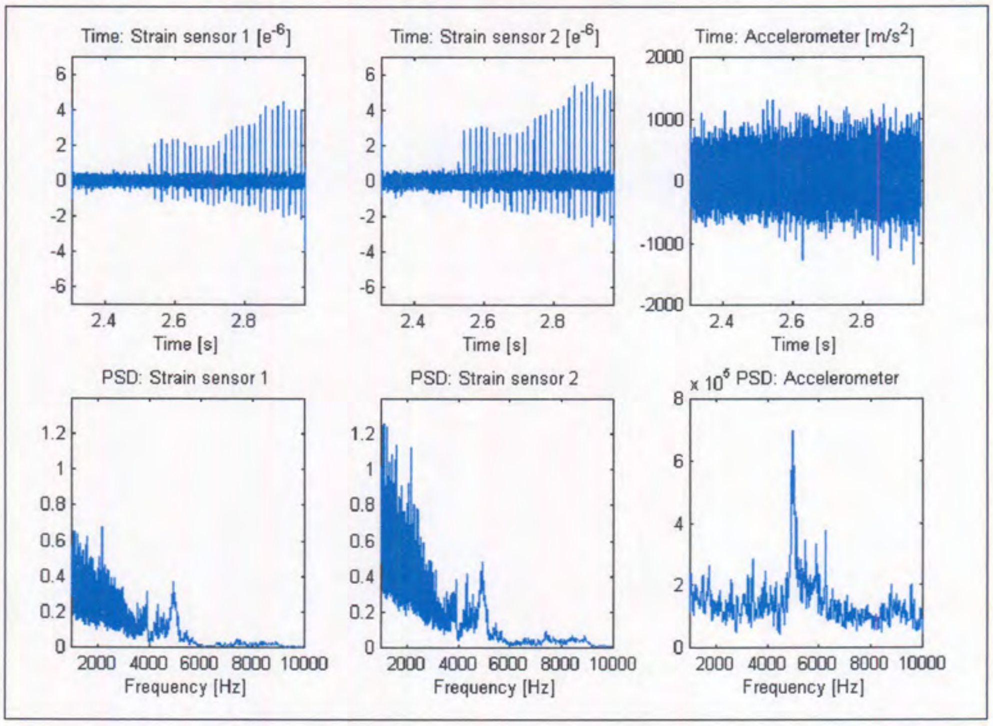

Figure 4.11: Typical part A of observation showing time and frequency components

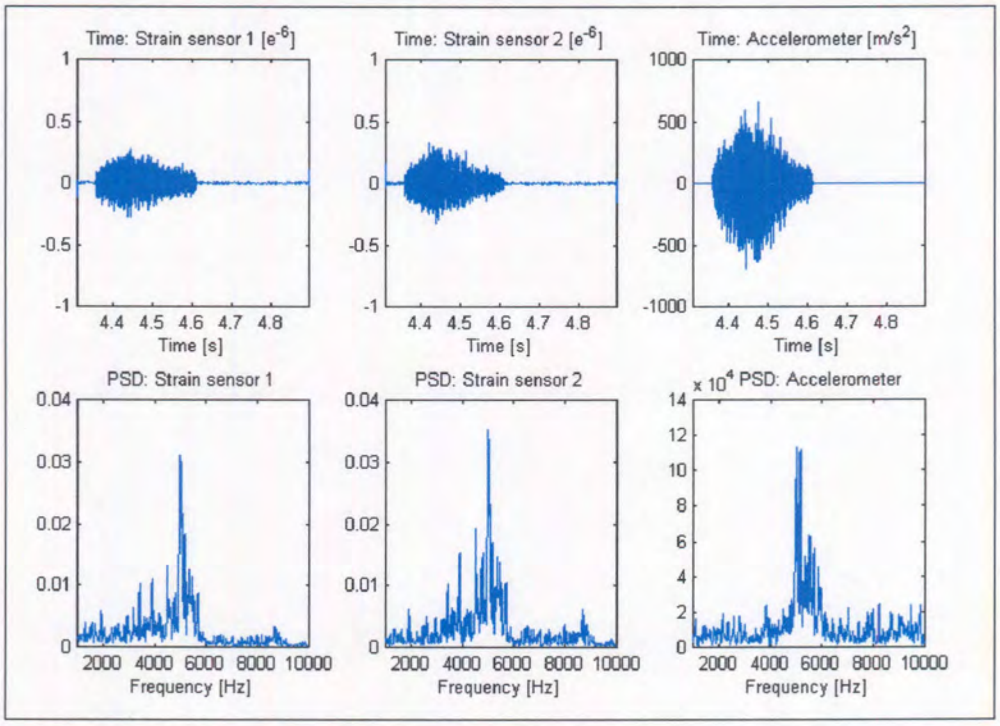

Figure 4.12: Typical part B of observation showing time and frequency components

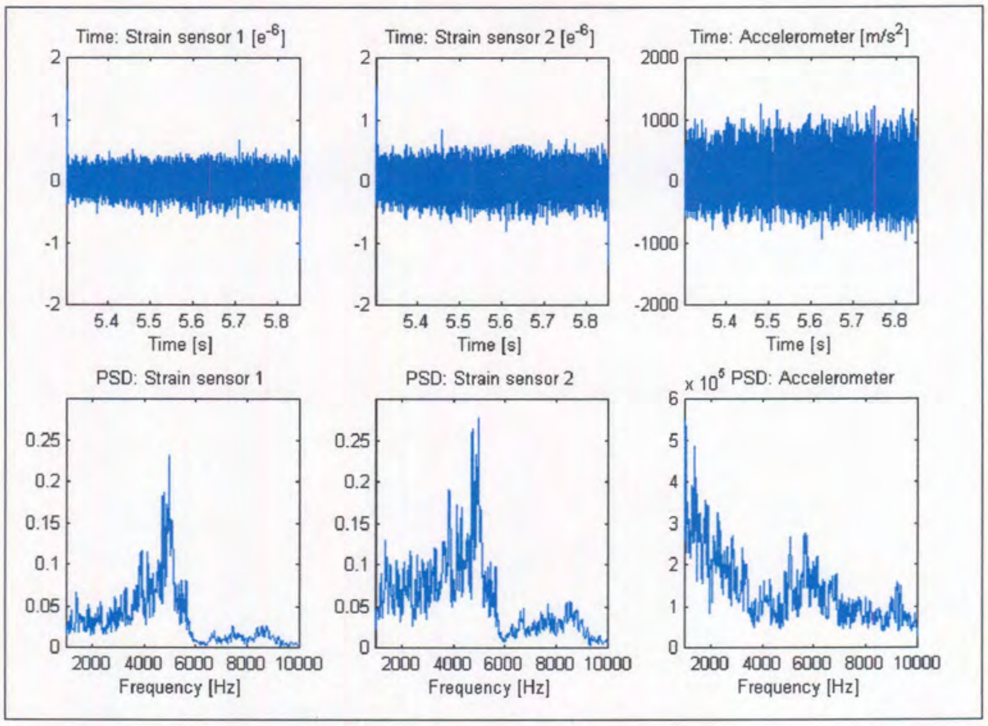

Figure 4.13: Typical part C of observation showing time and frequency components

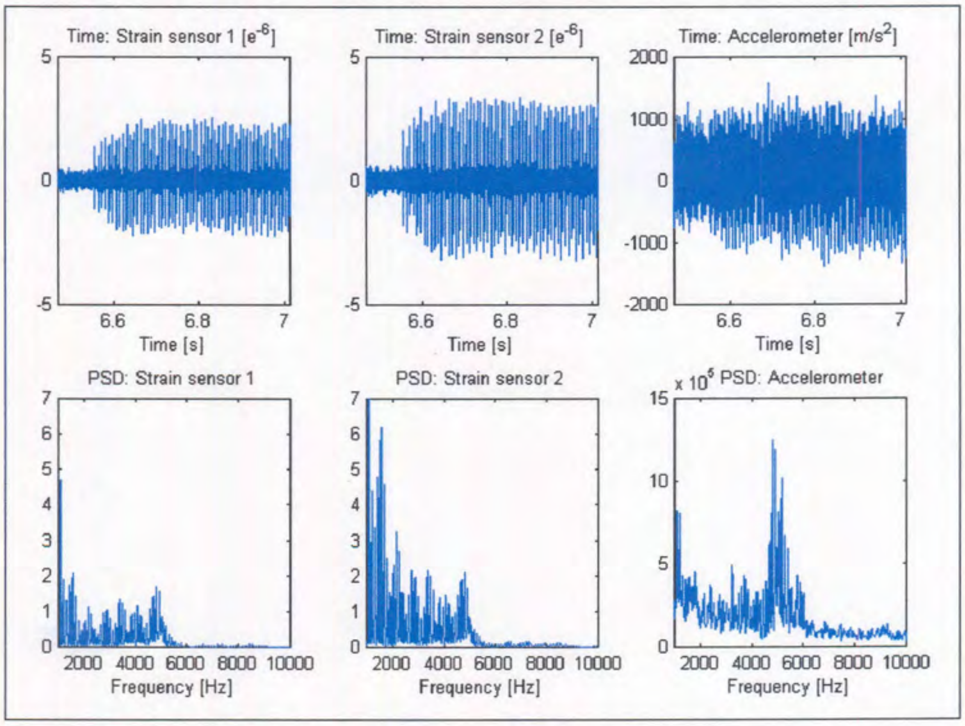

Figure 4.14: Typical part D of observation showing time and frequency components

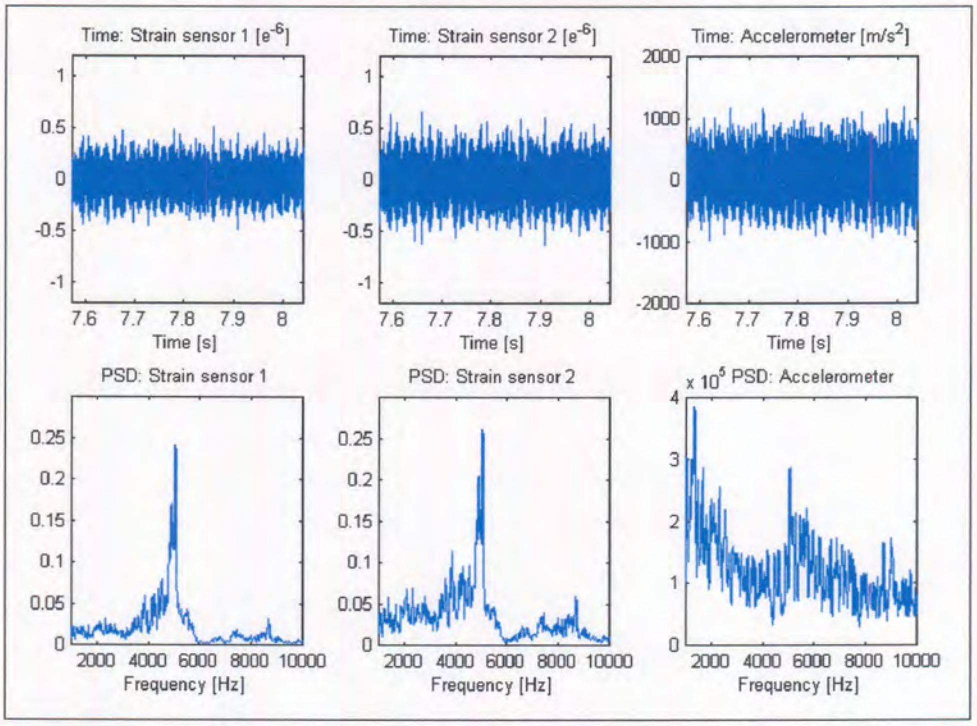

Figure 4.15: Typical part E of observation showing time and frequency components

Wavelet analysis and its significance in process monitoring were also discussed in Chapter 2. An approach proposed by Wu and Du [97], was adapted for this study for feature extraction from wavelet packet analysis. The method requires that a reliable wavelet packet analysis be established for the given signal. The reliability of the wavelet packet analysis can be investigated in a number of ways, such as assessing the cross-correlation, rms error and cross-coherence between the original signal and the reconstructed signal.

A number of packets containing the most energy representative of the original signal must then be chosen. The order of the decomposition tree will determine the maximum number of representative packets that may be chosen. In this case, four packets were decided upon. The different parts of the original signal yielded different choices for the packets containing the most energy. The Shannon entropy formula, as discussed in Chapter 2, was used to choose the packets containing the most energy.

The four representative packets containing the wavelet coefficients are then treated as separate signals, and each is characterised according to their rms, standard deviation, crest factor and kurtosis. These wavelet coefficient characteristics are then treated as features for wear classification. Figure 4.16 display a schematic representation of the wavelet packet tree, and figure 4.17 display the specific wavelet chosen for the analysis, which was the coiflet 3 wavelet. The coiflet 3 wavelet was chosen because it yielded the best results after experimentation with a number of different wavelets.

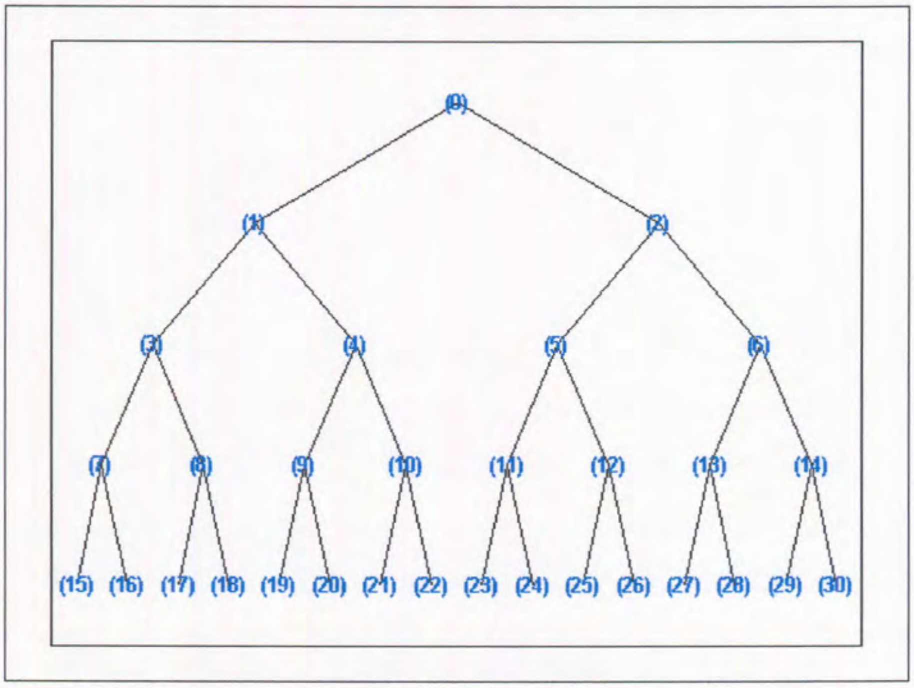

Figure 4.16: Second order with depth four wavelet packet decomposition tree

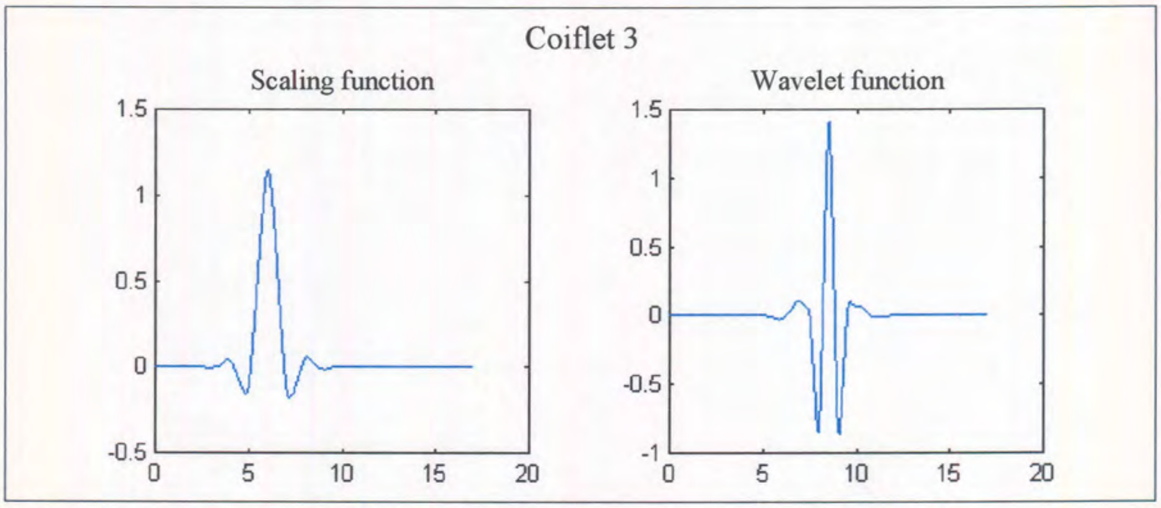

Figure 4.17: The coiflet 3 wavelet chosen for the analysis

Figure 4.18 display an example of an original signal (part A), with the chosen packets containing most energy *(E)*, calculated by Shannon entropy formula. In this case the chosen packets on the tree were packets 1, 2, 3 and 4.

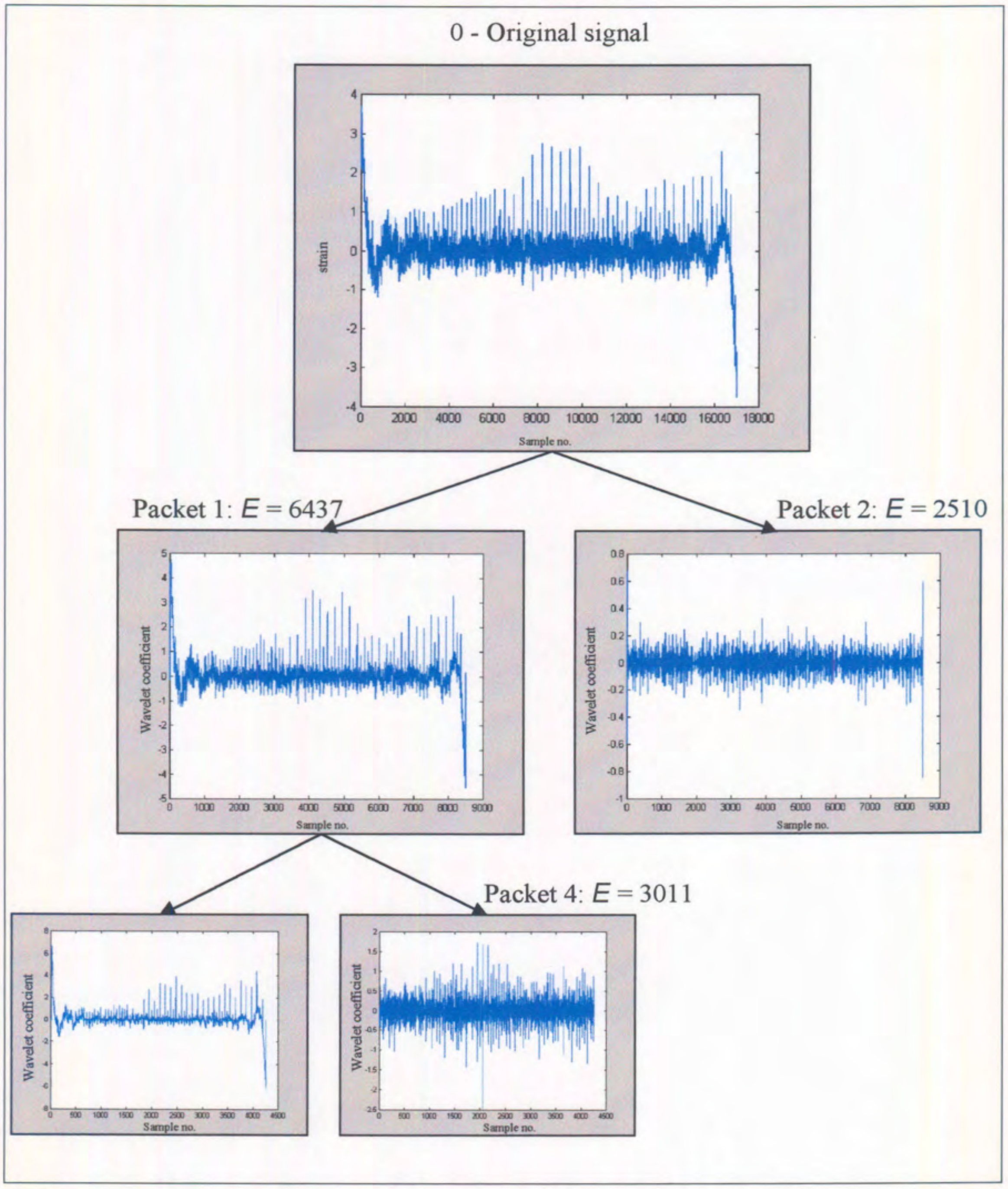

Figure 4.18: Wavelet packets containing the most energy

4.3.4 Feature selection

The total number of acquired features was 6 time, 3 model, 2 frequency and 16 wavelet features, which is a total of 27. These features were calculated for the data from all five parts of the signal, thus 27 x 5 = 135. Of course, there were three measurement channels, which makes it 135 x 3 = 405 individual features from which the best ones must be selected. Many of these features will not show significant trends towards tool wear, and therefore some means of feature reduction must be implemented.

In most similar studies, authors have correlated the trend in the features with the measured tool wear in order to select the best features. In this case it was not possible to disturb the production process for wear measurement. Also, due to the specific wear mode of the synthetic diamond tools, and the fact that the process is a not finishing operation, surface roughness analysis did not yield information on progressive tool wear. Calculating the correlation coefficient between the feature vector and an 'ideal trend' function solved the problem. The ideal trend function was taken as a straight line with a slope of 40 degrees. Although this is not representative of the true tool wear, it can give an indication of which features show consistent trend in time, and whether the trend is towards higher or lower values of the feature. The correlation coefficient can be expressed as a percentage, and features with a correlation higher than a certain threshold value were taken as the final features for tool wear classification. This is an adapted version of the correlation coefficient approach proposed by previous authors, such as Quan *et al.* [45].

The correlation coefficient (expressed as a percentage) between the selected feature x and ideal trend value y can be calculated as follows:

$$\rho = \left| \frac{\sum_i (x_i - \bar{x})(y_i - \bar{y})}{\sum_i (x_i - \bar{x})^2 \sum_i (y_i - \bar{y})^2} \right| \times 100 \qquad (4.1)$$

where $\bar{x}$ and $\bar{y}$ are the means of x and y, respectively; ρ is the correlation coefficient whose value indicate linearity between x and y. When ρ is approaching 100%, there exists a relationship between x and y. The lower the value of ρ, the lesser the chance for the selected feature to show any trend towards tool wear. A last test to determine if the trend of a certain feature is due to chance is to check if roughly the same correlation coefficient is reached for the same feature in the two training data sets.

4.3.5 Wear estimation

The final features are used in a self-organising neural network for wear classification. Different SOM geometries were experimented with in order to obtain the best results. The whole system of vibration measurement, feature extraction, feature reduction and the final wear classification cumulates to a complete monitoring system. This system, with some adjustments, can be implemented on-line if required. Figure 4.19 shows a diagrammatic representation of the proposed monitoring system.

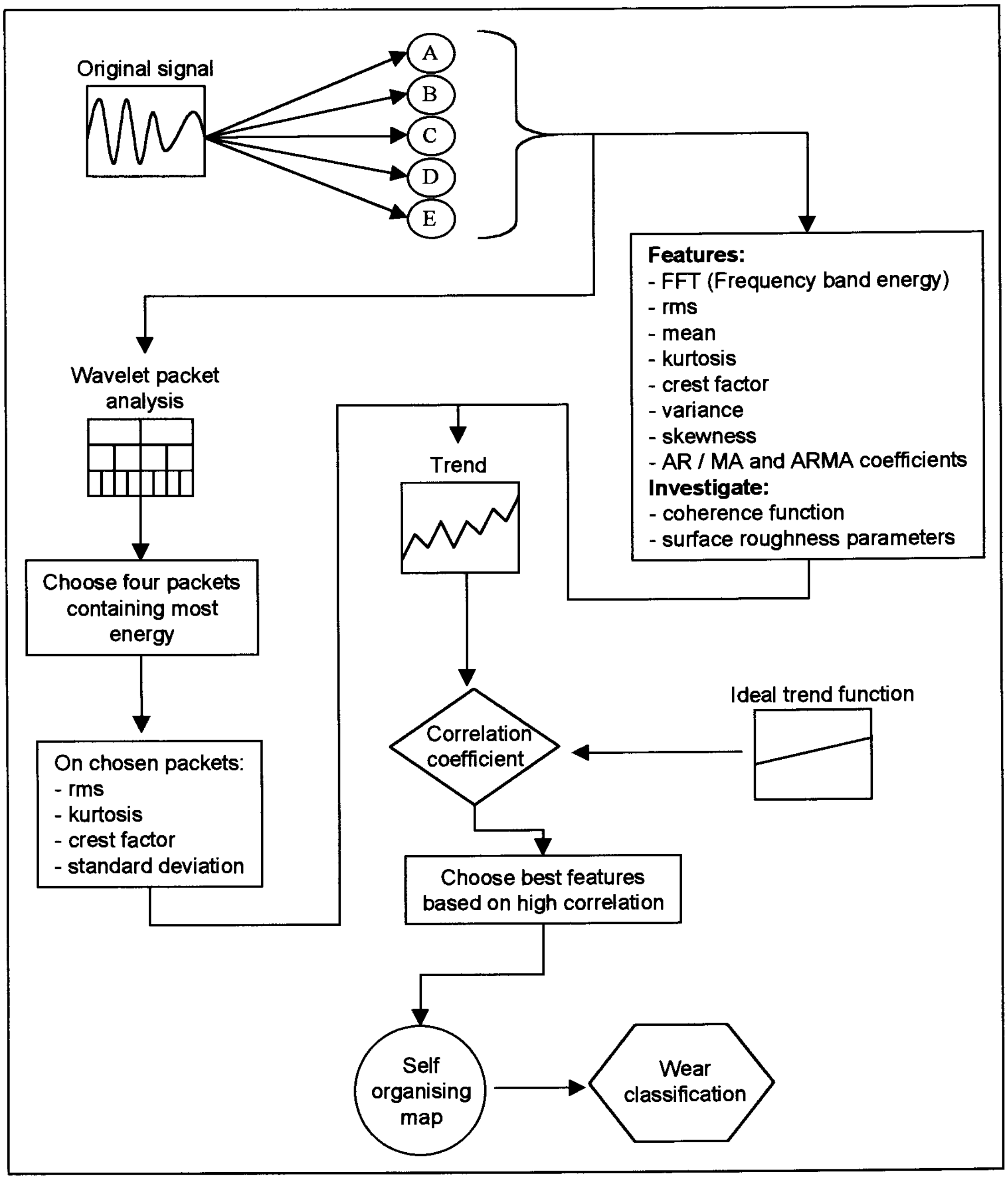

Figure 4.19: Diagrammatic representation of monitoring system

4.4 Experimental results

4.4.1 Selected features

The features selected by the automated monitoring strategy as described above, are shown in Table 4.2. Although a number of other features also displayed considerable trends towards tool wear, only thirteen were selected due to the fact that a limited number of observations for training the SOM were available. The normal practice is to have ten times more observations than features .

Table 4.2

Selected features for wear classification

Feature	Channel	Part
mean	1	B
rms	2	C
rms wavelet packet 1	2	C
rms wavelet packet 3	2	C
mean	2	C
rms	2	D
a1 from AR model	2	D
spectral energy 5 kHz	2	D
rms wavelet packet 1	2	D
kurtosis	2	E
rms	2	E
kurtosis wavelet packet 1	2	E
rms wavelet packet 1	2	E

It is also interesting to note that that no features were selected from the accelerometer signal. Although some features from the accelerometer did display consistent trend towards tool wear (especially the frequency band energy features), the trends were not consistent enough to be selected by the monitoring system. The strain sensor signals were more sensitive to the tool wear. This discovery leads to the conclusion that force sensors are more fit for the purpose of tool wear monitoring than accelerometers, which corresponds to results obtained by previous authors for another process [18].

However, the placement of the sensors, the type of sensor mounting and the specific process which is monitored, have a very strong influence on the final results. It would seem that the channel 2 strain sensor was most sensitive to tool wear. The reason for this could be because the channel 2 sensor was mounted nearest to the tool tip, and because it was mounted in the y-direction, which is the direction of the thrust force, which is normally the direction most sensitive to tool wear, depending on the operation. The channel 3 strain sensor was mounted in the direction of the feed force, which can also be very sensitive to tool wear under some circumstances.

Tool breakage occurred shortly after the last observations were recorded. Unfortunately, data on the breakage event is not available. This means that the monitoring system could not be trained to identify the onset of a breakage event. In principle, however, the system could be trained to set off an alarm when the risk of tool breakage becomes high. For this to be possible, data on the breakage event would have to be collected, which may be a difficult task, due to the high expense of breaking a diamond tool, together with down time on the machine and scrapping a part.

The selected features with respect to the number of machined components are shown in Figures 4.20 to 4.22. The three coloured lines on the graphs represent the features extracted from the three data sets (blue = 1, red = 2, green = 3). Note that the irregular shapes of the graphs are due to the changes in the feed rate, and other dynamic influences on the process. A very irregular deviation is visible in the kurtosis features in figure 4.22. The kurtosis is especially sensitive to any sudden changes in the process. The two big irregularities in the first data set may be due to an unwanted hard spot in the workpiece material formed during casting, or some other external factor.

These irregular trends make decision making very difficult when it is based on a normal thresholding or some other conventional technique. However, artificial neural networks such as the SOM, can handle such noisy inputs efficiently. Irregularities such as the ones visible in figure 4.22 does not have a very large influence on the final classification if enough training samples are available. The effect of the events causing the irregularities are 'smeared out' on the SOM with values from the other features.

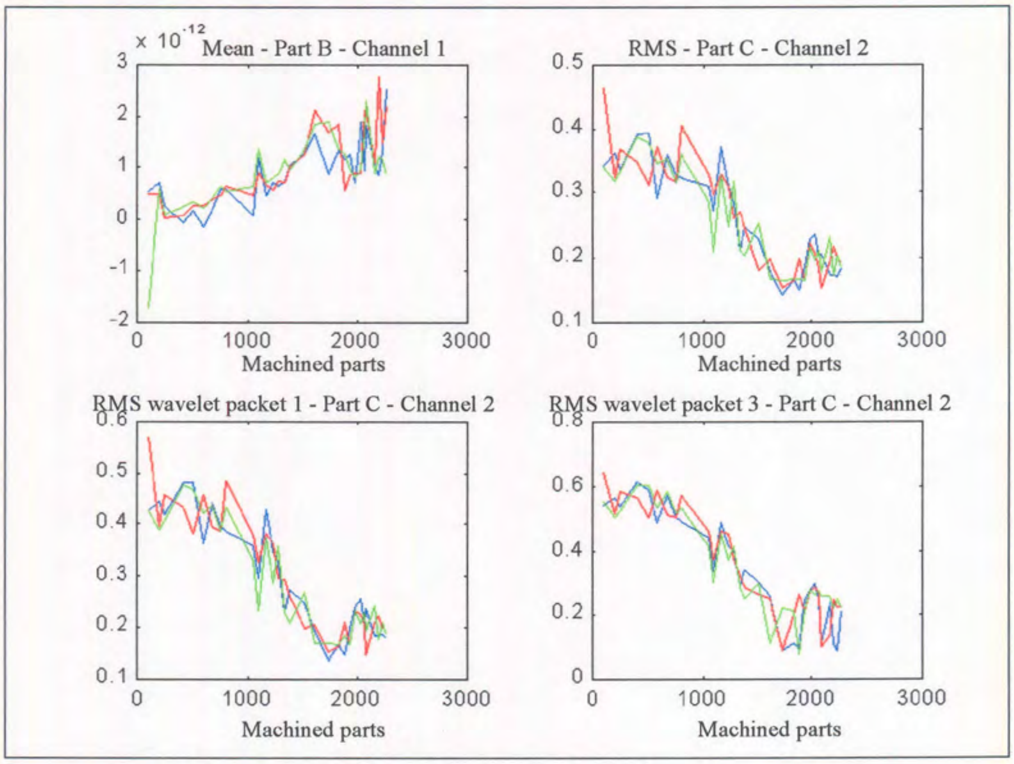

Figure 4.20: Selected features for wear classification

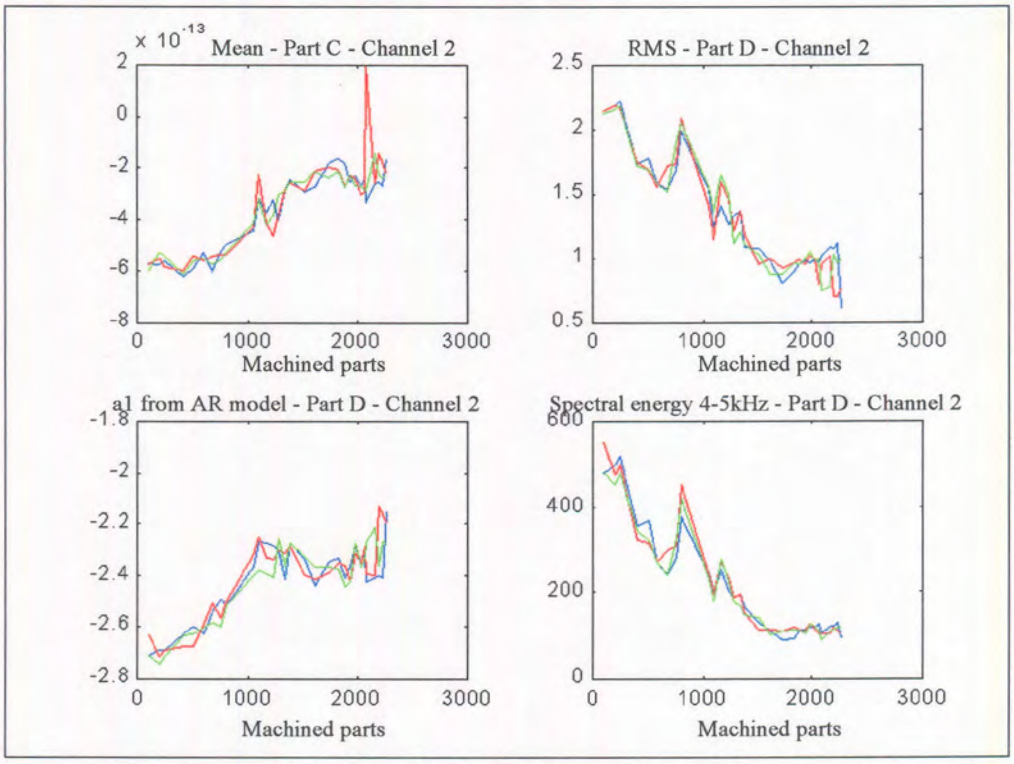

Figure 4.21: Selected features for wear classification

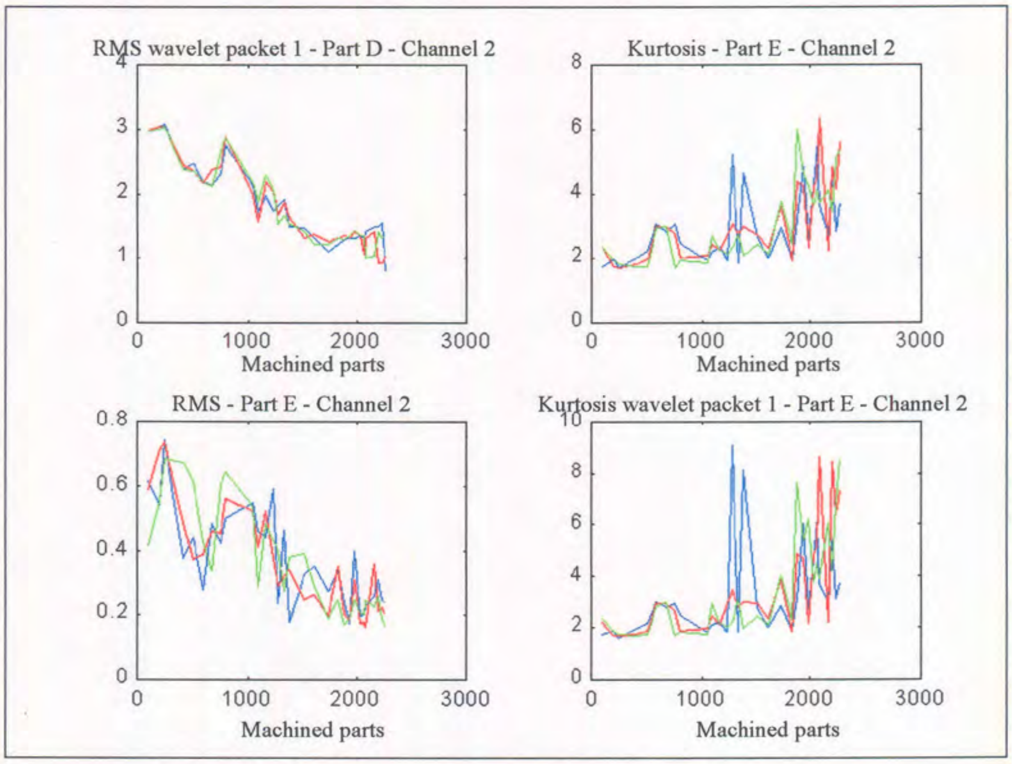

Figure 4.22: Selected features for wear classification

4.4.2 Classification

The selected features from the two learning data sets were used to train a SOM. Two map sizes were used to illustrate the classification capabilities of the SOM. In the first case, a small number of neurones were used. The reason why only a small number of neurones were used, was because it makes classification easier. In this case, only two or three neurones correspond to a new tool, and one correspond to a worn tool. The other neurones all correspond to a used or medium worn tool. In the second instance, when more neurones are used in the network, the regions corresponding to a certain classification becomes larger, and classification becomes more flexible.

The data is normalised before map training commences, although the figures presented here display the data without normalisation. The data is normalised to prevent ill-conditioned calculations during map training. Different normalisation techniques are available, but in this case, a linear normalisation between 0 and 1 for each feature were used.

Some pattern recognition algorithms (k-means, fuzzy and Gaussian clustering) were also tested on the training data. The algorithms could not succeed in forming clusters indicative of tool condition. This does not mean that the algorithms cannot be used for tool condition monitoring, because previous authors have used them with much success [38]. It would rather seem that neural networks are less sensitive to random disturbances in the data, and is more fit for process monitoring in some instances. The fact that the SOM is based on unsupervised learning makes it even more attractive because it is easier to use, and much more flexible.

A. Results with 3×3 SOM

For each of the selected features, a 3×3 representative SOM can be shown. It is important to note that although a SOM for each feature is available, the SOM is actually a single entity. A view on a selected feature is only the view in the direction of that dimension. The SOM can represent multidimensional data in this manner. This is illustrated in figure 4.23, where all the selected variables are shown on a single figure. From this figure, it is easy to observe how the values of the features relate to one another.

The observations in the data sets were all labelled 'new', 'used' or 'worn', corresponding to the number of machined components. The best matching units for this data were looked up on the SOM, and the program was instructed to place the labels of the test data on the corresponding best matching neurones. In figure 4.24, it can be seen that neurones 1 and 4 correspond to a new tool and neurone 9 to a worn tool (neurones are numbered from top to bottom and from left to right). The neurones in-between correspond to used or medium worn tools. The number of hits on a certain neurone is also shown in brackets in figure 4.24. It is important to note that the third data set displays very good results. This data set was not used to train the map, but only for testing.

In figure 4.25, a trajectory was drawn corresponding to the best matching units of the test data. It can be observed that the trajectory moves in time from the 'new' to the 'used' to the 'worn' region. The monitoring system obtained a near 100% success rate in distinguishing between new and worn tools. In figures 4.15 and 4.16, the selected feature is the rms of part C of the signal, from channel 2.

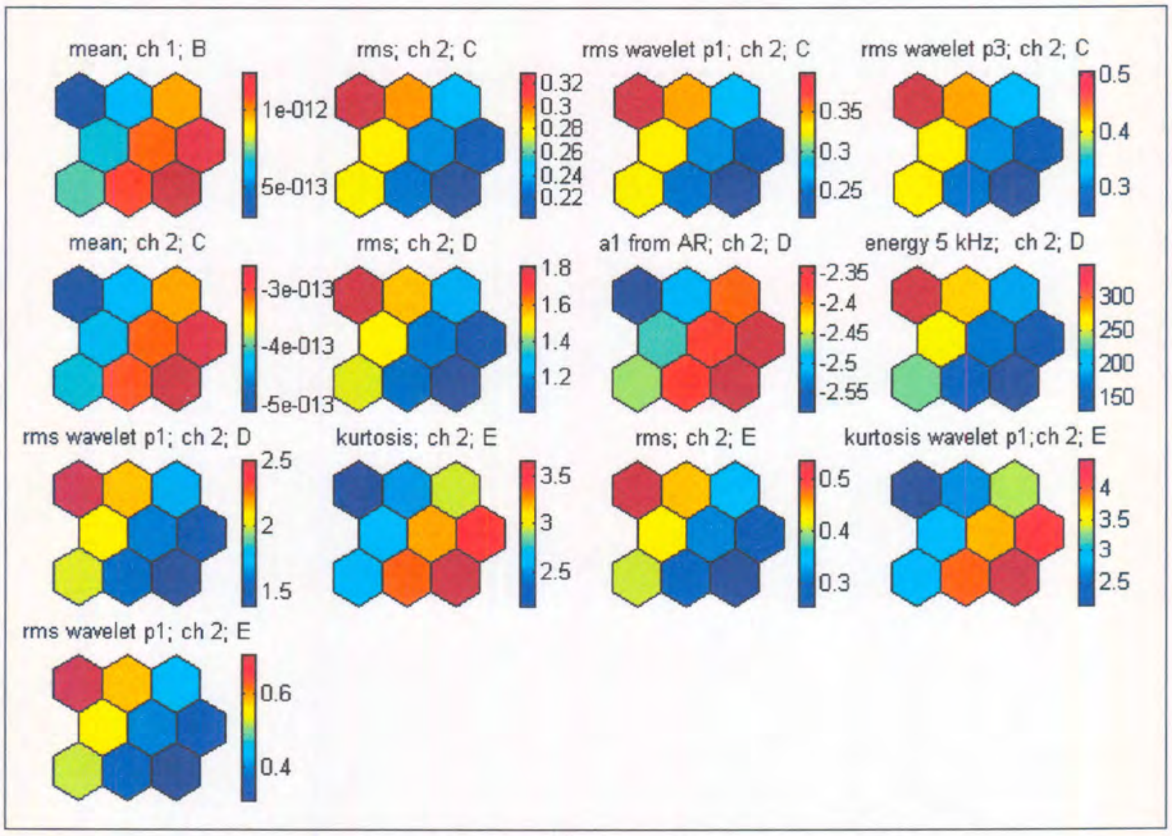

Figure 4.23: 3 × 3 SOM displaying all the selected features

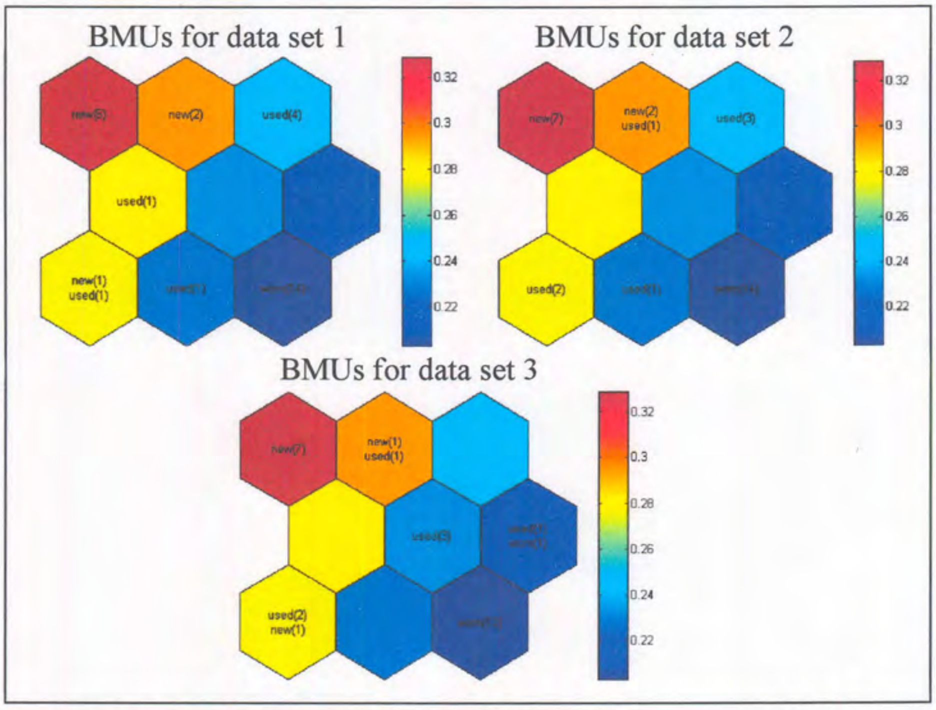

Figure 4.24: BMUs for three data sets, displaying frequency of tool status hits

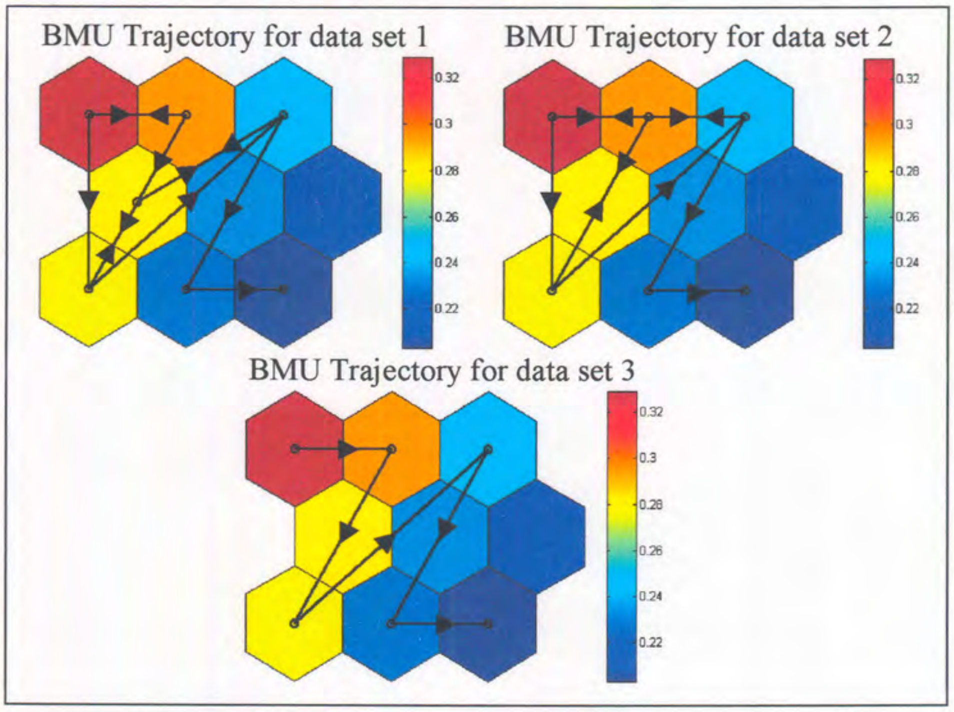

Figure 4.25: BMU trajectories for three data sets

B. Results with 12×8 SOM

In order to make the classification of the tool wear more flexible, a 12×8 SOM were also trained in the same manner as before, with two training data sets and one testing data set. A map containing more neurones can, for example, enlarge the 'worn' region on the map in order to distinguish between a worn tool and a severely worn tool. Training a map with more neurones, is computationally much more challenging and therefore training takes longer.

Figure 4.26 displays the multidimensional view on all the selected features, where the hidden relationships between the features are revealed. It can be seen which features are related to one another, and which tend to display a unique characteristic. For example, the rms from wavelet packets one and three from part C of the signal, seem to display more or less the same trend. However, some of the features trend towards lower values and some features trend towards higher values. The physical explanation for this behaviour will be discussed in the next section.

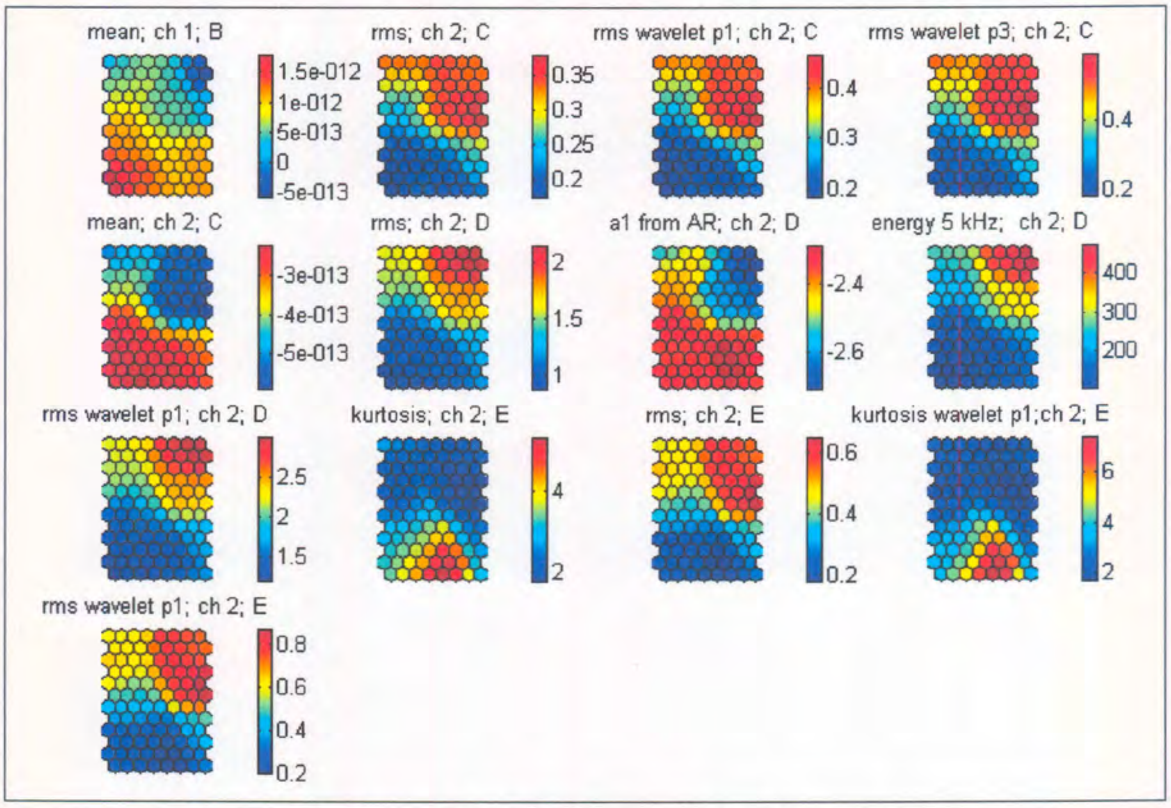

Figure 4.26: 12 x 8 SOM displaying all the selected features

Figure 4.27 displays the number of hits and hit labels for the BMUs of the three data sets. The time trajectory of the BMUs are displayed in figure 4.28. Once again, it can be noted that the trajectory moves from a 'new', to a 'med' to a 'worn' region. It would seem like the trajectory moves around the dark blue area in the worn region and then stops somewhere in this region. Due to the fact that data on the tool breakage is not available, as explained earlier, a single neurone where the risk of tool breakage becomes high cannot be identified here. However, it would be safe to say that a hit in the dark blue region is evident of a worn tool, with some risk of tool breakage in the near future.

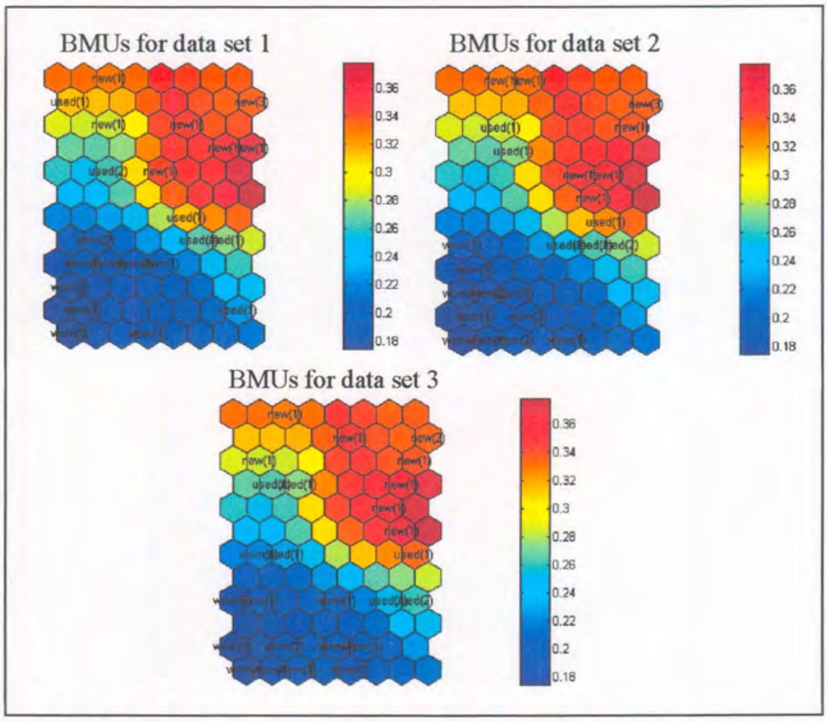

Figure 4.27: BMUs for three data sets, displaying frequency of tool status hits

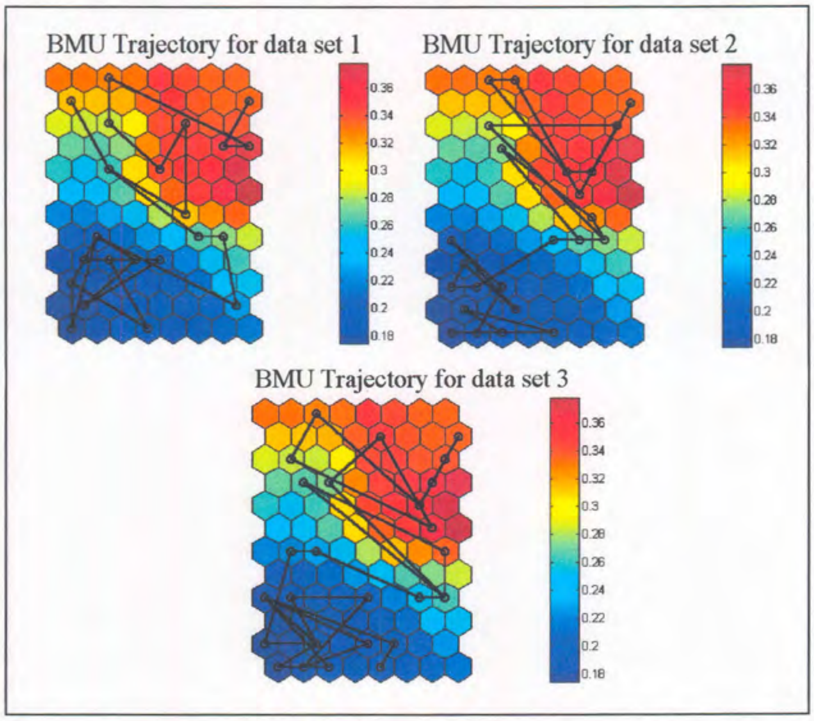

Figure 4.28: BMU trajectories for three data sets

4.5 Investigation

4.5.1 Introduction

Due to the fact that the wear status of the diamond tool could not be investigated during the experimental process, conclusions regarding the mode of failure of the diamond tool are based on the trends in the features and the investigation of the surface roughness of the machined parts. A physical explanation for the trends in the selected features must be found in order to validate the accuracy of the proposed monitoring system.

4.5.2 Surface roughness

The surface roughness of the machined parts were investigated throughout the experimental monitoring process. A Talysurf 10 stylus were used to analyse and record the surface roughness. Various surface roughness parameters were recorded: R_a, R_q, R_y, R_{tm} and R_{pm}. None of these parameters displayed any trends that could be correlated with tool wear. Although certain set limits for each of the parameters are specified for the operation, none of them were violated before tool breakage occurred.

The reason for this is twofold:

1. The process is not a finishing operation, but a metal removal operation, which means that surface finish is not very important during this operation.
2. The mode of progressive failure of the tool is such that it does not influence the surface roughness significantly, which means that flank wear is not the dominant tool failure mode. This is a very important conclusion.

4.5.3 Tool failure mode

It is in actual fact very difficult to identify a single failure mode that caused the visible trends in the features for this case study. A number of failure modes are probably present, and some are more dominant in certain parts of signal than others. At this stage, it is definitely possible to say that channel 2, which was a piezoelectric strain sensor in the thrust direction, was most sensitive to tool wear. In second place was channel 1, which was also a piezoelectric strain sensor. The acceleration signal was less sensitive to the tool wear. This result is similar to the results of another recent study with diamond tools [66], which found that force signals are more sensitive to the diamond tool wear than acceleration signals.

The so-called 'bathtub' behaviour of the tool could not be proved by the selected features. However, it may be possible that these tools exhibit such behaviour, because it is a common characteristic of most machine tools. Due to all the external influences on the process, it was not possible to prove that the initial and final wear stages during this case study occurred faster than the regular wear stage.

An attempt to find an explanation for the tool failure modes are made here, treating each part of the observation signal separately:

A. Part A

No features from part A of the signal were chosen for wear classification, although some features from this part of the signal displayed a trend towards tool wear. This operation is the removal of metal from the face of the piston. It is most likely that the part of the tool tip which is in contact with the workpiece during this operation differs slightly from the rest of the operations, because the direction of the cut differs. Because this part is also a shorter cut than the rest of the operations, it may be that the tool wear in this direction is relatively small compared to the other operations. This information could be of value to the manufacturer because it shows that excessive tool wear will not occur due to this part of the cut.

B. Part B

This part of this signal did not contain much information on the tool wear. Only one feature from this part of the signal were selected for classification. The mean value in this part of the signal increases with progressive tool wear, which in itself cannot give an indication of the dominant wear mode. The cut performed in this case is metal removal on the edge of the piston, and may cause a little flank wear on a small section of the diamond tool.

C. Part C

This part of the signal contained significant information on the tool wear. The selected features from this part of the signal are all related to the rms of the signal, which is an indication of the energy contained within the signal. However, in this part of the signal, the energy decreases, which is an indication that the dominant failure mode is not flank wear. The decrease of energy could have been caused by crater wear or micro-chipping. The mean of the signal, on the other hand, showed an increase, which is an indication of increasing force which is caused by the wear at the tool tip, especially after many components have been manufactured. This may be an indication that micro chipping at the tool tip is present. However, it is not possible determine which failure mode is dominant, because the tool could not be investigated during manufacturing.

D. Part D

This part of the signal contained the most significant information on the tool wear, with four features selected for wear classification. The same arguments as in part C applies here. All the features indicates a decrease of energy. The 5 kHz spectral energy also indicates a decrease of energy, which is again an indication that flank wear is not the dominant wear mode for this cut. The fact that the most features were selected from this part of the signal, indicates that this part of the signal would be the best choice for analysing with an on-line wear monitoring system.

E. Part E

Three features were selected from this part of the signal, but all of them are very noisy and the trends in these features are not really visible with the naked eye. The selected features in this case are once more the rms, which displays a decrease, as well as the kurtosis of the signal and the first wavelet packet. It is also very interesting to note that the crest factor also displayed a trend towards tool wear in this part of the signal, although it was not selected for final classification. This could be attributed to the dominant failure mode, which may be micro-chipping. The cut at the edge of the piston cause a bigger instantaneous force which can cause features like the kurtosis and the crest factor to increase. Although these features are normally not very reliable, as found in the earlier case study and by previous authors, they could be useful when used with a process like this. However, the results obtained here are not very smooth, and these features alone would not be sufficient for a monitoring scheme.

4.6 Conclusion

A diamond tool wear monitoring strategy, based on vibration measurements, was presented. Measurements were taken from a piston manufacturing process, and information on the progressive wear of the diamond tip was unavailable. Due to the fact that the diamond tool wear induces very small variations in the overall machine vibration, a large number of monitoring features were extracted from the data. The monitoring system automatically selected features displaying the most consistent trends towards tool wear, by evaluating a correlation coefficient with an ideal trend function. The selected features were used to train and test a self-organising neural network. A near 100% correct classification was obtained with the test data set. Although the SOM was not originally developed for process classification, very good results can be obtained if the best features for the specific process are selected.

The monitoring system can extract and select features quick enough to enable the implementation of an on-line monitoring system. This system will enable the manufacturer to optimise the use of the diamond tools, which will be a significant cost saving. Further conclusions will be discussed in the following chapter.

CHAPTER 5

CONCLUSIONS AND RECOMMENDATIONS FOR FUTURE RESEARCH

5.1 Conclusions

5.1.1 Introduction

In this chapter the final conclusions are discussed regarding the different aspects of the study. Recommendations for future research are also made based on conclusions drawn from this study. The different aspects of the study from which conclusions are made, are some aspects regarding the two case studies, the use of the Self-Organising Map and wavelet analysis.

5.1.2 Case study 1: Wear monitoring of a coated carbide insert in turning

In this case study two important aspects were investigated under controlled experimental conditions. The first important conclusion was the fact that vibration monitoring is suitable for tool wear identification in a normal turning process. Further conclusions regarding this are:

- The dominant failure mode for this process is flank wear.
- The spectral energy at the natural frequency of the tool post system increase with increasing flank wear.
- The increase in the energy of the signal also causes an increase in certain features extracted from the signals.

The second important investigation of this case study was to determine if the Self-Organising Map can be used for wear classification based on features extracted from sensor data. It was demonstrated that the SOM can be used successfully to distinguish between new and worn tools. The unsupervised learning capability of the SOM allows automatic wear classification without human interaction. The only interaction the SOM requires is data inset and map size specification. As with all other neural networks, the training data must be reliable in order to obtain an accurate classification. A general rule of thumb is that the number of observations supplied to the network must be at least ten times the number of features. The map can be trained with the original training data, and when more observations become available, they can also be used to update the training of the map.

The use of the SOM with discrete variables was also demonstrated for this case study. If threshold values for the variables are known, their values can be fixed to a discrete 0 or 1. This can make classification more accurate, and allows for the definition of a new feature which is the intersection value of all the other features.

5.1.3 Case study 2: Monitoring of the synthetic diamond tool wear in a manufacturing process

This study investigated a number of aspects regarding synthetic diamond tool wear monitoring. Conclusions from case study 1 were used for the planning of this investigation, like the use of vibration sensors and the use of a SOM classification strategy. The study was conducted in a real manufacturing environment under which the experimental conditions had to comply with the manufacturer's demands. Conclusions from this study are similar to conclusions from case study 1, as well as conclusions made by previous authors in similar investigations. However, certain aspects of this case study are quite unique, and these aspects will be highlighted in the following section.

The highlights of this investigation were:

- The use of synthetic diamond tools instead of normal carbide coated tools.
- Accelerometers and piezoelectric strain sensors used for process monitoring.
- The implementation of an automatic feature extraction and feature selection strategy.
- The use of wavelet packet analysis to extract features for tool wear monitoring.
- The use of a SOM for wear classification.

The synthetic diamond tools used in this investigation displayed quite unique wear characteristics. It has been shown that failure modes such as micro-chipping and crater wear dominates diamond tool wear. Flank wear of the diamond did not have a large influence on the diamond wear and resulting tool breakage. It can be concluded from this and previous studies, that diamond tools display unique modes of failure which are not fully understood by researchers yet.

The fact that the failure modes of the diamond tools differ from that of other tools have a large influence on the features that can be selected for wear monitoring, as well as the resulting trends of these features. This is the reason why an automatic feature extraction and feature reduction strategy were implemented. A correlation coefficient approach was used for feature selection. Very good results were obtained with this strategy, which can be implemented in an on-line monitoring system. The conclusion from this part of the study is that it is sometimes necessary to generate large numbers of features, and then select the most appropriate ones for classification with a neural network. This enables monitoring of a process which cannot be characterised in any other way.

It was also shown that the features extracted from the piezoelectric strain sensors showed more consistent trends towards tool wear than the accelerometer. This means that the force signal is more sensitive to tool wear than the vibration signal. In this case, the thrust force was more sensitive to tool wear than the feed force. Previous authors also found that the force signal can sometimes produce better results than the vibration signal. However, accelerometers are sometimes more fit for the purpose of process monitoring due to reasons discussed in Chapter 1.

The piezoelectric strain sensors used in the study are a relatively new type of sensor, and have many advantages above other sensors. One advantage is that the sensors are extremely small, and can be mounted comfortably on the tool holder without obstructing the process. Another advantage is that the sensors are sensitive to tool wear and can also sample within the same frequency range as the accelerometer. A disadvantage is still the fact the sensors must be protected against cutting fluid and chips, but this is the case with almost all sensors. A definite conclusion is that these sensors are fit for process monitoring, if they can be protected when used in an aggressive environment.

Wavelet packet analysis were used for feature extraction, based on a method proposed by previous authors. It was shown that wavelet analysis can be very useful for feature generation, because the original signal is de-noised and compressed by wavelet analysis. This means that only the most relevant information from the original signal are present in the wavelet packets. Another advantage of wavelet analysis is that the calculation is fairly quick, which makes it an option for an on-line monitoring system. The conclusion from this study is that wavelet analysis is a very useful tool for process monitoring, and should be experimented with in other processes as well.

The SOM was investigated for wear classification of the diamond tools. Although the input data contained much noise, very good results were obtained. The input data was chosen to be noisy (refer to Chapter 4) in order to design a robust monitoring system. Different map topologies were experimented with, and the advantage between choosing more or less neurones for the map was demonstrated.

The SOM produced much better results than a pattern recognition algorithm that was also tested with the tool wear data. As was concluded in case study 1, the SOM can be used for process monitoring, although it was originally intended as a data visualisation tool.

5.1.4 Contribution of study

In Chapter 1 a range of literature regarding TCM studies were discussed. Table 1.1 was used to place this study in context with some of the recent relevant literature. This table is also very useful to summarise the contributions made to the literature by this study. From table 1.1 it can be seen that the study contribute to the literature in terms of the following:

- A unique type of tool is investigated.
- The monitoring strategy proposed in the study combines many of the methods investigated in other recent studies.
- The use of the SOM for wear classification is also fairly unique, with only two other studies also investigating the use of SOMs [6,44].
- The large number of features generated and investigated is also a contribution with regard to the literature.

There still exist many unanswered questions regarding this particular field of study, and recommendations for future research are made in a forthcoming section.

5.1.5 Summary of conclusions

To summarise, the conclusions can be described as follows:

- Accelerometers and piezoelectric strain sensors can be used for tool wear monitoring.
- The force signal is more sensitive to the diamond tool wear than the vibration signal.
- The thrust force is more sensitive to the diamond tool wear than feed force.
- Wavelet packet analysis can be used for feature generation in tool wear monitoring
- Feature reduction can be done successfully with a correlation coefficient approach.
- The SOM can be used for classification of tool wear data.
- An automated diamond tool wear monitoring system was developed, that can be implemented on-line if the manufacturer requires it.
- The monitoring system was designed to be robust to changes in process, and can be modified to monitor a wider range of processes than the one discussed in case study 2.
- Synthetic diamond tools display unique wear characteristics, by which failure modes such as crater wear and micro-chipping dominates the flank wear.

5.2 Recommendations for future research

5.2.1 Tool wear monitoring systems

The justification for the purchase of tool monitoring systems by manufacturers were discussed in Chapter 1. Although some tool monitoring systems are commercially available today, there still exist many research opportunities in this field. Most of the commercially available systems monitors tool breakage, and are also limited to a specific process.

However, recent developments in sensor technology will enable manufacturers to purchase sensor integrated tool holders. The recommendation from this study is that the sensors used for such systems are of the piezoelectric strain sensor type, with adequate shielding characteristics when built into the tool holder.

A recommendation for future work from this study is to investigate the possibility of smart sensor integrated tool holders that can be supplied to industry on a cost-effective basis. These monitoring systems must be able to operate with inexpensive software on a PC (or 'black box' format) that can adjust to a certain process or range of processes (similar to the system developed in the study).

5.2.2 Self-Organising Map

Although the data from case study 2 were analysed with the SOM and with a pattern recognition algorithm, the data was not analysed with any other neural network. It would be interesting to compare results from the SOM with other neural networks. Unfortunately, not many neural networks are based on unsupervised learning, which will make the training procedures more complex.

Many neural network strategies today are also combined with fuzzy modelling, and it would be very interesting to investigate the possibility of combining a unsupervised neural network with a fuzzy modelling procedure, especially in the field of process monitoring. The implementation of the SOM with other process monitoring systems could also be very interesting subjects for future research.

5.2.3 Diamond tools

The wear mechanisms of diamond tools in general are not fully understood yet. More studies investigating diamond tools are necessary before the failure modes of these tools will be fully understood. Data on the wear of diamond tools must be made available by researchers in order to achieve a better understanding of the subject by researchers world wide. It is a great advantage for any study to be conducted and implemented in a real manufacturing environment. The disturbances always present in manufacturing plants force the design of robust monitoring systems. Robust monitoring systems can easily be adjusted to monitor other processes as well. However, laboratory experiments with diamond tools could reveal some of the hidden wear characteristics that have not been widely researched yet.

5.3 Epilogue

The development of an automated tool wear monitoring system was the main objective of this study. It was shown that such a system can be implemented in a real manufacturing environment successfully. The system can adjust to changes in process, and will also be able to adjust to the manufacturing of other parts as well. TCM systems for virtually any combination of machines, tools and workpieces will be available soon thanks to the wide variety of research already conducted in this field. The on-line implementation of such systems is the next step. These systems will be a standard commodity on most machines used in manufacturing plants in the future.

REFERENCES

[1] G. Byrne, D. Dornfeld, I. Inasaki, G. Ketteler, W. König and R. Teti, *Tool Condition Monitoring (TCM) - The Status of Research and Industrial Application*, Annals of the CIRP, vol. 44, no. 2, pp. 541-567, 1995.

[2] T. Pfeifer and H. Thrum, *Open systems link sensors and measurement applications to machine tool control units*, Measurement, vol. 19, no. 2, pp. 113-121, 1996.

[3] Janusz Bryzek, *Smarter, less costly sensors are on the way*, Process and Control Engineering, vol. 47, no. 6, pp. 40-43, 1994.

[4] Ian Kinghorn, *Smart sensor technology - the next generation*, Paper Technology, vol. 35, no. 2, pp. 39-41, 1994.

[5] N. Tanaka, S.D. Snyder and C.H. Hansen, *Distributed parameter modal filtering using smart sensors*, Journal of Vibration and Acoustics, Transactions of the ASME, vol. 118, pp. 630-640, 1996.

[6] R. G. Silva, R. L. Rueben, K. J. Baker and S. J. Wilcox, *Tool wear monitoring of turning operations by neural network and expert system classification of a feature set generated form multiple sensors*, Mechanical Systems and Signal Processing, vol. 12, no. 2, pp. 319-332, 1998.

[7] J. Kopac, *Influence of cutting material and coating on tool quality and tool life*, Journal of Materials Processing Technology, vol. 78, pp. 95-103, 1998.

[8] A.K.M.Nurul Amin *et al.*, *Selection of cemented carbide turning tools using EMF and optimization criteria*, Journal of Materials Processing Technology, vol. 77, pp. 59-63, 1998.

[9] M.E.R. Bonifacio and A.E. Diniz, *Correlating tool wear, tool life, surface roughness and tool vibration in finish turning with coated carbide tools*, Wear, vol. 173, no. 1-2, pp. 137-144, 1994.

[10] P.J.A. Lever, M.M. Marefat and T. Ruwani, *A Machine Learning Approach to Tool Wear Behavior Operational Zones*, IEEE Transactions on Industry Applications, vol. 33, no. 1, pp. 264-273, 1997.

[11] S.B. Rao, *Tool wear monitoring through the dynamics of stable turning*, Journal of Engineering for Industry, vol. 108, pp. 184-189, 1986.

[12] S. A. Coker and Y. C. Shin, *In-process control of surface roughness due to tool wear using a new ultrasonic system*, International Journal of Machine Tools & Manufacture, vol. 36, no. 3, pp. 411-422, 1996.

[13] I. Grabec, E. Govekar, E. Susic and B. Antolovic, *Monitoring manufacturing processes by utilizing empirical modeling*, Ultrasonics, vol. 36, pp. 263-271, 1998.

[14] A. Ruiz, D. Guinea and L.J. Barrios, F. Betancourt, *An empirical multi-sensor estimation of tool wear*, Mechanical Systems and Signal Processing, vol. 7, no. 2, pp. 105-199, 1993.

[15] W.J. Braun, M.H. Miller and J.F. Schultze, *The development of machine-tool force reconstruction for wear identification*, Proceedings of the 17th International Modal Analysis Conference, Florida, U.S.A., pp. 94-98, 1999.

[16] H.V. Ravindra, Y.G. Srinivasa and R. Krishnamurthy, *Modeling of tool wear based on cutting forces in turning*, Wear, vol. 169, no. 1, pp. 25-32, 1993.

[17] Tamas Szecsi, *Automatic cutting-tool condition monitoring on CNC lathes*, Journal of Materials Processing Technology, vol. 77, pp. 64-69, 1998.

[18] L.J. Barrios *et al.*, *Experimental Comparison of sensors for tool-wear monitoring on milling*, Sensors and Actuators A, vol. 37-38, pp. 589-595, 1993.

[19] M. Santochi, G. Dini and G. Tantussi, *A Sensor-Integrated Tool for Cutting Force Monitoring*, Annals of the CIRP, vol. 46, no. 1, pp. 49-52, 1996.

[20] T.I. El-Wardany, D. Gao and M.A. Elbestawi, *Tool condition monitoring in drilling using vibration signature analysis*, International Journal of Machine Tools & Manufacture, vol. 36, no. 6, pp. 687-711, 1996.

[21] X.Q. Li, Y.S. Wong and A.Y.C. Nee, *Tool wear and chatter detection using the coherence function of two crossed accelerations*, International Journal of Machine Tools & Manufacture, vol. 37, no. 4, pp. 425-435, 1997.

[22] C.Y. Jiang, Y.Z. Zhang and H.J. Xu, *In-Process monitoring of tool wear stage by the frequency band energy method*, Annals of the CIRP, vol. 36, no. 1, pp. 45-48, 1987.

[23] S. Kim, B.E. Klamecki, *Milling Cutter Wear Monitoring Using Spindle Shaft Vibration*, Journal of Manufacturing Science and Engineering, vol. 119, no. 1, pp. 118-119, 1997.

[24] Joseph M. Shea, *Using forced vibration to determine machine tool condition*, IRD Mechanalysis Technical Report, no. 129, 1990.

[25] D. Meredith, *Practical tool condition monitoring*, Manufacturing Engineering, January '98, pp. 34-39, 1998.

[26] D. Bähre, M. Müller and G. Warnecke, *Basic characteristics on cutting effects in correlation to dynamic effects*, 1997 Technical Papers of the North American Manufacturing Research Institution of SME, pp. 21-26, 1997.

[27] K. Jemielnak and O. Otman, *Tool failure detection based on analysis of acoustic emission signals*, Journal of Materials Processing Technology, vol. 76, pp. 192-197, 1998.

[28] H.V. Ravindra, Y.G. Srinivasa and R. Krishnamurthy, *Acoustic emission for tool condition monitoring in metal cutting*, Wear, vol. 212, pp. 78-84, 1997.

[29] T.A. Carolan, S.R. Kidd, D.P. Hand, S.J. Wilco, P. Wilkonson, J.S. Barton, J.D.C. Jones and R.L. Reuben, *Acoustic emission monitoring of tool wear during the face milling of steels and aluminum alloys using a fibre optic sensor Part 1: Energy Analysis*, Proceedings of the Institute of Mechanical Engineers, vol. 211, part B, pp. 299-309, 1997.

[30] T.A. Carolan, S.R. Kidd, D.P. Hand, S.J. Wilco, P. Wilkonson, J.S. Barton, J.D.C. Jones and R.L. Reuben, *Acoustic emission monitoring of tool wear during the face milling of steels and aluminum alloys using a fibre optic sensor Part 2: Frequency Analysis*, Proceedings of the Institute of Mechanical Engineers, vol. 211, part B, pp. 311-319, 1997.

[31] I.N. Tansel, M.E. Trujillo, W. Bao and T.T. Arkan, *Detection of tool breakage in micro-end-milling operations by monitoring acoustic emission*, 1997 Technical Papers of the North American Manufacturing Research Institution of SME, pp. 69-74, 1997.

[32] N. H. Abu-Zahra and T. H. Nayfeh, *Calibrated method for ultrasonic on-line monitoring of gradual wear during turning operations*, International Journal of Machine Tools & Manufacture, vol. 37, no. 10, pp. 1475-1484, 1997.

[33] F. Caiazzo, G.S. Palazzo and R. Pasquino, *The influence of working parameters on the response of a capacitive sensor used in-process for the measurement of tool wear*, International Journal of Machine Tools & Manufacture, vol. 38, pp. 871-879, 1998.

[34] S. Kurada and C. Bradley, *A machine vision system for tool wear assessment*, Tribology International, vol. 30, no. 4, pp. 295-304, 1997.

[35] A. Novak and H. Wiklund, *On-line prediction of the tool life*, Annals of the CIRP, vol. 45, no. 1, pp. 93-96, 1996.

[36] Y.S. Wong, A.Y.C. Nee, X.Q. Li and C. Reisdorf, *Tool condition monitoring using laser scatter pattern*, Journal of Materials Processing Technology, vol. 63, pp. 205-210, 1997.

[37] A. Karthick, S. Chandra, B. Ramamoorthy and S. Das, *3D Tool wear measurement and visualization using stereo imaging*, International Journal of Machine Tools & Manufacture, vol. 37, no. 11, pp. 1573-1581, 1997.

[38] S. A. Kumar, H.V. Ravindra and Y.G. Srinivasa, *In-process tool wear monitoring through time series modeling and pattern recognition*, International Journal of Production Research, vol. 35, no. 3, pp. 739-751, 1997.

[39] D.E. Dimla, P.M. Lister and N.J. Leighton, *Investigation of a single-layer perceptron neural network to tool wear inception in a metal turning process*, Proceedings of the 1997 IEE Colloquium on Modeling and Signal Processing for Fault Diagnosis, pp. 3/1 - 3/4, 1996.

[40] K. Venkatesh, M. Zhou and R.J. Caudill, *Design of artificial neural networks for tool wear monitoring*, Journal of Intelligent Manufacturing, vol. 8, no. 3, pp. 215-226, 1997.

[41] D.E. Dimla, P.M. Lister and N.J. Leighton, *Tool condition monitoring in metal cutting through application of MLP neural networks*, Proceedings of the 1997 IEE Colloquium on Fault Diagnosis in Process Systems, no. 174, pp. 9/1-9/3, 1997.

[42] Q. Zhou, G.S. Hong and M. Rahman, *A new tool life criterion for tool condition monitoring using a neural network*, Engineering Applications of Artificial Intelligence, vol. 8, no. 5, pp. 579-588, 1995.

[43] S. Das, R. Roy and A.B. Chattopadhyay, *Evaluation of wear of turning carbide inserts using neural networks*, International Journal of Machine Tools & Manufacture, vol. 36, no. 7, pp. 789-797, 1996.

[44] G. Luetzig, M. Sanchez-Castillo and R. Langari, *On tool wear estimation through neural networks*, Proceedings of the 1997 IEEE International Conference on Neural Networks - part 4 of 4, Houston, TX, USA, no. 4, pp. 2359-2363, 1997.

[45] Y. Quan, M. Zhou and Z. Luo, *On-line robust identification of tool-wear via multi-sensor neural network fusion*, Engineering Applications of Artificial Intelligence, vol. 11, pp. 717-722, 1998.

[46] S.K. Choudhury, V.K. Jain and Ch. V. V. Rama Rao, *On-line monitoring of tool wear in turning using a neural network*, International Journal of Machine Tools & Manufacture, vol. 39, pp. 489-504, 1999.

[47] S. Das, A.B. Chattopadhyay and A.S.R. Murthy, *Force parameters for on-line tool wear estimation: A neural network approach*, Neural Networks, vol. 9, no. 9, pp. 1639-1645, 1996.

[48] J.H. Lee, D.E. Kim and S.J. Lee, *Statistical analysis of cutting force ratios for flank-wear monitoring*, Journal of Materials Processing Technology, vol. 74, pp. 104-114, 1998.

[50] T.I. Liu, W.Y. Chen and K.S. Anatharaman, *Intelligent detection of drill wear*, Mechanical Systems and Signal Processing, vol. 12, no. 6, pp. 863-873, 1998.

[51] C.M. Talbott, *Prognosis of residual machine life*, Proceedings of the Maintenance and Reliability Conference (MARCON 98), University of Tennessee, Knoxville, pp. 11-14, 1998.

[52] A. Chukwujekwu Okafor and O. Adetona, *Predicting quality characteristics of end-milled parts based on multi-sensor integration using neural-networks: individual effects of learning parameters and rules*, Journal of Intelligent Manufacturing, vol. 6, no. 6, pp. 389-400, 1995.

[53] K. Lou and C. Lin, *An Intelligent Sensor Fusion System for Tool Monitoring on a Machining Center*, International Journal of Advanced Manufacturing Technology, vol. 13, pp. 556-565, 1997.

[54] J.C. Chen and JT. Black, *A Fuzzy-nets-in-process (FNIP) system for tool breakage monitoring in end-milling operations*, International Journal of Machine Tools & Manufacture, vol. 37, no. 6, pp. 783-800, 1997.

[55] L. Xiaoli, Y. Yingxue and Y. Zhejun, *On-line tool condition neural network with improved fuzzy neural network*, High Technology Letters, vol. 3, no. 1, pp. 30-38, 1997.

[56] P. Fu, A.D. Hope and M.A. Javed, *Fuzzy classification of milling tool wear*, Insight, vol. 39, no. 8, pp. 553-557, 1997.

[57] S. Li and M.A. Elbestawi, *Fuzzy clustering for automated tool condition monitoring in machining*, Mechanical Systems & Signal Processing, vol. 10, no. 5, pp. 533-550, 1996.

[58] R.J. Kuo and P.H. Cohen, *Multi-sensor integration for on-line tool wear estimation through radial basis function networks and fuzzy neural network*, Neural Networks, vol. 12, pp. 355-370, 1999.

[59] R.J. Kuo and P.H. Cohen, *Intelligent tool wear estimation system through artificial neural networks and fuzzy modeling*, Artificial Intelligence in Engineering, vol. 12, pp. 229-242, 1998.

[60] D. Y. Jang, Y. Choi, H. Kim and A. Hsiao, *Study of the correlation between surface roughness and cutting vibrations to develop an on-line roughness measuring technique in hard turning*, International Journal of Machine Tools & Manufacture, vol. 36, no. 4, pp. 453-464, 1996.

[61] P. Wilkinson, R.L. Reuben, J.D.C. Jones, J.S. Barton, D.P. Hand, T.A. Carolan and S.R. Kidd, *Surface finish parameters as diagnostics of tool wear in face milling*, Wear, vol. 205, pp. 47-54, 1997.

[62] S. Vajpayee, *Analytical study of surface roughness in turning*, Wear, vol. 70, pp. 165-175, 1981.

[63] Y. K. Chou and C.J. Evans, *Tool wear mechanism in continuous cutting of hardened tool steels*, Wear, vol. 212, no. 1, pp. 59-65, 1997.

[64] M. Thomas *et al.*, *Effect of tool vibration on surface roughness during lathe dry turning process*, Computers & Industrial Engineering, vol. 31, no. 3-4, pp. 637-644, 1996.

[65] *Talysurf 10 Operators Handbook*, Rank Taylor Hobson Limited, Leicester, England, no. 241-7, pp. 6-8 and 38-39.

[66] In-Hyu Choi and Jeong-Du Kim, *Development of monitoring system on the diamond tool wear*, International Journal of Machine Tools & Manufacture, vol. 39, pp. 505-515, 1999.

[67] J.E.D. Afaghani, K. Yamaguchi, T. Nakamoto and K. Yoshino, *Tear-off wear mechanism of sintered diamond tool in cutting SiC-particle-strengthened epoxy composites*, Wear, vol. 206, pp. 221-229, 1997.

[68] C. Wilson and I.D. Marinescu, *Tool wear and temperature using PDC cutters in granite turning*, Transactions of the North American Manufacturing Research Institution of SME, vol. 25, pp. 99-104, 1997.

[69] E. Paul, C.J. Evans, A. Mangamelli, M.L. McGlauflin and R.S. Polvani, *Chemical aspects of tool wear in single point diamond turning*, Precision Engineering, vol. 18, pp. 4-19, 1996.

[70] A.G. Khurshudov, K. Koji, H. Koide, *Wear of the AFM diamond tip sliding against silicon*, Wear, vol. 203-204, pp. 22-27, 1997.

[71] S. Durante, G. Rutelli and F. Rabezzana, *Aluminum-based MMC machining with diamond-coated cutting tools*, Surface and Coatings Technology, vol. 94-95, pp. 632-540, 1997.

[72] Kyung Sam Park and Soung Hie Kim, *Artificial intelligence approaches to determination of CNC machining parameters in manufacturing: a review*, Artificial Intelligence in Engineering, vol. 12, pp. 127-134, 1998.

[73] D.S. Ermer, *Optimization of the constrained machining economics problem by geometric programming*, Journal of Engineering for Industry, vol. 93, no. 4, pp. 1067-1072, 1971.

[74] Z. J. Da, J.P. Sadler and I.S. Jawahir, *Predicting optimum cutting conditions for turning operations at varying tool-wear states*, Transactions of the North American Manufacturing Research Institution of SME, vol. 25, pp. 75-80, 1997.

[75] S.K. Choudhury, E. Kumar and A. Ghosh, *A scheme of adaptive turning operations*, Journal of Materials Processing Technology, vol. 87, pp. 119-127, 1999.

[76] Chen Zhou and R.A. Wysk, *Tool status recording and its use in probabilistic optimization*, Journal of Engineering for Industry, vol. 114, pp. 494-499, 1992.

[77] D.W. Yen and P.K. Wright, *Adaptive Control in Machining - a new approach based on the physical constraints of tool wear mechanisms*, Journal of Engineering for Industry, vol. 105, pp. 31-38, 1983.

[78] T. Obikawa, C. Kaseda, T. Matsumura, W.G. Gong and T. Shirakashi, *Tool wear monitoring for optimizing cutting conditions*, Journal of Materials Processing Technology, vol. 62, pp. 374-379, 1996.

[79] D.Y. Jang and A. Seireg, *Machining parameter optimization for specified surface conditions*, Journal of Engineering for Industry, vol. 114, pp. 254-257, 1992.

[80] Y.S. Tarng, S.T. Chen and Y.S. Wang, *Adaptive Control of Machining Operations*, Key Engineering Materials, vol. 138-140, pp. 263-287, 1998.

[81] Y. Hatamura, T. Nagao and M. Mituishi, *A fundamental structure for intelligent manufacturing*, Precision Engineering, vol. 15, no. 4, pp. 266-273, 1993.

[82] Allan Davies, *The intelligent machine*, Manufacturing Engineer, vol. 73, no. 4, pp. 182-185, 1994.

[83] Th. Lundholm and B. Lindstrom, *A flexible real-time control system for turning*, Annals of the CIRP, vol. 40, no. 1, pp. 441-444, 1991.

[84] Angus Jeang, *Reliable tool replacement policy for quality and cost*, European Journal of Operational Research, vol. 108, pp. 334-344, 1998.

[85] M.S. Akturk and S. Avci, *Tool allocation and machining conditions optimization for CNC machines*, European Journal of Operational Research, vol. 94, pp. 335-348, 1996.

[86] B. Gopalakrishnan and F. Al-Khayyal, *Machine parameter selection for turning operations with constraints: an analytical approach based on geometric programming*, International Journal of Production Research, vol. 29, no. 9, pp. 1897-1908, 1991.

[87] Cornel Mihai Nicolescu, *On-line Identification and Control of Dynamic Characteristics of Slender Workpieces in Turning*, Journal of Material Processing Technology, vol. 58, pp. 374-378, 1996.

[89] D.R. Martinez, T.D. Hinnerichs and J.M. Redmond, *Vibration Control for Precision Manufacturing Using Piezoelectric Actuators*, Journal of Intelligent Materials Systems and Structures , vol. 7, pp. 182-191, 1996.

[90] S.B. Billatos and P. Tseng, *Knowledge-based optimization for intelligent manufacturing*, Journal of Manufacturing Systems, vol. 10, no. 6, pp. 464-475, 1991.

[91] S.S. Rao, *Mechanical Vibrations*, Addison Wesley Publishing Company, Massachusetts, 3rd Edition, 1995.

[92] Lennart Ljung, *System Identification - theory for the user*, PTR Prentice Hall Inc., Englewood Cliffs, New Jersey, 1987.

[93] J.H. Williams, *System monitoring and the use of models*, Handbook of Condition Monitoring, Chapman & Hall, London, pp. 219-239, 1998.

[94] A. Swami, J.M. Mendel and C.L. Nikias, *Higher-Order Spectral Analysis Toolbox for use with MATLAB user's guide*, Version 2, Available from Mathworks at http://www.mathworks.com, 1999.

[95] G.S. Hong, M. Rahman and Q. Zhou, *Using neural network for tool condition monitoring based on wavelet decomposition*, International Journal of Machine Tools & Manufacture, vol. 36, no. 5, pp. 551-566, 1996.

[96] L. Xiaoli, Y. Yingxue and Y. Zhejun, *On-line tool condition monitoring system with wavelet fuzzy neural network*, Journal of Intelligent Manufacturing, vol. 8, no. 4, pp. 271-276, 1997.

[97] Y. Wu and R. Du, *Feature extraction and assessment using wavelet packets for monitoring of machining processes*, Mechanical Systems and Signal Processing, vol. 10, no. 1, pp. 29-53, 1996.

[98] M. Misiti, Y. Misiti, G. Oppenheim and J.P. Poggi, *Wavelet Toolbox for use with MATLAB user's guide*, Version 1, Available from Mathworks at http://www.mathworks.com, 1999.

[99] Teuvo Kohonen, *The self-organizing map*, Neurocomputing, vol. 21, pp. 1-6, 1998.

[100] Jari Kangas and Teuvo Kohonen, *Developments and applications of the self-organizing map and related algorithms*, Mathematics and Computers in Simulation, vol. 41, pp. 3-12, 1996.

[101] A.S. Tolba and A.N. Abu-Rezeq, *A self-organizing feature map for automated visual inspection of textile products*, Computers in Industry, vol. 32, pp. 319-333, 1997.

[102] Kimmo Kiviluoto, *Predicting bankruptcies with the self-organizing map*, Neurocomputing, vol. 21, pp. 191-201, 1998.

[103] L. Cser, A.S. Korhonen, P. Mantyla and O. Simula, *Data mining in improving the geometric quality parameters of hot rolled strips*, Proceedings of the 1999 International Conference on Quality Manufacturing, Stellenbosch, South Africa, pp. 8-15, 1999.

[104] Helsinki University of Technology, Neural Networks Research Centre, *The Self-Organizing Map*, http://www.cis.hut.fi/nnrc, 1999.

[105] Helsinki University of Technology, Laboratory of Computer and Information Science, *The Self-Organizing Map Toolbox for MATLAB*, http://www.cis.hut.fi/cis, 1999.